MODEL-BASED ON-BOARD DIAGNOSTICS FOR SCR-ASC

by

Kaushal Kamal Jain

A Dissertation

Submitted to the Faculty of Purdue University

In Partial Fulfillment of the Requirements for the degree of

Doctor of Philosophy

School of Mechanical Engineering

West Lafayette, Indiana

May 2023

THE PURDUE UNIVERSITY GRADUATE SCHOOL
STATEMENT OF COMMITTEE APPROVAL

Dr. Peter H. Meckl, Chair

School of Mechanical Engineering

Dr. Gregory M. Shaver

School of Mechanical Engineering

Dr. Kartik B. Ariyur

School of Mechanical Engineering

Dr. Pingen Chen

School of Mechanical Engineering, Tennessee Tech University

Dr. Oleg Wasynczuk

School of Electrical and Computer Engineering

Approved by:

Dr. Nicole Key

To the loving memory of my father, Sh. Kamalesh Kumar Jain

Papa, I miss you every day and wish that you were here.
But, I have always felt your love and support from wherever you are.
Your unconditional love has and will always be my biggest strength.

ACKNOWLEDGMENTS

First and foremost, I would like to thank Dr. Peter Meckl for giving me the opportunity to join his research group and for his patience, guidance, and support throughout. It has been an utmost pleasure working with him and I consider myself very lucky to have someone like Prof. Meckl as my major professor. I would do myself proud if I could become half as meticulous and kind as him. I would also like to thank Dr. Pingen Chen for his invaluable guidance and help as our collaborator in this project. Further, I would also like to thank Dr. Greg Shaver, Dr. Oleg Wasynczuk, and Dr. Kartik Ariyur for serving on my PhD advisory committee. I am grateful to Dr. Ariyur for many stimulating discussions and providing many valuable suggestions and ideas.

It wouldn't have been possible for us to do this project without the data and sponsorship from Cummins Inc. We are grateful to Dr. Michael Haas and Dr. Lyle Kocher at Cummins for their efforts and support to provide the data and sponsorship and also for their immense guidance, regular constructive feedback, and mentorship. I would also like to thank the School of Mechanical Engineering for providing me TA support for a major part of my graduate studies.

I have had the fortune of forming some great friendships with several colleagues. I would especially like to express my gratitude to Jagdish Hiremath and Rohinish Gupta for their mentorship and friendship over the years. From helping me get started with the fundamentals of aftertreatment control to providing great insights and ideas at every stage of my PhD, Jagdish has played an instrumental role in my progress. Hanging out with Jagdish and Shivani during my trips to Columbus remains one of my fondest memories as a grad student. I fondly remember the time I spent with Rohinish during my first year at Purdue when I learned the ropes of using a chassis dynamometer and spent countless hours with him in trying to fix it. I have always counted on him to provide great suggestions and advice whenever I need help. I would also like to thank Rajakumar Ganne for the amazing time I had working with him, playing Chess, having random discussions, and many more fond memories. Special thanks also to Harshil Angre, Atharva Tandale, Mrunal Chavan, Suyash

Jadhav, Shrenik Zinage, Abhilash Reddy, Kuo Yang, Sachin Joshi, and Zifei Su as I had a great time working, interacting and learning from them.

Moving to a new country on the other side of the world could have been an intimidating experience, but I was lucky to have several friends from IIT Guwahati join Purdue around the same time as me. Words can't do justice to the amazing time I spent with Abhishek Chaurasia, Naveen Madapana, Ashish Chaudhari, Harsh Ranjan, Parth Paritosh, Abhimanyu Baruah, Rohit Singh, Ashutosh Pandey, Mayank Gupta, Shamiek Mangipudi, and Sagar Swetambar. I can call up any of these guys whenever I need to uplift my mood. I was also fortunate to forge several amazing friendships at Purdue that have given me many memories to cherish: cooking (mis)adventures and fun times at McCormick with Vikram Ravindra and Rohith Chandrasekar; random drives, racquetball, discussions on cricket, philosophy, math, movies, and everything under the sun with Akash Kumar, Abhiram Natarajan, and Vikram Ravindra; banter with Suyash Gupta; the most fun and carefree times with Ashutosh Srivastava, Vatsal Patel, Niranjan Rajendra, and Rakesh Balachandra; grading memories, discussions on controls and some truly-random topics with Niraj Vipra; fun times with Akancha Pandey, Kanishka Misra, Ananya Sheth, Janav Udani, Raghavendra Yesaswi, Tanya Purwar, Ankit Manerikar, Malavika Panicker, Shatakshi Gupta, Karna Patel, Ayan Hazra, and Chirag Nimani. I would like to thank all of them for their friendship. I would also like to thank my friends from IIT Guwahati: Harshit Gupta, Arpit Jain, Puru Rastogi, Ajay Zambare, Rupesh Verma, Sivapuram Raghavendra, Saurabh Samant, Anmol Mukati, Abhilash Ajmera, Manoj Rahul; my childhood friends: Shivam Gupta, Shreya Binaykiya; and my cousin Shreya Agrawal for their friendship, love, and support through thick and thin.

Most importantly, I would like to express immense gratitude towards my parents, Kokilah Jain and Kamalesh Kumar Jain, for their unconditional love and support, and to my elder brother Kalpit, who has been a pillar of support as he has helped me with everything from high school mathematics to graduate school and beyond. Special thanks also to my younger brother Kartikeya, sister-in-law Ankita, and my little nephews Kritin and Tryaksh, who are the sources of unlimited joy for our family.

TABLE OF CONTENTS

LIST OF TABLES

LIST OF FIGURES

LIST OF SYMBOLS

A_i	Pre-exponential coefficient for reaction i
E_i	Activation energy for reaction i in J/mol
F	Exhaust gas volume flow rate in m^3/sec
K	SCR Catalyst NH_3 storage capacity in moles
R	Universal gas constant in J/mol-K
S_{NOx}	ASC's selectivity to NOx
$S_{\mathrm{N_2O}}$	ASC's selectivity to N_2O
T	Catalyst bed temperature in K
u_1	Concentration of injected NH_3 in mol/m^3
$u_{1,\mathrm{ideal}}$	Ideal u_1 assuming instant and 100% conversion from urea to NH_3
u_2	Concentration of SCR-in NOx in mol/m^3
V	Catalyst volume in m^3
x_1	Concentration of SCR-out NH_3 slip in mol/m^3
x_2	Concentration of SCR-out NOx in mol/m^3
x_3	Fraction of SCR catalyst storage capacity occupied by NH_3

α_{ads}	Reaction rate for NH_3 adsorption to SCR catalyst
α_{des}	Reaction rate for NH_3 desorption from SCR catalyst
α_{oxi}	Reaction rate for oxidation of adsorbed NH_3 in SCR catalyst
α_{SCR}	Reaction rate for NOx reduction by adsorbed NH_3 in SCR catalyst
$\eta_{\mathrm{NH_3}}$	ASC's NH_3 conversion efficiency
η_{urea}	Urea to NH_3 conversion efficiency
τ	Time-constant for Urea to NH_3 conversion

ABBREVIATIONS

ASC	Ammonia Slip Catalyst
CARB	California Air Resource Board
DEF	Diesel Exhaust Fluid
DG	Degreened
DOC	Diesel Oxidation Catalyst
DPF	Diesel Particulate Filter
EPA	Environment Protection Agency
EUL	End of useful life
FTP	Federal Test Procedure
GVWR	Gross Vehicle Weight Rating
HDT	Heavy-duty Truck
HDV	Heavy-duty Vehicle
IUMPR	In-use Monitor Performance Ratio
LDT	Light-duty Truck
LDV	Light-duty Vehicle
MIL	Malfunction Indicator Light
OBD	On-board Diagnostics
RMC	Ramped Mode Cycle
SCR	Selective Catalytic Reduction
SET	Supplemental Emissions Test

ABSTRACT

Selective Catalytic Reduction (SCR) and Ammonia Slip Catalyst (ASC) are important components of the diesel engine aftertreatment. SCR reduces the engine-out NOx into harmless N_2 and H_2O using NH_3, which is injected into the system as Diesel Exhaust Fluid or DEF. ASC is responsible for oxidizing SCR-out NH_3. Thus, SCR-ASC system minimizes tailpipe NOx and NH_3 emissions.

A major challenge with the SCR-ASC system is degradation or aging of the SCR catalyst with time, which leads to increase in tailpipe NOx emissions. Therefore, it is important for diesel-engine vehicles to be equipped with effective on-board diagnostics (OBD), which can monitor and report catalyst degradation before it degrades beyond acceptable levels. The primary objective of this work is to develop a robust model-based non-intrusive on-board diagnostics algorithm that can monitor catalyst health using commercial NOx sensors under real-world on-road driving conditions.

Cummins Inc. has generously provided on-road data for four trucks, and test-cell data for cold Federal Test Procedure (cFTP), hot Federal Test Procedure (hFTP), and Ramped Mode Cycle (RMC) cycles for degreened (DG) and end-of-useful-life (EUL) catalysts. This thesis presents a diagnostics-oriented aging model for combined SCR-ASC system, along with two model-based OBD methods applied to both test-cell data and on-road data from commercial trucks. The key challenge with model development was unavailability of NOx and NH_3 measurements between SCR and ASC. Since it would have been very difficult to calibrate both SCR and ASC dynamics without any measurements between SCR and ASC, therefore ASC was modeled using static look-up tables to determine ASC's NH_3 conversion efficiency and its selectivity to NOx and N_2O as a function of temperature and flow rate. The traditional three-state single-cell ordinary differential equation (ODE) model was used for SCR. Hot FTP was used to calibrate the model. Cold FTP and RMC were used for validation. Results show that the SCR-ASC model can capture the aging signatures in tailpipe NOx, NH_3, and N_2O reasonably well for cFTP, hFTP, and RMC cycles in the test-cell data. After slight re-calibration and combining with a simple model for commercial NOx sensor's cross-sensitivity to NH_3, the model works reasonably well for on-road data from

commercial trucks. Two model-based on-board diagnostic (OBD) methods are presented with enable conditions designed to detect operating conditions suitable for detecting aging signatures, while minimizing false positives and false negatives. It was demonstrated that the enable conditions increase the robustness of the OBD methods to model inaccuracy, uncertainty in initial NH_3 storage, and NOx sensor's cross-sensitivity to NH_3.

The first OBD method does a binary classification at each sample point to label it as either degreened or EUL. This OBD method is applied to both test-cell and real-world truck data with commercial NOx sensors. Results on test-cell data showed that this method is capable of correctly identifying the aging levels of degreened and EUL catalysts with zero false positives and very few false negatives. The method was also shown to be robust to NOx sensor's cross-sensitivity to NH_3 and measurement noise when the tailpipe NOx and NH_3 signals in test-cell data were combined with Gaussian noise to simulate worst-case cross-sensitivity and measurement noise. Results on truck data show encouraging trends between relative degradation level and the number of miles on the four trucks. The trends reported by the method on truck data were shown to be robust to uncertainty in the initial value of NH_3 storage. A drawback with this method was that very few sample points were selected from the test-cell data after applying the enable conditions, which demonstrate the challenge with designing model-based enable conditions that are robust to false positives and false negatives but still lead to good In-use monitoring performance ratio (IUMPR).

Unlike the first method, the second OBD method assigns a non-binary value to each sample point, which is proportional to the probability of that point belonging to a degreened or an EUL catalyst. This method uses a stochastic version of the proposed SCR-ASC model, which is derived using a simplified version of the Bayesian approach for model calibration. This method results in a much better IUMPR than the first one and can still correctly classify the degreened and EUL catalysts for all three cycles in the test-cell data. Even though this work presents a preliminary implementation of the stochastic OBD method, the detailed framework presented in this thesis along with a complete set of enable conditions lays a strong foundation for developing a more detailed version of the method in future based on a rigorous implementation of the Bayesian approach.

1. INTRODUCTION TO SCR-ASC OBD: MOTIVATION, CHALLENGES, AND CURRENT APPROACH

Due to their high compression ratio, diesel engines have low operation cost and high fuel efficiency, which makes them a popular choice for automotive applications. However, diesel emissions include pollutants such as unburnt hydrocarbons (UHC), carbon monoxide (CO), nitrogen oxides (NOx) and particulate matter (PM). These pollutants are the result of undesirable processes during combustion, including incomplete fuel combustion, combustion of engine lubricating oil and non-hydrocarbon components, and reactions between mixture components under high temperature and pressure [1].

These pollutants combine in the atmosphere to form ground-level ozone, which leads to health issues such as respiratory problems [2]. Hence, government bodies like the United States Environment Protection Agency (EPA) and California Air Resources Board (CARB) enforce regulations on the amount of pollutants a vehicle can emit. In order to meet the EPA/CARB regulations, the diesel engine aftertreatment system employs diesel particulate filter (DPF) to filter PM, diesel oxidation catalyst (DOC) to oxidize CO and UHC, Urea-SCR (Selective Catalytic Reduction) to reduce NOx into harmless Nitrogen and water vapors, and Ammonia Slip Catalyst (ASC) to oxidize SCR-out NH_3 into Nitrogen.

The increasingly stringent regulations warrant effective and robust control strategies for all aftertreatment components. Another major challenge with the aftertreatment system is degradation or aging of its components with time. Though all components of the aftertreatment age, the focus of this work will be SCR and ASC. Degradation of SCR catalyst leads to decline in deNOx efficiency resulting in an increase in tailpipe NOx emissions. A robust urea-dosing controller can adapt to catalyst age, to a certain extent, to keep NOx emission under permissible limits. However, this would lead to an increase in Diesel Exhaust Fluid (DEF or AdBlue, a mixture of 32.5% urea and 67.5% distilled water) consumption, and the NOx emissions will go beyond permissible limits once the catalyst degrades beyond a certain level. This can have severe environmental and financial implications. A drastic example of this from recent times was when Cummins Inc. had to recall 500,000 medium-and heavy-duty trucks in 2018, because the SCR catalysts degraded faster than expected, leading to excess NOx emissions [3]. Therefore, it is very important for diesel-engine vehicles to be equipped with effective on-board diagnostics (OBD), which can monitor and report catalyst degradation before it degrades beyond acceptable levels. The objective of this work is to develop effective model-based OBD algorithm(s) to detect SCR catalyst degradation, which can work under real-world on-road conditions. This chapter starts with a brief description of aftertreatment components, followed by a summary of EPA's OBD regulations. Then, the motivation, objective and key challenges for this work will be discussed. The chapter will conclude with an overview of the rest of the document.

1.1 Diesel engine aftertreatment system

A schematic of the diesel-engine aftertreatment system is shown in Figure 1.1. The following subsections (text for DOC, DPF, and SCR is borrowed from the author's M.S. thesis [4]) will summarize important functions of the components of the diesel engine aftertreatment system.

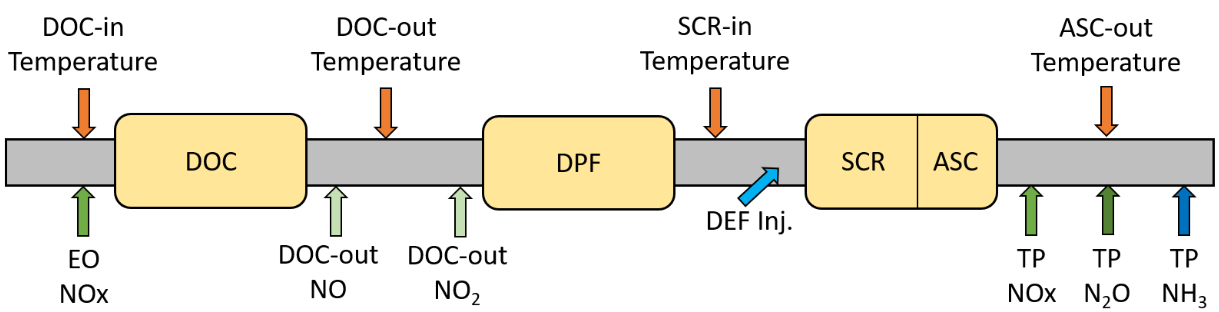

Figure 1.1. Schematic of the diesel engine aftertreatment system. Exhaust gas flows from left to right.

1.1.1 Diesel Oxidation Catalyst (DOC)

As quoted from [5], the DOC has 3 major functions:

1. "Oxidation of CO to CO_2.

2. Oxidation of unburnt and partially burnt hydrocarbons.

3. Oxidation of NO to NO_2". This helps to bring the NO/NO_2 ratio in NOx from about 9:1 to 1:1. This function is important for good SCR performance which relies on almost equal quantities of NO and NO_2 in NOx [5].

As a sub-function, the heat generated from the DOC due to oxidation helps in DPF regeneration [5].

1.1.2 Diesel Particulate Filter (DPF)

DPF is a soot filter responsible to trap PM in the exhaust stream. It needs periodic cleaning of the soot which is called DPF regeneration. Depending on the heat source to burn off the soot particles, the regeneration is called active or passive. Active regeneration involves controlled heating whereas passive relies on high exhaust gas temperature and heat from DOC oxidation reactions [5].

1.1.3 Urea - Selective Catalytic Reduction (SCR) system

The Urea-SCR system employs NH_3 to reduce NOx into molecular nitrogen (N_2) and water (H_2O). DEF is injected into the system as a source of NH_3 because it is difficult and dangerous to store NH_3.

Urea gets converted into NH_3 through thermolysis and hydrolysis because of high exhaust gas temperature. The catalyst adsorbs some NH_3. Adsorbed NH_3 is involved in oxidation, desorption and NOx reduction. Unadsorbed and desorbed NH_3 constitute NH_3 slip which goes out of the tailpipe with unreacted NOx. The schematic representation of this process along with the corresponding reactions (according to the Eley Rideal mechanism) is shown in Figure 1.2.

1.1.4 Ammonia Slip Catalyst (ASC)

Very high urea injection leads to excessive SCR-out NH_3 slip and too little leads to excessive NOx emissions. Hence, it is challenging to simultaneously achieve low SCR-out NH_3 and low NOx. The Ammonia Slip Catalyst oxidizes SCR-out NH_3 into harmless N_2.

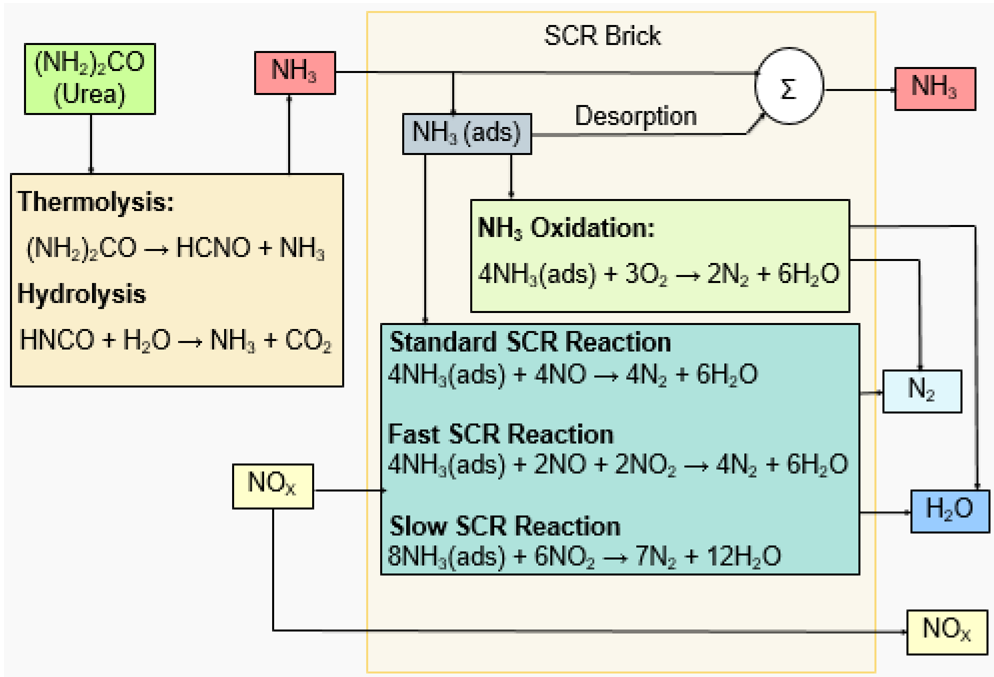

Figure 1.2. Schematic representation of SCR reactions, taken from [4].

Therefore, an SCR+ASC system allows the urea-dosing controller to inject higher amounts of urea than an SCR-only system, leading to better deNOx with low tailpipe NH_3 slip. However, the ASC is not perfect and it oxidizes some SCR-out NH_3 into NO and N_2O. Therefore, the urea-dosing controller still needs to ensure optimum urea injection as excessive SCR-out NH_3 can contribute to increase in tailpipe NO and N_2O, due to the ASC.

1.2 Important OBD Terminology

1. **Degreened (DG) catalyst:** A fresh catalyst that has not aged at all is called degreened catalyst.

2. **End-of-useful-life (EUL) catalyst:** In the context of this work, a catalyst that has degraded to the least-acceptable performance by EPA/CARB is called an EUL catalyst. So for this work, DG and EUL will be considered the extreme ends of the degradation spectrum with no degradation and maximum degradation, respectively.

3. **Enable conditions or Monitoring conditions:** Unlike a controller, OBD doesn't run at all times. The operating conditions when OBD is activated are called enable or monitoring conditions.

4. **False positive:** False indication of malfunctions is called false positive. For example, reporting a degreened catalyst as aged.

5. **False negative:** False passing of a malfunctioning part is called false negative. For example, reporting an aged catalyst as degreened.

6. **Driving cycle:** As per sections 1968.2 [6] and 1971.1 [7], title 13 of California Code of Regulations (CCR), this is defined as: "A trip that meets any of the four conditions below:

   (a) Begins with engine start and ends with engine shutoff;

   (b) Begins with engine start and ends after four hours of continuous engine-on operation;

   (c) Begins at the end of the previous four hours of continuous engine-on operation and ends after four hours of continuous engine-on operation; or

   (d) Begins at the end of the previous four hours of continuous engine-on operation and ends with engine shutoff."

7. **IUMPR (In-use monitor performance ratio):** This is defined in [6], [7] as the ratio of:

   (a) Numerator: The number of times OBD has been activated or the enable conditions have been encountered during vehicle operation. This is an integer and can not be incremented by more than one during a single driving cycle.

   (b) Denominator: The number of drive cycles.

   Both numerator and denominator can be increased by more than one under very specific ambient and vehicle operating conditions, which won't be listed here for brevity. Sections 1968.2 [6] and 1971.2 [7] of CCR can be referred for more details.

1.3 Types of OBD

SCR OBD can be classified as follows:

1. Based on intrusion:

   (a) **Intrusive Diagnostics:** A diagnostic algorithm is called intrusive if it overrides the urea-dosing controller with a diagnostics-oriented dosing routine to monitor catalyst health. In other words, intrusive diagnostics and urea-dosing controller can not run simultaneously. The controller is turned off when diagnostics is running and vice versa. Controller's urea dosing profile is designed to maximize SCR's performance (or minimize emissions), whereas an intrusive diagnostic algorithm's urea dosing profile is designed to excite the system to reveal its age. Therefore, emissions may increase when intrusion is active.

   (b) **Non-intrusive Diagnostics:** A non-intrusive diagnostics algorithm monitors catalyst health without interfering with the controller and hence, does not affect emissions.

2. Based on OBD goal:

   (a) **Binary Classification:** CARB/EPA require OBD to illuminate the malfunction indicator light (MIL) and store a fault code when catalyst degrades enough to cause tailpipe NOx emissions to exceed acceptable limits (quantified based on drive-cycle tests defined by CARB/EPA) [6] [7]. Such diagnostic algorithm only needs to classify the catalyst as good (MIL off) or bad (MIL on). So, it won't be able to distinguish between a degreened and an aged catalyst, which still doesn't cause the emissions to exceed the specified threshold.

   (b) **Distinguish multiple aging levels:** Although binary classification is sufficient to meet EPA/CARB requirements, it is important to distinguish between several levels of degradation among both "good" and "bad" catalysts in order to monitor the rate of catalyst degradation. This category needs more advanced algorithm(s) that can report several levels of degradation. Both OBD goals are visually demonstrated in Figure 1.3.

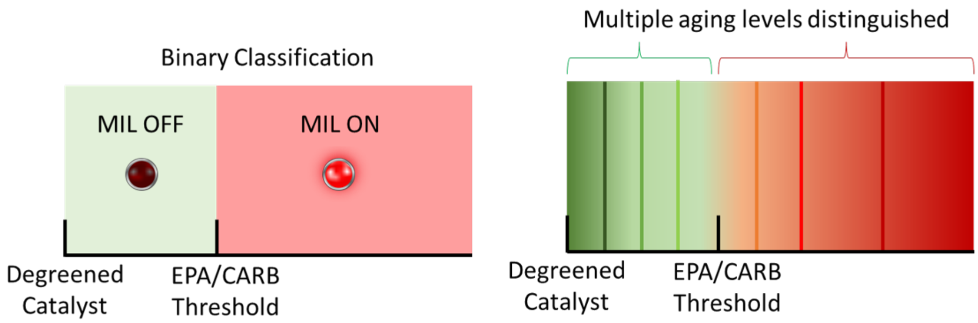

Figure 1.3. Two categories of OBD goals: 1) Binary classification; 2) Distinguishing multiple aging levels.

1.4 EPA/CARB Regulations for OBD

Since OBD performance has very significant environmental impact, EPA and CARB have specific OBD requirements for SCR. Here is the timeline of CARB OBD regulations in US, as quoted from [8]:

1. "OBD I: The first OBD regulation in the United States, which required manufacturers to monitor some of the emission control components on all 1991 and newer vehicles sold in California.

2. OBD II: This more rigorous OBD regulation started to be phased-in in 1994. Since 1996, its implementation has been required on all new gasoline and alternate fuel passenger cars and trucks sold in California. All 1997 and newer diesel fueled passenger cars and trucks are also required to meet OBD II requirements."

Quoted from [9]: "Following the introduction of OBD requirements in California, OBD regulations were also adopted by the US EPA. The following have been the most important steps in the development of federal OBD requirements:

1. Beginning with the 1994 model year, the EPA has required OBD systems on light-duty vehicles (LDVs) and light-duty trucks (LDTs).

2. Since 2005, OBD systems became mandatory for heavy-duty vehicles and engines up to 14,000 lbs Gross Vehicle Weight Rating (GVWR).

3. In December 2008, EPA finalized OBD regulations for 2010 and later heavy-duty engines used in highway vehicles over 14,000 lbs GVWR and made changes to the OBD requirements for heavy-duty applications up to 14,000 lbs GVWR to align them with requirements for applications over 14,000 lbs GVWR."

Although several engine and aftertreatment components fall under the scope of these regulations, we will focus on the ones for SCR.

1.4.1 SCR Faults to Monitor

Several faults can affect the performance of SCR-ASC system, resulting in lower deNOx efficiency or excess emissions. Therefore, EPA/CARB require vehicle manufacturers to monitor the following as part of OBD for the SCR-ASC system [10], [6], [7]:

1. Faults with urea-dosing system such as:
    - Faults with the injector or the pump.
    - Empty urea tank.
    - Urea tank filled with something other than DEF.
2. Faults with urea-dosing control, such as [6], [7]:
    - Control doesn't start within the expected time.
    - Fault with feedback causes open-loop operation.
    - Emission targets can't be reached even with the controller saturated at maximum urea dosing.
3. Catalyst degradation resulting in increased emissions.

1.4.2 Regulations

Here are the key OBD regulations for SCR from CARB. EPA regulations are very similar, with some slight differences [9], which are not presented here. Also, since the focus of this work is catalyst degradation, only the regulations relevant to that are presented:

1. **Malfunction criterion:** For 2016 and subsequent model year vehicles, OBD must illuminate the MIL if catalyst degrades enough to exceed acceptable NOx emissions (during an SET (Supplemental Emission Test) or FTP (Federal Test Procedure)) for a degreened catalyst by 0.2 gm/bhp-hr.

2. **Enable conditions:** The enable or monitoring conditions must be designed such that:

   (a) false positives and false negatives are minimized;

   (b) OBD must be activated at least once during FTP;

   (c) the enable conditions must “reasonably be expected to be encountered in normal vehicle operation and use" [6], [7].

   (d) the IUMPR should not be less than 0.3 for 2024 and subsequent model year vehicles (there are some subtle differences between the IUMPR requirements for model year 2024-2027 and model year 2028 and subsequent year vehicles, but those are not detailed here). For heavy-duty vehicles, CARB estimates that an IUMPR is approximately equivalent to around 500 miles or 10 hours per monitoring event [11].

3. **Intrusive diagnostics:** The most recent CARB regulations dictate that intrusive diagnostics will only be allowed if it has minimal impact on tailpipe emissions. If the impact on emissions is significant, then intrusion is only allowed when the MIL is already on as a result of non-intrusive monitoring.

1.5 Current Research

1.5.1 Motivation

Here is a summary of some key gaps identified from the literature:

1. **On-road vs test-cell/simulations:** EPA and CARB have rigorous and effective test-cell routines to certify vehicles. However, their findings, shown in Figure 1.4, from logging over a month's on-road OBD data from 68 trucks show that there is significant discrepancy between real-world and test-cell emissions [11]–[13]. This challenge is also reflected in academic literature, where most aging models and diagnostic strategies have only been demonstrated in simulation [14]–[16]. A few that have demonstrated hardware results have used a catalyst that was aged in a controlled environment through accelerated hydrothermal aging. Although this is a good simulation, it is still not a perfect replication of on-road aging [17].

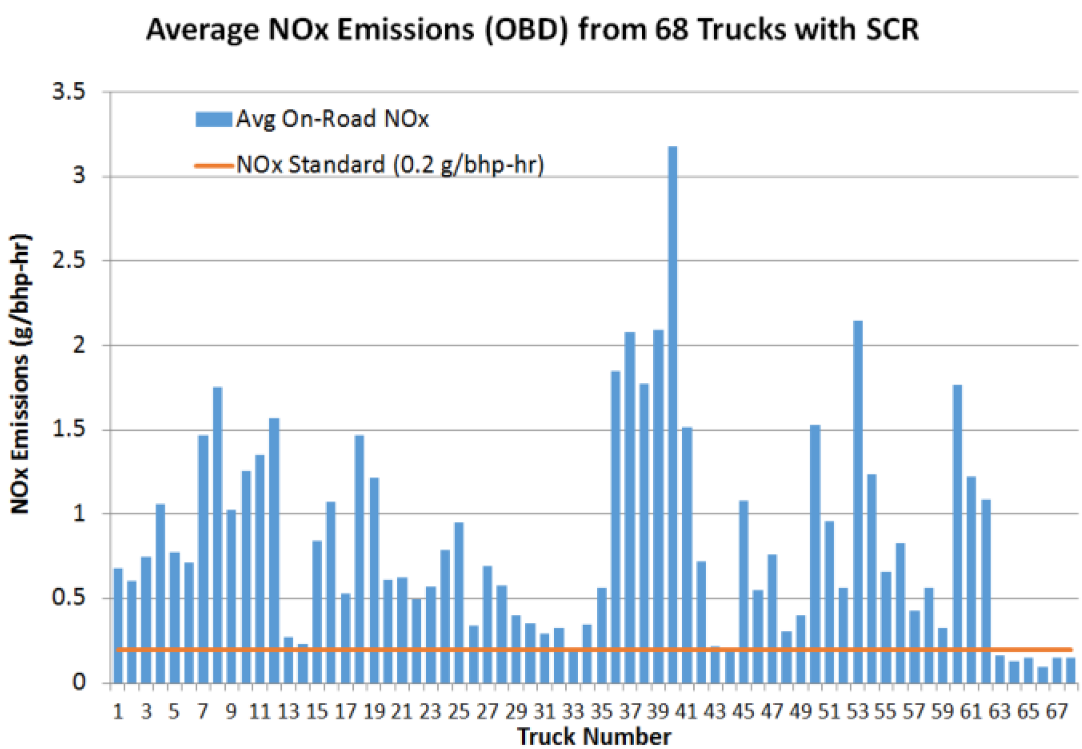

Figure 1.4. On-road emissions data collected by CARB, taken from [11].

2. **Intrusive vs non-intrusive**: There are patents from industry that have proposed diagnostic algorithms designed to work under on-road conditions. However, most of these algorithms are intrusive [18]–[20]. Since the most recent regulations contain stringent restrictions on intrusive diagnostics, it is important to develop non-intrusive methods that can work under on-road conditions.

3. **Commercial aftertreatment system:** To the best of our knowledge, most existing literature has not considered the presence of ASC or absence of tailpipe NH_3 sensors in commercial aftertreatment system. Therefore, diagnostic algorithms that can monitor the SCR-ASC system using a commercial tailpipe NOx sensor must be developed.

1.5.2 Objective

The objective of this work is to contribute towards filling the aforementioned gaps by developing model-based non-intrusive diagnostics for SCR-ASC that can work with commercial NOx sensors, and demonstrate the results on real-world on-road truck data.

In this work, the focus would be to monitor catalyst age assuming that the dosing system, controller, and sensors do not have any fault. This is summarized in Figure 1.5.

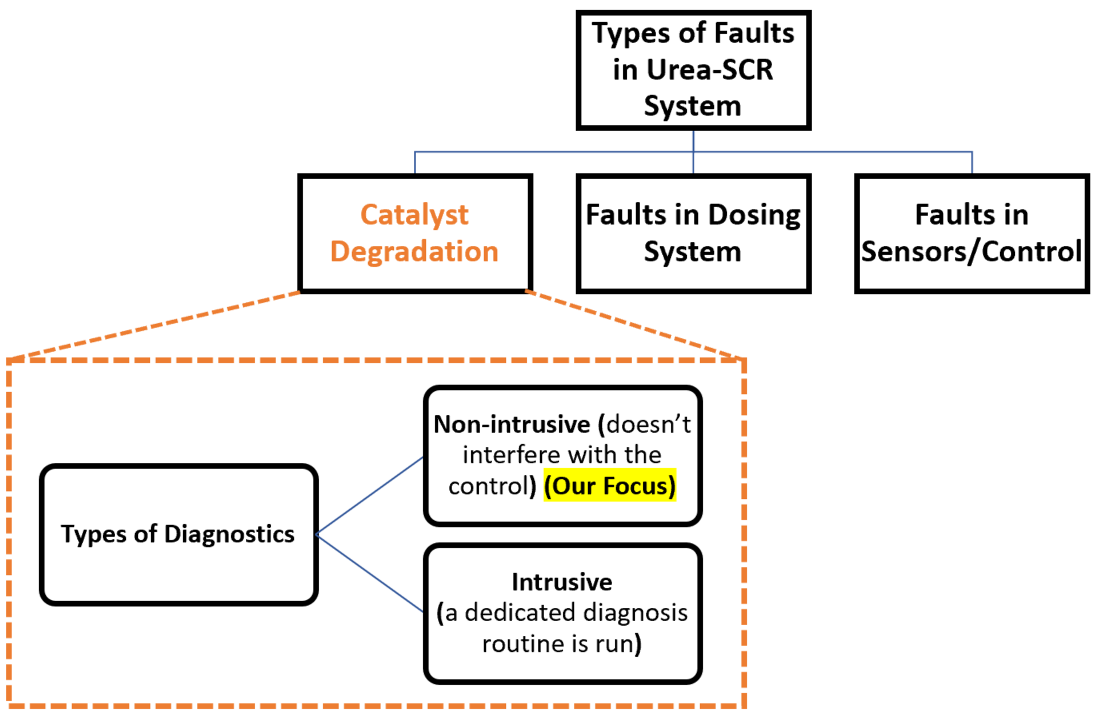

Figure 1.5. Summary of the focus of this work.

1.5.3 Approach

Cummins Inc. has generously provided on-road data for four trucks, and test-cell data for cold FTP, hot FTP, and RMC cycles for degreened (DG) and end-of-useful-life (EUL) catalysts. After thoroughly studying the data, the first task in the project was to develop diagnostics-oriented aging models for SCR-ASC using test-cell data. Once the modeling results were satisfactory for test-cell data, the model was calibrated and validated on truck data. Modeling work was followed by development of two model-based OBD methods with well-defined enable conditions and diagnostic metrics. The first OBD method does a binary classification at each time sample by labeling it as either degreened or EUL. This OBD method was first applied to test-cell data with perfect measurements. After achieving satisfactory performance with perfect measurements, the OBD's robustness was tested by simulating worst-case NOx sensor cross-sensitivity and noise in test-cell data. After robustness analysis, the OBD algorithm was applied to truck data to demonstrate that the method can report relative aging levels of the SCR-ASC system on trucks with commercial NOx sensors. Unlike the first method, the second OBD method assigns a non-binary value to each sample point, which is proportional to the probability of that point belonging to a degreened or an EUL catalyst. This method uses a stochastic version of the proposed SCR-ASC model, which is derived using a simplified version of the Bayesian approach for model calibration. This method results in a much better IUMPR than the first one and can still correctly classify the degreened and EUL catalysts for all three cycles in the test-cell data.

Based on this approach, the key contributions of this work are:

1. Observations about the effects of real-world catalyst degradation on tailpipe NOx, NH_3, and N_2O are presented based on data from test-cell experiments on a degreened and an aged catalyst, which degraded to end-of-useful-life (EUL) on the road.

2. Insights from the test-cell data and observations from on-road truck data are then used to describe challenges with designing model-based on-board diagnostics that could work for the aftertreatment system on commercial trucks.

3. A novel diagnostics-oriented SCR-ASC model is presented, which is shown to work reasonably well, for the purpose of model-based OBD, for both test-cell data and on-road data from commercial trucks. The model is calibrated on the hot FTP cycle and validated on the cold FTP and RMC cycles in test-cell data. After slight re-calibration and combining with a simple model for NOx sensor's cross-sensitivity to NH_3, the model works reasonably well for the purpose of model-based OBD on the truck data as well.

4. Two model-based OBD methods are presented with model-based enable conditions designed to detect operating conditions suitable for diagnostics, while minimizing false positives and false negatives due to model uncertainties, NOx sensor's cross-sensitivity to NH_3, measurement noise, and uncertainty in initial NH_3 storage.

5. The first OBD method does a binary classification at each time sample by labeling it as either degreened or EUL. This method was applied to both test-cell data and real-world truck data with commercial NOx sensors. The method is shown to be robust to cross-sensitivity, measurement noise, and uncertainty in initial NH_3 storage but very few sample points were selected from the test-cell data after applying the enable conditions. This demonstrated the challenge with designing model-based enable conditions that are robust to false positives and false negatives but still lead to good IUMPR.

6. Unlike the first method, the second OBD method assigns a non-binary value to each sample point, which is proportional to the probability of that point belonging to a degreened or an EUL catalyst. This method uses a stochastic version of the proposed SCR-ASC model, which is derived using a simplified version of the Bayesian approach for model calibration. This method was applied to the test-cell data. Results show that it has a much better IUMPR than the first method and can still correctly classify the degreened and EUL catalysts for all three cycles in the test-cell data. Similar to the first method, detailed enable conditions are defined for this method as well. The enable

conditions are shown to make the method robust to NOx sensor's cross-sensitivity to NH_3 and uncertainty in initial NH_3 storage.

1.6 Structure of the document

This document has six chapters. Chapter 2 reviews existing catalyst aging mechanisms, models and OBD methods in literature. The first step in the project after receiving the data was to carefully analyze and observe it. Chapter 3 contains details about the data, along with these observations. This lays the groundwork for Chapter 4, which discusses the SCR-ASC model in detail with calibration and validation results from test-cell and truck data. Chapter 5 presents the two model-based diagnostic algorithms, with clearly defined enable conditions and diagnostic metrics, and results on both test-cell and truck data. Chapter 6 concludes the document and proposes the directions for future work.

2. LITERATURE REVIEW: SCR-ASC AGING MECHANISMS, MODELS AND EXISTING OBD STRATEGIES

2.1 SCR Aging Mechanisms and Effects

Following are some key aging mechanisms and their effects reported in literature:

1. Hydothermal aging leads to irreversible structural and chemical changes. Several publications such as [21], [22] report reduction in NH_3 storage capacity as a result of hydothermal aging. Another observation in [21] was that in-oven aging doesn't change the overall NOx conversion efficiency but changes the axial NH_3 storage and NO, NO_2 and NH_3 concentration profiles.

2. Sulphur or Phosphorous poisoning and injected urea-related deposits block active sites for NH_3 adsorption, causing reduced NH_3 storage capacity [22].

3. Trace levels of Pt volatize from DOC and deposit on the front section of SCR [23], [24]. This leads to increase in NH_3 oxidation, which reduces the NH_3 available for deNOx.

4. There are aging mechanisms specific to catalyst formulation, such as dealumination of the zeolite for Fe-zeolite [23] or sintering of anatase (higher surface area/mass) TiO_2 to form rutile (lower surface area/mass) TiO_2 in $V_2O_5/WO_3/TiO_2$ [25], that lead to reduction in surface area for NH_3 adsorption, resulting in reduced storage capacity. Therefore, robustness to aging depends on catalyst formulation. It is reported in [26], [27] that state-of-the-art Cu-SSZ 13 is more robust to hydrothermal aging than Cu-Zeolite and Fe-Zeolite.

Since it takes several years for the catalyst to age on-road, electrical heating in an oven and accelerated on-engine aging are used to prepare aged catalysts in labs for research studies. Oven-heating causes uniform heating across catalyst length and cross-section. On-engine dynamometer accelerated aging causes the front part of the catalyst to degrade more than the rear [22]. This may not necessarily be due to front part's exposure to slightly higher temperature [23]. Primary reason could be higher exposure to Sulphur poisoning, urea, and Pt deposits [22]. On-road aging is found to cause non-uniform aging across catalyst length and cross-section due to non-uniform exposure to exotherms, urea, Sulphur and other poisoning components [28].

2.2 SCR Aging Models

A very popular approach to capture catalyst degradation in control-oriented models is changing the value of certain parameters. This theme is common across different types of control-oriented models. For example, [14] and [15] use the four-state model from [29], [30]; [31], [32], and [33] (three-cell model) use the three-state CSTR model from [34]; and [16] (two-cell model) uses the three-state model from [35], [29]. But they all model aging by multiplying some model parameter by an "aging factor", which decreases from 1 to, say 0.5, as the catalyst degrades. The aging factor is used to scale catalyst's NH_3 storage capacity in [14], [15], [31], and [16]. In [33], it is used to scale the NH_3 adsorption reaction rate, and scales the NOx reduction rate in [32]. It should be noted that none of these aging models have been validated on an actual aged catalyst yet.

Instead of capturing age through a single parameter, an alternate approach is to perform separate calibration for degreened and aged catalysts as done in [21]. This resulted in different values for all parameters across degreened and aged catalysts.

Recent publications from Cummins Inc. on high-fidelity aging models, such as [26], [27], report that there are various types of active sites, where NH_3 storage happens: Bronsted acid sites, Cu sites and physisorbed NH3 sites. It is recommended in [27] that at least two sites should be used in aging models. These are called S1 and S2 in [27]. The following observations about the impact of aging on S1 and S2 were reported in [26] and [27]:

1. Number density of active sites in S1 decreases and in S2 increases until mild aging occurs. Then both decrease with severe aging. Overall number density of active sites remains constant until some aging occurs and then decreases with severe aging.

2. Adsorption and desorption reaction rates don't change until mild aging occurs. They might change with severe aging.

3. Standard and fast reaction rates were almost unaffected with aging in [27] showing the catalyst's robustness.

4. Standard SCR reaction mainly happens on S1 for fresh catalyst and on S2 for aged.

5. NH_3 oxidation increases with aging at S1.

2.3 Non-intrusive OBD

2.3.1 "Aging Factor" Estimation

The common idea among [14], [15], [31], and [16] for diagnosing catalyst degradation is to design an observer to estimate the aforementioned aging factor. Lyapunov-based nonlinear observers are presented in [14] and [15], whereas [31] and [16] have used the Extended Kalman Filter (EKF) and Unscented Kalman Filter (UKF), respectively. The observers in all four papers rely on accurate tailpipe NOx and NH_3 feedback, except [15], who have presented an additional observer that can work with just tailpipe NOx feedback. Simulation results for all the observers show good performance for aging factor estimation.

2.3.2 Benchmark Approach

Reference [17] is the most promising paper so far as it presents an OBD method that considers the presence of ASC, works with the commercial tailpipe NOx sensor, and is demonstrated for real-world driving conditions. A two-cell SCR model and a single-cell ASC model are calibrated individually using SCR-in, SCR-out, and ASC-out measurements. Both SCR and ASC models are DAE-type models, except that a discretized equation is used to calculate NH_3 storage and the equations for tailpipe NOx and NH_3 are slightly different from the common CSTR equations. Each reaction is calibrated individually using steady-state tests. The SCR-ASC model is calibrated for both fresh and aged catalysts. The fresh and aged catalyst models are used to calculate the worst acceptable performance (highest possible value that could be reported by tailpipe NOx sensor for a good catalyst) and the best unacceptable performance (lowest possible value that could be reported by tailpipe NOx sensor for an aged catalyst), respectively at each operating point. OBD is enabled only when the tailpipe NOx sensor value for the best unacceptable performance is more than that for the worst acceptable performance by a threshold. The OBD can only do binary classification. It can not report multiple aging levels. The OBD is shown to work with reasonable IUMPR for New European Driving Cycle (NEDC) and about ten other driving patterns which customers actually drive. The workflow in this paper is very similar to our project. However, an additional challenge for us is that we don't have access to SCR-out measurements. Also, the aged catalyst in this work was prepared via accelerated aging in an electrical furnace, whereas the aged catalyst in our work degraded on the road.

2.3.3 Other non-intrusive approaches

A 2010 patent from Delphi [18] proposed the idea of adapting the reference to the urea-dosing control and detecting fault if the reference goes out of an acceptable range. Such method could work with the fault-tolerant controllers proposed in [14] and [31], which used both tailpipe NH_3 and NOx signals. However, the controller proposed in [18] uses only tailpipe NH_3 measurements.

Reference [36] implemented the idea of comparing the outputs of a fixed-parameter model to the actual measurements for OBD of a Lean NOx Trap (LNT). In this work, we will explore this method for SCR OBD.

A classification method that is a combination of grid search (GS), particle swarm optimization (PSO) and support vector machine (SVM) called the GS-PSO-SVM algorithm is used to detect catalyst age in [32]. Simulation runs with multiple aging vectors for the European Transient Cycle (ETC) are used to train and test the algorithm. The first half of ETC is used for training and the second for testing. Simulation results show that the algorithm can achieve 92% classification accuracy to detect aging accuracy during ETC.

2.4 Intrusive OBD

Due to the restrictions imposed by government agencies, and their undesirable impact on emissions, the literature on intrusive OBD is limited. The authors for reference [18] have proposed perturbing the control reference under steady-state conditions and monitoring the catalyst based on NH_3 slip response. Another idea is to infer catalyst degradation by comparing upstream and downstream NOx sensor measurements [19], [20].

3. DATA

Cummins Inc. has kindly provided test-cell and truck data to support this work. This chapter will discuss the details of these data-sets, along with some observations to set the base for the modeling work presented in the following chapters.

3.1 Test-cell Data

The test-cell data consists of six data-sets. These data-sets contain emissions data for a degreened and an aged aftertreatment system, for three drive cycles: 1) Cold Federal Test Procedure (cFTP), 2) Hot Federal Test Procedure (hFTP), and 3) Ramped Mode Cycle (RMC) Supplemental Emissions Test (SET). Each data-set contains the following measurements:

Engine torque

Engine speed

Diesel Exhaust Fluid (DEF) injection

Engine-out (EO) NOx

DOC-out NO, NO_2

Tailpipe (TP) NOx, NH_3, N_2O

DOC-in, DOC-out, SCR-in, ASC-out temperature

Exhaust flow rate

The exhaust layout, with the sensors available in test-cell, is shown in Figure 3.1. Table 3.1 shows the dimensions of the exhaust components.

Table 3.1. Dimensions of the key aftertreatment components in Cummins aftertreatment system used in this work.

	DOC	DPF	SCR	ASC
Diameter (in)	13	13	13	13
Length (in)	4	7	9.5	2

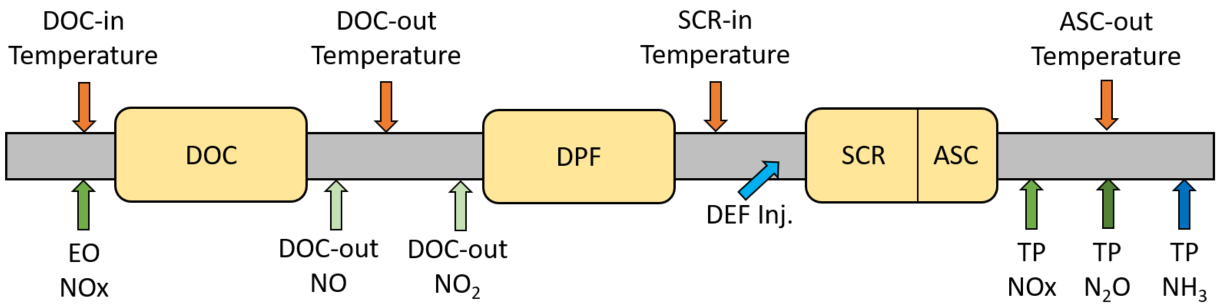

Figure 3.1. Exhaust layout with the sensors available in test-cell

3.1.1 Comparing operating conditions across drive cycles

Some observations regarding the operating conditions across drive cycles are as follows:

1. **Engine-out NOx and Exhaust Flow Rate:** The FTP cycles have transient changes in engine torque and speed, which lead to transient engine-out NOx and exhaust flow rate. On the other hand, RMC-SET has step changes in engine torque, speed, engine-out NOx, and exhaust flow rate. Also, both cFTP and hFTP have almost identical. engine-out NOx and flow rate throughout the cycle. Engine torque, speed, engine-out NOx, and exhaust flow rate for all three cycles are shown in Figure 3.2.

2. **Exhaust-gas temperature** The exhaust-gas temperature during the RMC-SET is higher than that for the FTP cycles. Among the FTP cycles, hot FTP has higher temperature than cold FTP during the first 600 seconds as shown in Figure 3.3.

3. **Urea Dosing** Figure 3.4 shows four phases of DEF dosing and ANR (Ammonia to NOx Ratio) vs time for the three cycles. It can be observed that during all four phases, the ANR stays steady for RMC-SET and is very transient for cFTP and hFTP. During phase 1, which is from $t = 0$ to $t = 424$ sec, there is zero DEF dosing for cFTP. In the next phase from $t = 424$ to $t = 520$ sec, cFTP has higher dosing than hFTP. In the third phase from $t = 520$ to $t = 600$ sec, a distinct step DEF dosing profile is observed for both cFTP and hFTP at different times. In the last phase beyond $t = 600$ sec, both cFTP and hFTP have almost the same dosing profile.

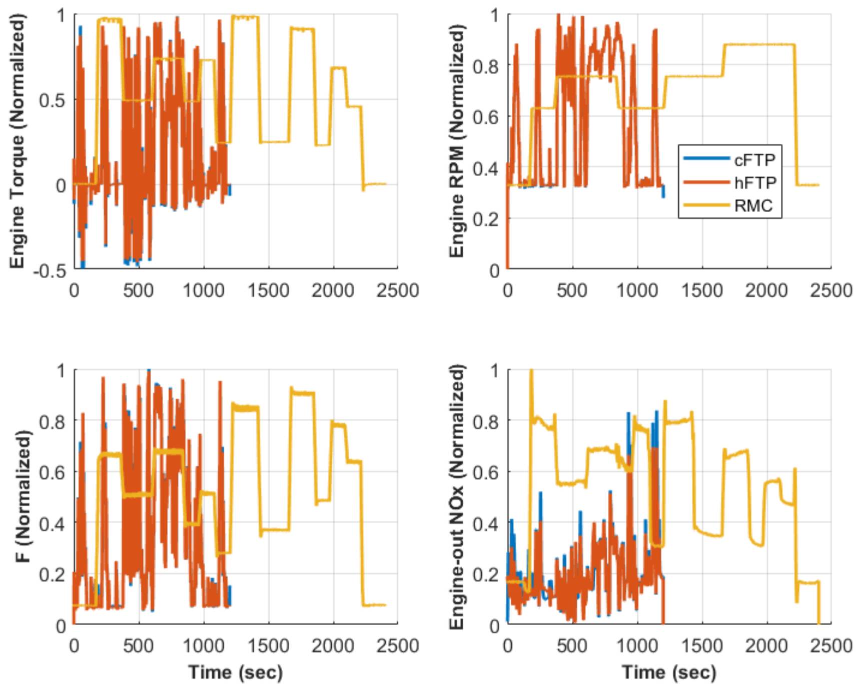

Figure 3.2. Engine torque, speed, engine-out NOx, and exhaust flow rate F for the three drive cycles in test-cell data. Each quantity was normalized by dividing by the maximum value across the three cycles.

3.1.2 Aging Signatures

The aged catalyst in the test-cell data was assumed to be degraded to EUL level on the road. As shown in Figure 3.5, both degreened and EUL aftertreatment systems were operated under the exact same operating conditions for each cycle. Therefore, the difference in DOC-out and tailpipe (TP) signals can be attributed to aging. And these differences in DOC-out and tailpipe signals due to aging are called aging signatures.

Following aging signatures were observed in the test-cell data:

1. **DOC-out NO, NO_2:** Engine-out NOx is rich in NO, leading to an NO_2/NO ratio of less than 1. DOC is responsible for oxidizing NO to NO_2. Aftertreatment aging leads to a decline in DOC performance, which decreases the DOC-out NO_2/NO ratio. This was clearly observed for all three cycles in the test-cell data as shown in Figure 3.6.

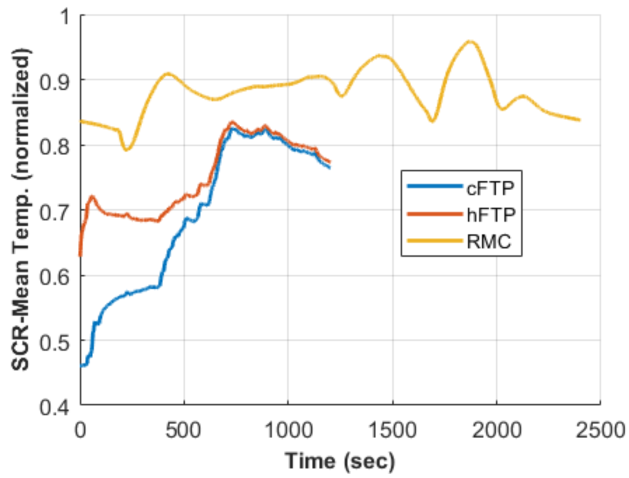

Figure 3.3. SCR mean temperature for the three drive cycles in test-cell data. Temperature was normalized by dividing by its maximum value across the three cycles.

2. **Tailpipe N_2O:** Figure 3.7 shows tailpipe N_2O for the three cycles. Aged catalyst produced significantly higher N_2O than degreened for cFTP and hFTP, from around 600 sec to 1000 sec. This could be because of higher SCR-out NH_3 slip from the aged catalyst, during those times, that gets converted to TP N_2O by the ASC. The RMC-SET shows the opposite trend as the TP N_2O for the degreened catalyst is higher. The reason for this is not entirely clear but it should be noted that TP N_2O in this case is very low (around 20 ppm), and hence the difference between degreened and aged catalyst is also very small.

3. **Tailpipe NH_3:** Tailpipe NH_3 slip for all three cycles was very low because of the presence of ASC. As shown in Figure 3.8, only hFTP showed slightly higher NH_3 slip (around 5 ppm) for the aged catalyst.

4. **Tailpipe NOx:** Aging is expected to cause a decline in SCR performance, leading to lower deNOx or higher tailpipe NOx. However, the test-cell data showed that TP NOx for the aged catalyst may not be higher than the degreened catalyst at all times. Only

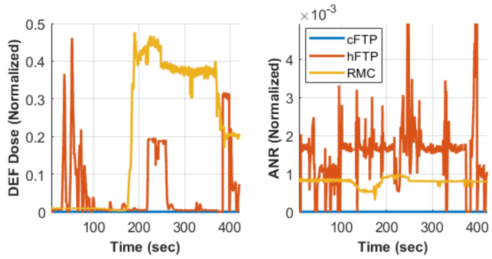

(a) Phase 1: $u_{\text{DEF,cFTP}} = 0$

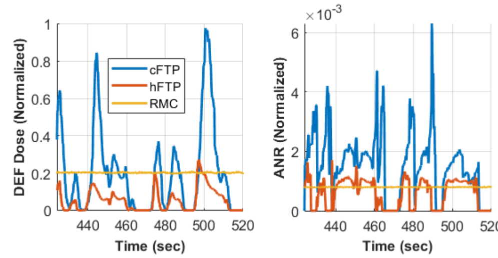

(b) Phase 2: $u_{\text{DEF,cFTP}} > u_{\text{DEF,hFTP}}$

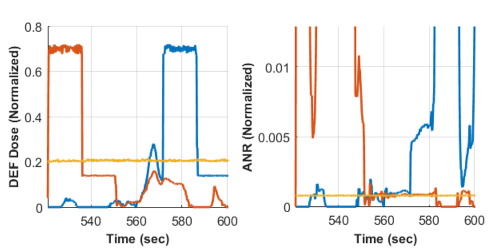

(c) Phase 3: Distinct dosing routine for cFTP and hFTP

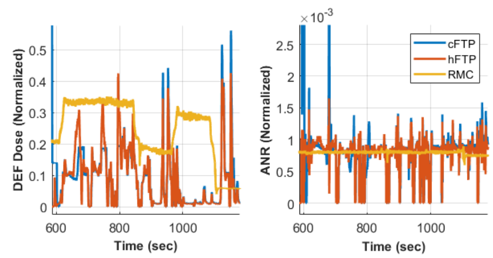

(d) Phase 4: $u_{\text{DEF,cFTP}} = u_{\text{DEF,hFTP}}$

Figure 3.4. DEF dosing and ANR for the three cycles, split into four phases. Both DEF dosing and ANR were normalized by dividing by the maximum value across the three cycles.

five segments of data, shown in Figure 3.9, across all three cycles showed reasonably higher (>10 ppm) tailpipe NOx for the aged catalyst.

Following are the key take-aways from these observations:

1. The effect of aging on DOC performance is evident from the smaller DOC-out NO_2/NO ratio for the aged catalyst across all three cycles.

2. The decline in SCR performance due to aging is expected to result in an increase in TP NOx and NH_3 slip. However, due to the presence of ASC, TP NH_3 stays low at all times and the increase in SCR-out NH_3 slip manifests through an increase in TP N_2O.

3. Only five aging signatures in TP NOx, i.e. reasonably higher (>10 ppm) tailpipe NOx for the EUL catalyst than the degreened catalyst, across the three drive cycles demon-

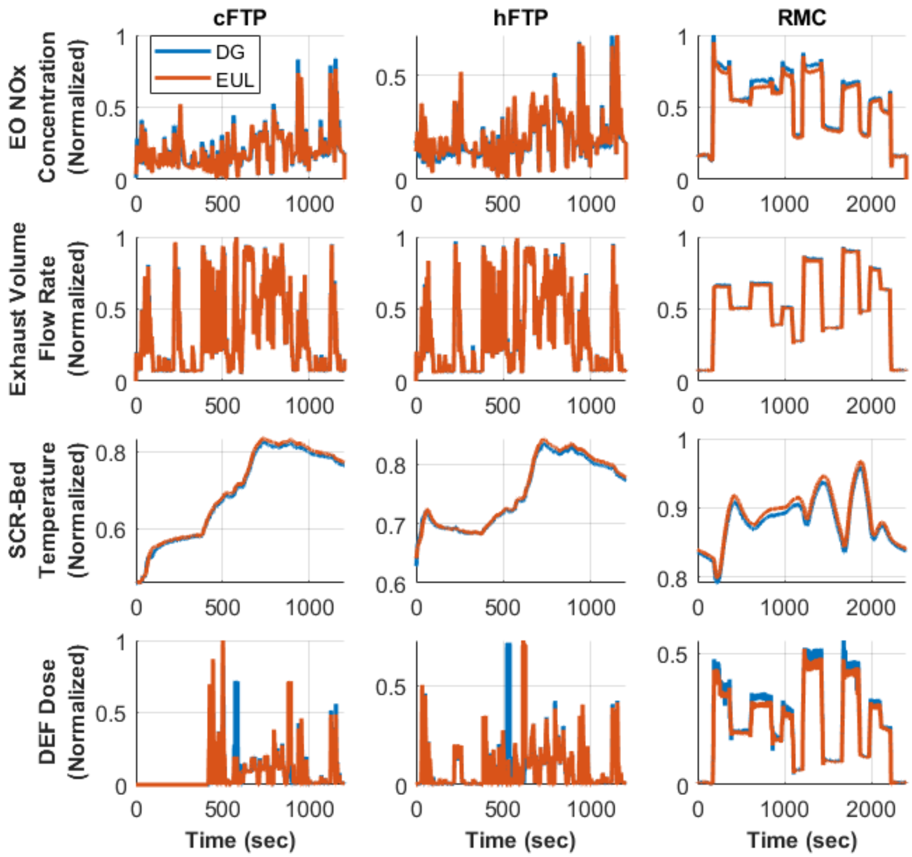

Figure 3.5. Input signals for both degreened and EUL catalyst for the three drive cycles.

strate that not all operating conditions will reveal the catalyst age. This establishes the importance of picking the right operating conditions to enable the diagnostics algorithm. This will be elaborated further in Chapter 6.

4. The RMC cycle presents a very interesting case where the effect of aging is very clear in DOC-out NO, NO_2, but doesn't show up in the tailpipe signals. This again shows that there are operating conditions where it may not be possible to distinguish degreened and aged catalysts based on tailpipe signals alone.

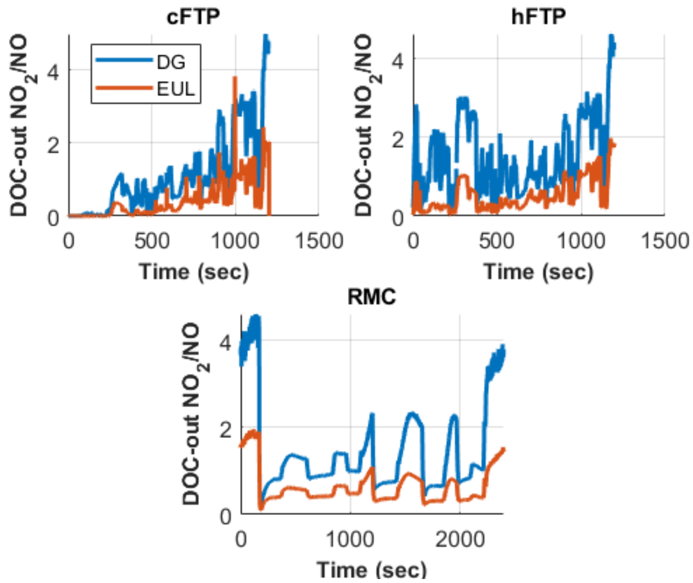

Figure 3.6. DOC-out NO_2/NO ratio for both degreened and EUL catalysts for the three drive cycles.

3.2 Truck Data

The truck data consists of four "day files". Each day file has on-road data collected using commercial on-board sensors during 24 hours-drive of a truck. The four day files are for four different trucks with 271k, 422k, 484k, and 711k miles on them. Each day file contains several measurements such as:

Engine torque, Engine speed

Truck speed

Cruise-control information

DPF-regeneration information

Diesel Exhaust Fluid (DEF) injection

Engine-out NOx

Tailpipe NOx

DOC-in, SCR-in, ASC-out temperature

Exhaust flow rate

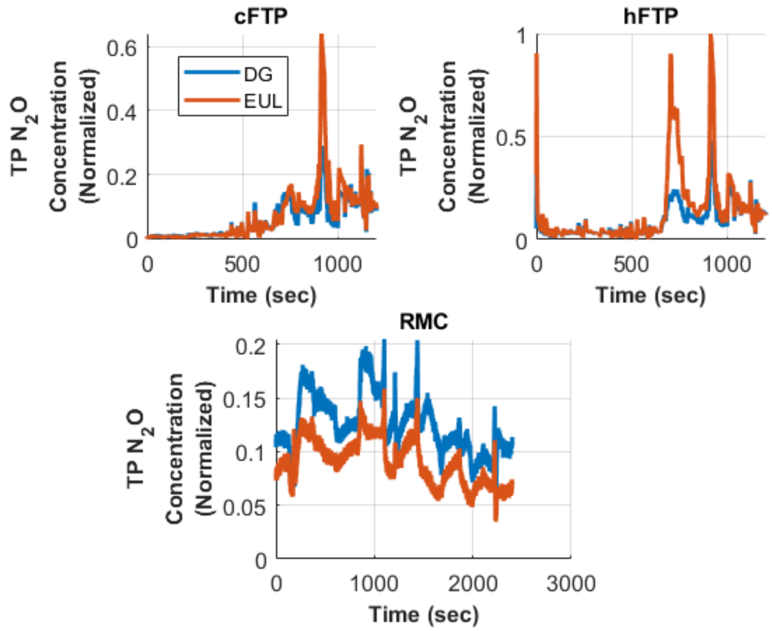

Figure 3.7. Tailpipe N_2O for degreened and EUL catalysts for the three drive cycles.

The aftertreatment system on these trucks is the same as the one used to collect test-cell data. The exhaust layout, with the sensors available on these trucks, is shown in Figure 3.10.

3.2.1 Operating conditions

Figure 3.11 shows a 7-minute segment of truck data. Differences in accelerator pedal position, altitude, and ambient temperature demonstrate that each driver has their own driving style, and every truck could be driven under different road, traffic, and weather conditions. Therefore, the operating conditions vary significantly across the four trucks.

Table 3.2 lists the minimum, maximum, and average values of engine-out NOx, exhaust flow, temperature and urea dosing over the entire day file for each truck. Notice that the average values of exhaust flow rate and temperature are very similar across the four trucks, but the ranges and average values of engine-out NOx and urea dose vary across the four trucks.

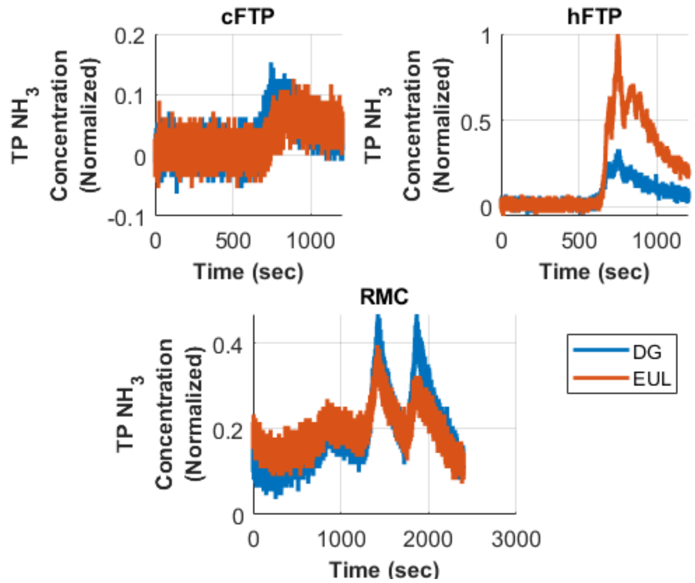

Figure 3.8. Tailpipe NH_3 for degreened and EUL catalysts for the three drive cycles.

Table 3.2. Operating conditions for the four trucks in truck-data day files.

Truck	kMiles	EO NOx (ppm)			Exh Volume Flow (m^3/sec)			SCR Bed Temp (^{0}C)			Urea Dose (ml/sec)		
		Min	Avg	Max	Min	Avg	Max	Min	Avg	Max	Min	Avg	Max
Truck 1	271	0	403	1371	0	0.35	0.61	50	244	314	0	0.34	2
Truck 2	422	0	408	1203	0	0.27	0.65	72	243	557	0	0.25	1.5
Truck 3	484	0	573	2237	0	0.35	0.77	44	253	354	0	0.44	2
Truck 4	711	0	490	1647	0	0.30	0.67	113	241	374	0	0.34	1.8

Since the inputs to the aftertreatment are unique for each truck, it is more challenging to attribute differences in tailpipe signals to aging as compared to the test-cell data.

3.3 Test-cell data vs Truck data

This section will compare some key aspects of the truck and the test-cell data and their implications for model-development and diagnostics:

1. **Aging signatures** As discussed earlier, since the test-cell data has experiments where degreened and aged aftertreatment were run under identical operating conditions, it is

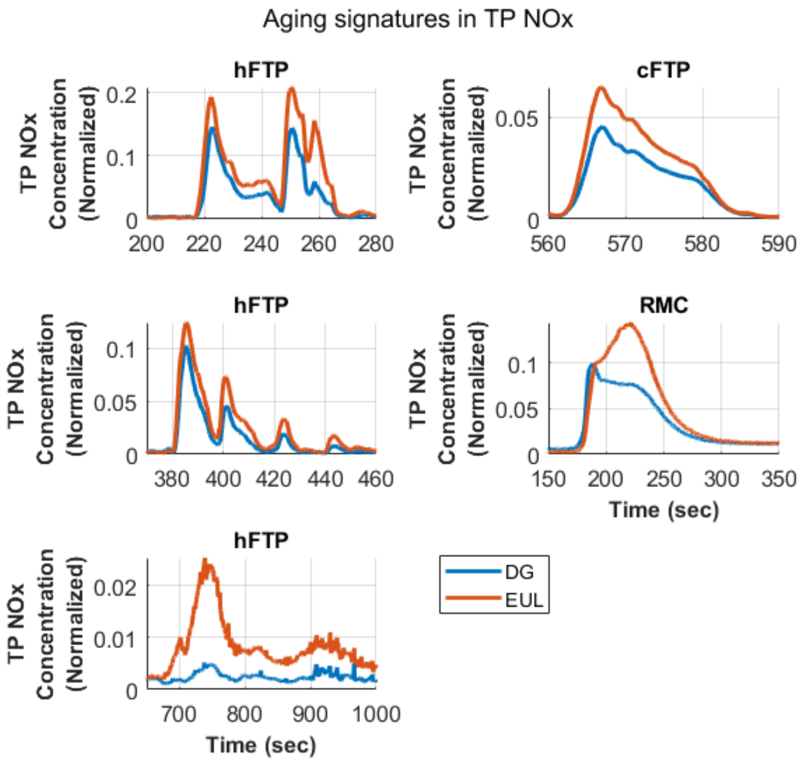

Figure 3.9. Aging signatures observed in tailpipe NOx for the three drive cycles. Note that the three subplots for hFTP, shown on the left side, are zoomed in sections from the same test.

easier to attribute changes in tailpipe signals to aging. Therefore, the test-cell data is more suitable for developing a model to capture aging.

2. **Available signals:** The test-cell data has DOC-out NO, NO_2, TP NH_3, TP NOx, and TP N_2O signals as compared to just the TP NOx signal in the truck data. It was shown in Subsection 3.1.2 that there are operating conditions where only a subset of these signals show aging signatures. Therefore, the test-cell data gives more insight about the effects of aging as compared to the truck data.

3. **Commercial NOx sensors vs FTIR:** Test-cell data has measurements from FTIR sensors, as opposed to the commercial NOx sensors in the truck data. Since the commercial NOx sensors have several limitations such as lower accuracy, cross-sensitivity to

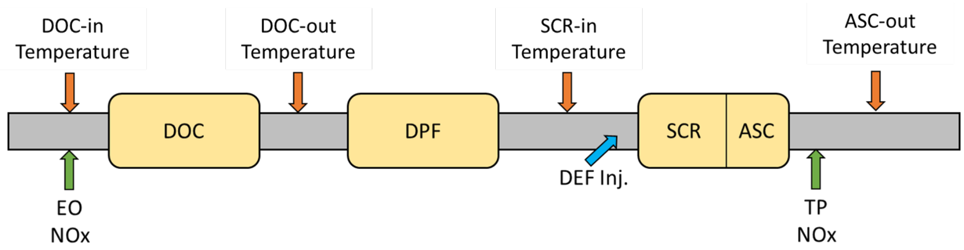

Figure 3.10. Exhaust layout with the sensors available on commercial trucks.

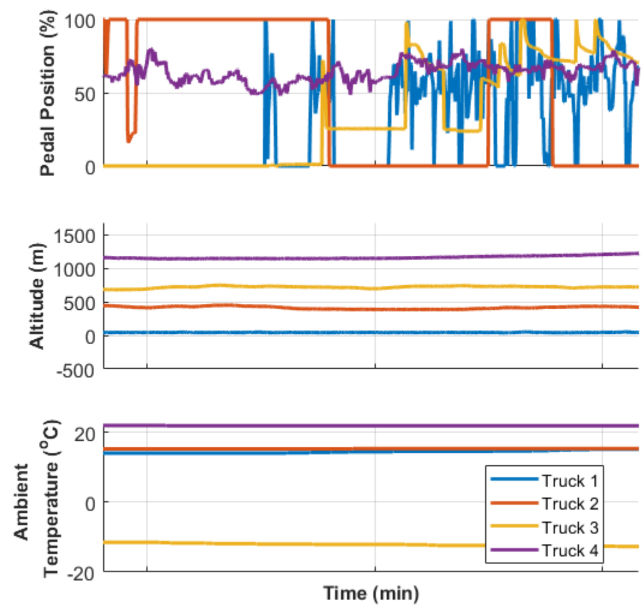

Figure 3.11. Segment of truck data showing differences in driving style and ambient conditions across the four trucks.

NH_3, and inability to operate below the light-off temperature, the FTIR measurements provide a more complete and cleaner data for modeling.

4. **On-road vs In-Lab Conditions:** Given the challenges with truck data, the test-cell data is clearly more suitable to build a model from scratch. However, the truck data provides great insights about the challenges posed by on-road conditions. These insights have played a key role in laying down the modeling requirements, which will be discussed in the next chapter.

4. MODELING

This chapter describes the diagnostics-oriented model, suitable for model-based OBD for SCR+ASC. The chapter starts by specifying the model requirements, based on observations from test-cell and truck data discussed in the previous chapter. This is followed by a description of SCR and ASC reactions and model structure. Then the chapter describes the model calibration process in detail, and concludes with the validation results on test-cell and truck data.

4.1 Model Requirements

Model requirements are elaborated in the following points:

1. **Accuracy requirement:** The model in this work is intended to be used for developing model-based diagnostic algorithm(s). To avoid false positives and false negatives, it is important to pick the right operating conditions to activate the diagnostic algorithm. Therefore, unlike a controller, a diagnostic method would not be running at all times and the model doesn't need to be accurate during operating conditions when the OBD would not be running.

   The model needs to be at its most accurate during operating conditions that are suitable for diagnostics such as the ones where a clear aging signature, i.e. reasonable difference between EUL and degreened catalysts, for tailpipe NOx can occur. But even under these operating conditions, the model doesn't need to capture the data accurately at each time-stamp of a drive cycle. Instead, the key requirement from a diagnostics-oriented model would be to capture the general trends in the tailpipe signals that occur as a result of aging.

2. **Ability to run with commercial sensors:** Apart from exhaust gas flow rate and temperature, commercial trucks only have engine-out and tailpipe NOx measurements. Therefore, it must be possible to run the model with just those measurements.

   Even though aging signatures were observed in DOC-out NO and NO_2 signals, DOC-out NOx will be used as the input to the model. This is because DOC-out NO and

NO_2 signals are not available in commercial trucks, and a DOC model will be required to calculate DOC-out NO and NO_2. Since the focus of current work is SCR+ASC, the DOC dynamics will not be taken into account at this stage.

Also, the outputs from the SCR+ASC model would be tailpipe NOx, NH_3, and N_2O concentration as these measurements are available in the test-cell data, and will be used to calibrate and validate the model. However, only the tailpipe NOx values will be used when testing the model on data from commercial trucks.

Model Objective: To summarize, the primary objective is to develop a diagnostics-oriented model for SCR+ASC that can capture aging signatures observed in the test-cell data, and is suitable for developing model-based OBD that can work with sensors available in the SCR-ASC system on commercial trucks.

4.2 Selective Catalytic Reduction (SCR)

The SCR catalyst is responsible for reducing engine-out NOx into harmless N_2 and H_2O. Diesel Exhaust Fluid (DEF), which is a mixture of 32.5% urea and 67.5% distilled water is injected into the exhaust. Exhaust heat converts urea to NH_3, which is then adsorbed by the catalyst. Some of the adsorbed NH_3 reduces the NOx, and the rest gets desorbed or oxidized.

4.2.1 SCR Reactions

The Eley Rideal mechanism is widely accepted to be an accurate representation of the Urea-SCR reactions [30], [37]. The key processes and corresponding chemical reactions in the Urea-SCR system as per the Eley Rideal mechanism are as follows:

1. Urea to NH_3 conversion.

   Thermolysis:

$$(NH_2)_2CO \longrightarrow HNCO + NH_3 \tag{4.1}$$

Hydrolysis:

$$HNCO + H_2O \longrightarrow NH_3 + CO_2 \tag{4.2}$$

2. NH_3 adsorption and desorption.

$$NH_3 + \theta_{\text{free}} \longleftrightarrow NH_3(\text{ads}) \tag{4.3}$$

where θ_{free} is the number of moles of catalyst sites available for NH_3 adsorption.

3. NOx reduction.

Standard SCR reaction:

$$4\,NH_3(\text{ads}) + 4\,NO + O_2 \longrightarrow 4\,N_2 + 6\,H_2O \tag{4.4}$$

Fast SCR reaction:

$$4\,NH_3(\text{ads}) + 2\,NO + 2\,NO_2 \longrightarrow 4\,N_2 + 6\,H_2O \tag{4.5}$$

Slow SCR reaction:

$$8\,NH_3(\text{ads}) + 6\,NO_2 \longrightarrow 7\,N_2 + 12\,H_2O \tag{4.6}$$

Slow reaction is usually ignored when writing the dynamic equations, as it is much slower than the fast and the standard reactions.

4. NH_3 oxidation.

$$4\,NH_3(\text{ads}) + 3\,O_2 \longrightarrow 2\,N_2 + 6\,H_2O \tag{4.7}$$

4.2.2 SCR Model

A high fidelity model for the Urea-SCR system will require partial differential equations (PDEs) to represent chemical reactions, gas flow and convective heat transfer [38], [37]. However, such model would be computationally too expensive to be embedded in a micro-controller. Hence, several references such as [30], [39] and [40] have used a lumped parameter zero-dimensional model by treating the catalyst as a continuous stirred tank reactor (CSTR) as shown in Figure 4.1. The CSTR model assumes homogeneous distribution of reacting species in the catalyst which allows using ordinary differential equations (ODEs) instead of PDEs to model the Urea-SCR system dynamics.

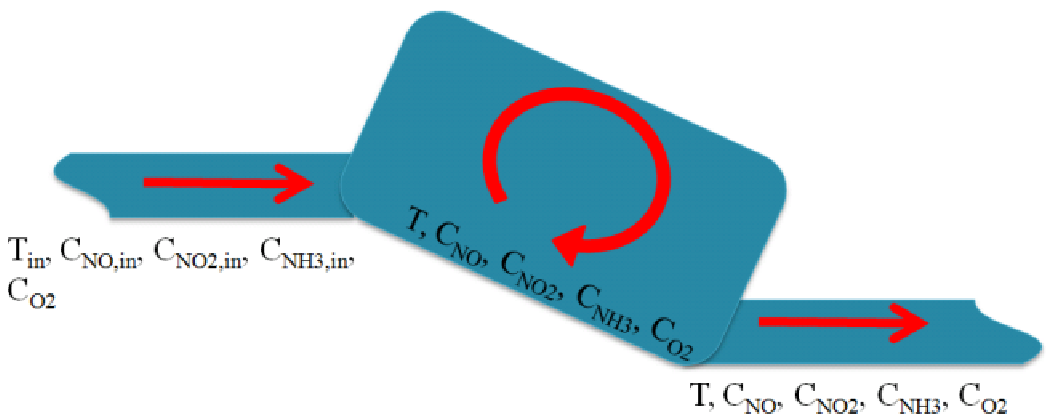

Figure 4.1. Schematic of the CSTR Model (Taken from [30]).

The system dynamic equations for the CSTR model can then be obtained using mass balance across the catalyst: Depending on whether or not NO_2 dynamics are considered, the CSTR model can have three or four states, respectively. In this work, the three-state CSTR model will be used for SCR because the aftertreatment system on commercial trucks does not have any sensor to measure NO_2 concentration upstream or downstream of SCR. The system dynamic equations for the three-state CSTR models are given by Equation 4.8.

$$
\begin{aligned}
\dot{x}_1 &= \frac{F}{V}(u_1 - x_1) - \alpha_{\text{ads}} x_1 (1 - x_3) K + \alpha_{\text{des}} x_3 K \\
\dot{x}_2 &= \frac{F}{V}(u_2 - x_2) - \alpha_{\text{SCR}}(x_2)(x_3 K) \\
\dot{x}_3 &= -\alpha_{\text{SCR}} x_2 x_3 + \alpha_{\text{ads}} x_1 (1 - x_3) - \alpha_{\text{des}} x_3 - \alpha_{\text{oxi}} x_3
\end{aligned} \tag{4.8}
$$

The temperature (T) dependence of the reaction rates (α_i) and catalyst NH_3 storage capacity (K) is given by

$$\alpha_i = A_i \mathrm{e}^{-\frac{E_i}{RT}}, K = \frac{S_1}{V} \mathrm{e}^{-S_2 T} \tag{4.9}$$

And the urea to NH_3 conversion dynamics is given by

$$\dot{u}_1 = \frac{1}{\tau}(-u_1 + \eta_{\text{urea}} u_{1,\text{ideal}}) \tag{4.10}$$

All the symbols in Equations 4.8 to 4.10 are described in Table 4.1.

Table 4.1. Symbols used in the SCR Model

Symbol	Meaning
x_1	Concentration of NH_3 slip in mol/m^3
x_2	Concentration of emitted NOx in mol/m^3
x_3	Fraction of catalyst storage capacity occupied by NH_3
u_1	Concentration of injected NH_3 in mol/m^3
$u_{1,\text{ideal}}$	Ideal u_1 assuming instant and 100% conversion from urea to NH_3
u_2	Concentration of incoming NOx in mol/m^3
F	Exhaust gas volume flow-rate in m^3/sec
T	Catalyst bed temperature in K
A_i	Pre-exponential coefficient for reaction i
E_i	Activation energy for reaction i in J/mol
V	Catalyst volume in m^3
K	Catalyst NH_3 storage capacity in moles
α_{ads}	Reaction rate for NH_3 adsorption to SCR catalyst
α_{des}	Reaction rate for NH_3 desorption from SCR catalyst
α_{oxi}	Reaction rate for oxidation of adsorbed NH_3 in SCR catalyst
α_{SCR}	Reaction rate for NOx reduction by adsorbed NH_3 in SCR catalyst
η_{urea}	Urea to NH_3 conversion efficiency
τ	Time-constant for Urea to NH_3 conversion

4.3 Ammonia Slip Catalyst (ASC)

It is difficult to get low SCR-out NOx and NH_3 simultaneously. ASC is responsible for oxidizing the SCR-out NH_3 to N_2. Therefore, for the same amount of tailpipe NOx, an SCR-ASC system will have lower tailpipe NH_3 than an SCR-only system. However, the ASC is not perfect and it can oxidize some SCR-out NH_3 into NO and N_2O.

4.3.1 ASC Reactions

The key reactions in an ASC are as follows [41]:

1. Conversion of NH_3 to N_2. This is the desired reaction.

$$4\,NH_3 + 3\,O_2 \longrightarrow 2\,N_2 + 6\,H_2O \tag{4.11}$$

2. Conversion of NH_3 to NO and N_2O. These are the undesired reactions.

$$4\,NH_3 + 5\,O_2 \longrightarrow 4\,NO + 6\,H_2O \tag{4.12}$$

$$2\,NH_3 + 2\,O_2 \longrightarrow N_2O + 3\,H_2O \tag{4.13}$$

4.3.2 ASC Model

An ODE model, with concentration of NH_3, NO, and N_2O as the three states, could be developed for ASC from the reactions 4.11 to 4.13 using mass balance and CSTR assumptions similar to the SCR model. Combining such model with the three-state SCR model would give us a six-state nonlinear ODE model for the SCR-ASC system. However, calibrating such model would be extremely difficult in the absence of SCR-out measurements. Therefore, instead of developing an ODE model for ASC, a look-up table model based on ASC's NH_3

conversion efficiency and selectivity to N_2, NO and N_2O is developed. Since the look-up table doesn't model ASC dynamics, it won't be able to capture the tailpipe signals accurately at each time-stamp in the drive cycles. However, the results will show that this model can capture the general trends caused due to aging, which should be sufficient for diagnostics as discussed earlier and will also be demonstrated in the later sections.

ASC's NH_3 conversion efficiency and selectivities to NOx and N_2O can be calculated using the following equations:

$$\eta_{\mathrm{NH_3}} = \frac{y_{\mathrm{NH_3,SCR}} - y_{\mathrm{NH_3,TP}}}{y_{\mathrm{NH_3,SCR}}} \tag{4.14}$$

$$S_{\mathrm{NOx}} = \frac{y_{\mathrm{NOx,TP}} - y_{\mathrm{NOx,SCR}}}{y_{\mathrm{NH_3,SCR}} - y_{\mathrm{NH_3,TP}}} \tag{4.15}$$

$$S_{\mathrm{N_2O}} = \frac{2y_{\mathrm{N_2O,TP}}}{y_{\mathrm{NH_3,SCR}} - y_{\mathrm{NH_3,TP}}} \tag{4.16}$$

where $\eta_{\mathrm{NH_3}}$ is ASC's NH_3 conversion efficiency and S_{NOx} and $S_{\mathrm{N_2O}}$ are selectivities to NOx and N_2O, respectively.

The curves, reported in [41], for ASC's NH_3 conversion efficiency and sensitivities vs temperature and flow rate are shown in Figure 4.2. Since ASC's NH_3 conversion efficiency and sensitivities are functions of temperature and flow rate, two-dimensional look-up tables can be developed to calculate NH_3 conversion efficiency and sensitivities for any given combination of temperature and flow rate. Due to the unavailability of detailed ASC-in and ASC-out data, it won't be possible to obtain the exact relation from temperature and flow rate to efficiency and selectivities. Therefore, the objective here is to maintain the qualitative curves reported in [41] and manipulate them empirically using the existing test-cell data such that the SCR+ASC model can match the tailpipe signals.

The curves shown in Figure 4.2 are a good starting point to develop the look-up tables because the temperatures in these curves cover the range of values in the test-cell data. The space velocities given by [41] in Figure 4.2 are 66k hr^{-1} and 265k hr^{-1}, but these exact space velocity values are not important as the curves at these values will be manipulated to obtain the curves at three flow rate values within the range of our data. The range of exhaust volume flow rate in the data is from 0.04 m^3/sec to 0.6 m^3/sec. Curves for 66k hr^{-1} will be manipulated to get selectivity vs temperature curves for a flow rate of 0.04 m^3/sec and 0.2 m^3/sec. And the curves for 265k hr^{-1} will be manipulated to get selectivity vs temperature curves for the flow rate of 0.7 m^3/sec. This will be further elaborated in Section 4.3.4.

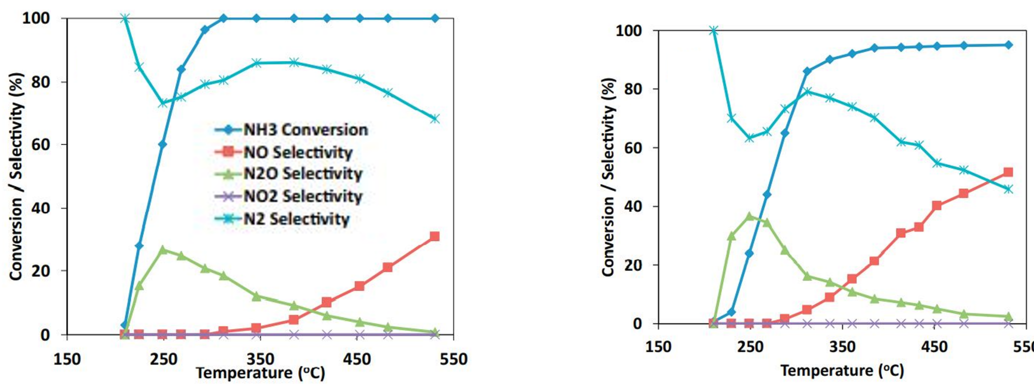

(a) 66k hr^{-1} space velocity (b) 265k hr^{-1} space velocity

Figure 4.2. Dependence of ASC's NH_3 conversion efficiency and selectivities on temperature and flow-rate, taken from [41]

The step-by-step implementation of the ASC model, based on these 2D look-up tables, is given as follows:

1. For a given temperature (T), flow rate (F) calculate $\eta_{\mathrm{NH_3}}$, S_{NOx}, and $S_{\mathrm{N_2O}}$ using the 2D look-up tables.

2. Calculate tailpipe NH_3 using $\eta_{\mathrm{NH_3}}$ and SCR-out NH_3.

$$y_{\mathrm{NH_3,TP}} = (1 - \eta_{\mathrm{NH_3}})\, y_{\mathrm{NH_3,SCR}} \tag{4.17}$$

3. Calculate tailpipe NOx using S_{NOx}, SCR-out NOx, SCR-out NH_3, and tailpipe NH_3.

$$y_{\mathrm{NOx,TP}} = y_{\mathrm{NOx,SCR}} + S_{\mathrm{NOx}}\,(y_{\mathrm{NH_3,SCR}} - y_{\mathrm{NH_3,TP}}) \tag{4.18}$$

4. Calculate tailpipe N_2O using S_{N_2O}, SCR-out NH_3, and tailpipe NH_3.

$$y_{N_2O,TP} = \frac{S_{N_2O}}{2}\left(y_{NH_3,SCR} - y_{NH_3,TP}\right) \tag{4.19}$$

4.3.3 Model Calibration

The combined SCR-ASC model is shown in Figure 4.3. Inputs to the SCR model are: T, F, Engine-out NOx (u_{NOx}), and Injected DEF (u_{DEF}). Outputs from the SCR model and the inputs to the ASC model are SCR-out NH_3 ($y_{NH_3,SCR}$) and NOx ($y_{NOx,SCR}$). Tailpipe NH_3 ($y_{NH_3,TP}$), NOx ($y_{NOx,TP}$), and N_2O ($y_{N_2O,TP}$) are the outputs from the ASC model.

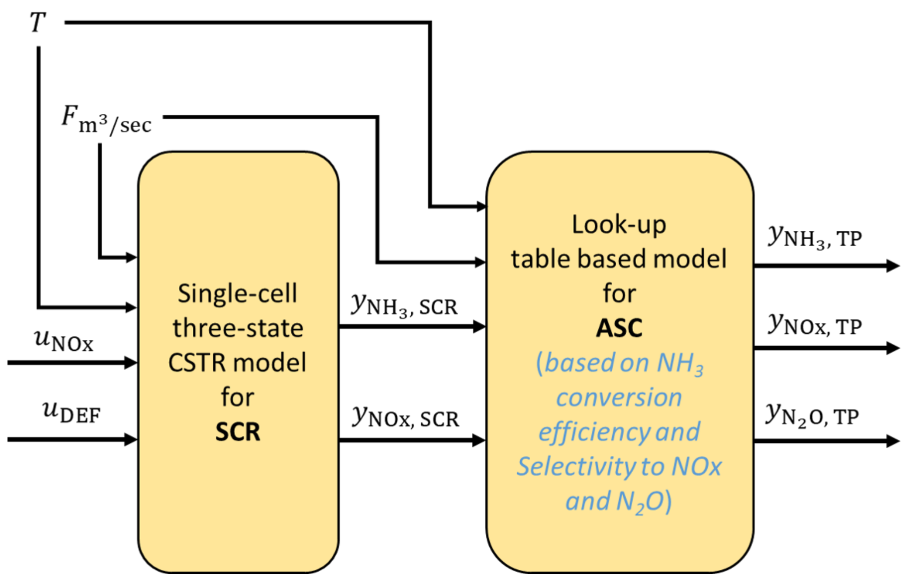

Figure 4.3. SCR+ASC model structure

Hot FTP cycle (hFTP) data is used to calibrate the SCR and ASC models for both degreened and EUL catalysts. Cold FTP (cFTP) and RMC cycles will be used for validation. Parameters for the SCR model are: Pre-exponential coefficients (A_i) and activation energies (E_i) for the reaction rates, storage capacity parameters S_1, S_2, Urea-to-NH_3 conversion efficiency (η_{urea}), and time constant for urea-to-NH_3 conversion (τ). Parametrization of the look-up tables for the ASC model will be discussed in Section 4.3.4.

4.3.4 Look-up tables for $S_{\mathbf{N_2O}}$, $\eta_{\mathbf{NH_3}}$, and $S_{\mathbf{NOx}}$

Look-up table for $S_{\mathbf{N_2O}}$: The step-by-step procedure to obtain the look-up table from temperature and flow rate to $S_{\mathrm{N_2O}}$ is given as follows:

1. Extract $S_{\mathrm{N_2O}}$ vs temperature data from Figure 4.2 for 66k hr^{-1} and 265k hr^{-1} space velocities. The values in Figure 4.2 are for the catalyst that was used in [41]. Therefore, these are not necessarily the true selectivities for the catalyst used in this work. These will be used as initial guesses, and will be parametrized by offsetting the curves for $S_{\mathrm{N_2O}}$ vs temperature in Figure 4.2. Let the initial values of $S_{\mathrm{N_2O}}$ from Figure 4.2 be $S_{\mathrm{N_2O,init66}}$ for 66k hr^{-1} space-velocity and $S_{\mathrm{N_2O,init265}}$ for 265k hr^{-1} space-velocity. Then the look-up table for $S_{\mathrm{N_2O}}$ can be parametrized as follows:

$$\begin{aligned} S_{\mathrm{N_2O,lowflow}} &= S_{\mathrm{N_2O,init66}} + p_1 \\ S_{\mathrm{N_2O,midflow}} &= S_{\mathrm{N_2O,init66}} + p_2 \\ S_{\mathrm{N_2O,highflow}} &= S_{\mathrm{N_2O,init265}} + p_3 \end{aligned} \tag{4.20}$$

   where $S_{\mathrm{N_2O,lowflow}}$, $S_{\mathrm{N_2O,midflow}}$, and $S_{\mathrm{N_2O,highflow}}$ are the values of ASC's selectivity to N_2O at the three flow rates of 0.04 m^3/sec, 0.2 m^3/sec, and 0.7 m^3/sec, respectively.

2. After the first step, $S_{\mathrm{N_2O}}$ values are obtained for several temperatures at each of the three flow rates. At each flow rate, $S_{\mathrm{N_2O}}$ is calculated for other temperatures in hFTP using piece-wise cubic Hermite interpolation. Then for each temperature, $S_{\mathrm{N_2O}}$ is calculated for other flow rates in hFTP using linear interpolation. Note that cubic interpolation is used to capture the nonlinear selectivity-vs-temperature curves in Figure 4.2, whereas linear interpolation is used for flow rate as selectivity values are known for only three flow rates, making it unnecessary and infeasible to use nonlinear interpolation.

3. After the second step, $S_{\mathrm{N_2O}}$ values are obtained for many temperatures and flow rates. Then the temperature, flow rate and selectivity values are stacked together to form a 2D interpolant using MATLAB's `scatteredInterpolant` function. This interpolant

is the 2D look-up table that can calculate $S_{\mathrm{N_2O}}$ for any combination of temperature and flow rate.

Look-up table for $\eta_{\mathrm{NH_3}}$: It is possible to obtain the look-up table for $\eta_{\mathrm{NH_3}}$ by extracting $\eta_{\mathrm{NH_3}}$ vs temperature data from Figure 4.2, and following a similar process to the look-up table for $S_{\mathrm{N_2O}}$. However, as shown in Figure 4.4, the SCR-out NH_3 slip, calculated using $\eta_{\mathrm{NH_3}}$ vs temperature curves from Figure 4.2, is less than $y_{\mathrm{NH_3,TP}} + 2y_{\mathrm{N_2O,TP}}$. This would imply that $S_{\mathrm{N_2O}} = 2y_{\mathrm{N_2O,TP}}/\left(y_{\mathrm{NH_3,SCR}} - y_{\mathrm{NH_3,TP}}\right) > 1$, which is not possible. Therefore, the

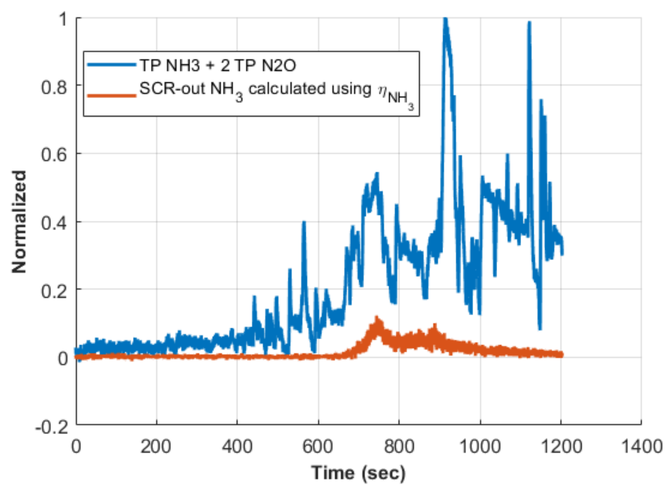

Figure 4.4. Comparison of $y_{\mathrm{NH_3,SCR}}$, calculated using $\eta_{\mathrm{NH_3}}$, and $y_{\mathrm{NH_3,TP}} + 2y_{\mathrm{N_2O,TP}}$.

look-up table for $\eta_{\mathrm{NH_3}}$ is created using the following alternate approach:

1. At each time-stamp in hFTP, calculate SCR-out NH_3 using $S_{\mathrm{N_2O}}$, tailpipe NH_3, and tailpipe N_2O using the following equation:

$$y_{\mathrm{NH_3,SCR}} = y_{\mathrm{NH_3,TP}} + \frac{2y_{\mathrm{N_2O,TP}}}{S_{\mathrm{N_2O}}} \tag{4.21}$$

2. Calculate $\eta_{\mathrm{NH_3}}$ from $y_{\mathrm{NH_3,SCR}}$ and $y_{\mathrm{NH_3,TP}}$ using Equation 4.14.

3. Stack temperature, flow rate, and $\eta_{\mathrm{NH_3}}$ at each time-stamp using `scatteredInterpolant` to obtain the look-up table from temperature and flow rate to $\eta_{\mathrm{NH_3}}$.

Look-up table for S_{NOx}: S_{NOx} can be calculated from $y_{\mathrm{NH_3,SCR}}$, $y_{\mathrm{NH_3,TP}}$, $y_{\mathrm{NOx,SCR}}$, and $y_{\mathrm{NOx,TP}}$ using Equation 4.15. However, since test-cell data does not have SCR-out measurements, $y_{\mathrm{NOx,SCR}}$ is unknown. Therefore, Equation 4.15 can be parametrized as follows:

$$S_{\mathrm{NOx}} = \frac{p_4(y_{\mathrm{NOx,TP}})}{y_{\mathrm{NH_3,SCR}} - y_{\mathrm{NH_3,TP}}} \tag{4.22}$$

where p_4 is the fraction of tailpipe NOx produced from NH_3 oxidation by ASC. This equation assumes that p_4 is a constant, which may not be true in general. However, this is a reasonable assumption to calculate approximate values of S_{NOx} for model calibration.

The look-up tables for both degreened and EUL catalysts were developed using these steps. The NH_3 conversion efficiency and selectivities vs temperature and flow rate, based on these look-up tables, are shown in Figure 4.5. Note that the curves for the degreened and EUL catalysts are generally very close to each other, which is a sanity check because the same $S_{\mathrm{N_2O}}$ vs temperature data was used for both degreened and EUL catalysts when creating the look-up table for $S_{\mathrm{N_2O}}$ and therefore it was expected that similar look-up tables will be obtained for both. The slight differences between the curves for degreened and EUL catalysts, shown in Figure 4.5, could be attributed to numerical differences caused due to slightly different operating conditions and tailpipe signals for the two catalysts.

Since these curves look qualitatively similar to the ones in Figure 4.2, these look-up tables could be used as reasonable initial guesses for the ASC model, which can be calibrated by tuning p_1, p_2, p_3, and p_4. Note that $\eta_{\mathrm{NH_3}}$, S_{NOx}, and $S_{\mathrm{N_2O}}$ are zero below 200^{o}C, which is the threshold for ASC activation.

4.3.5 Current Calibration Approach for SCR+ASC Model

As mentioned earlier, hFTP is used to calibrate the SCR+ASC model. The following steps summarize the procedure to run the SCR+ASC model:

1. Integrate the three-state ODE Equations 4.8 to get SCR-out NH_3 and NOx.

2. Calculate $\eta_{\mathrm{NH_3}}$, S_{NOx}, and $S_{\mathrm{N_2O}}$ at each time point using the look-up tables from T, F.

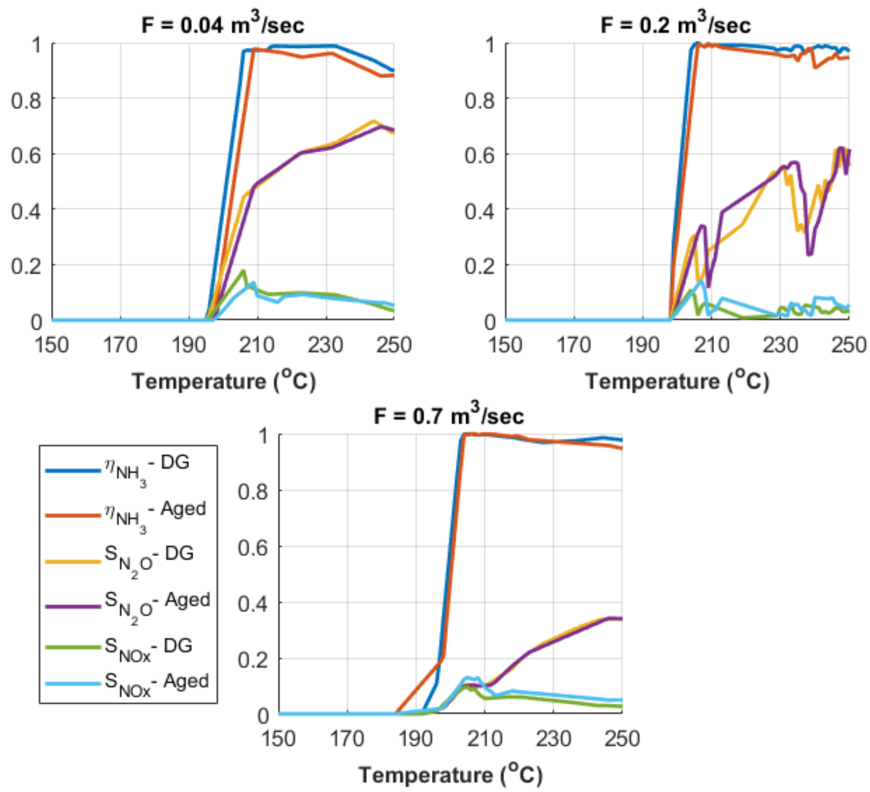

Figure 4.5. $\eta_{\mathrm{NH_3}}$, S_{NOx}, and $S_{\mathrm{N_2O}}$ vs temperature and flow rate, based on the 2D look-up tables for degreened (DG) and EUL catalyst.

3. Calculate tailpipe NH_3 from $\eta_{\mathrm{NH_3}}$ and $y_{\mathrm{NH_3,SCR}}$.

4. Calculate tailpipe NOx from S_{NOx}, $y_{\mathrm{NOx,SCR}}$, $y_{\mathrm{NH_3,TP}}$, and $y_{\mathrm{NH_3,SCR}}$.

5. Calculate tailpipe N_2O from $S_{\mathrm{N_2O}}$, $y_{\mathrm{NH_3,TP}}$, and $y_{\mathrm{NH_3,SCR}}$.

The parameters for the SCR-ASC model can be identified by solving the following optimization problem:

$$
\begin{aligned}
\min_{\theta_{\text{SCR}},\theta_{\text{ASC}}} \quad & J = \sum_{t=t_1}^{t_2} \left(e^2_{NH_3,TP} + e^2_{NOx,TP} + e^2_{N_2O,TP} \right) \\
\text{subject to} \quad & A_i, E_i, S_1, S_2 > 0 \\
& 0 < \eta_{\text{urea}} < 1 \\
& 0 < \tau < 50 \\
-1 &< p_1, p_2, p_3 < 1 \\
& 0 < p_4 < 1 \\
\text{where} \quad & \\
& e_{i,\text{TP}} = y_{i,\text{TP}} - \hat{y}_{i,\text{TP}} \\
& \theta_{\text{SCR}} = [A_i, E_i, S_1, S_2, \eta_{\text{urea}}, \tau] \\
& \theta_{\text{ASC}} = [p_1, p_2, p_3, p_4]
\end{aligned}
\tag{4.23}
$$

where $y_{i,\text{TP}}$ are the true tailpipe signals and $\hat{y}_{i,\text{TP}}$ are the model-out values. Also note that t_1 and t_2 denote the times during which clear aging signature was observed in hFTP data. This implies that good model accuracy is required only when the operating conditions are favorable for diagnostics.

The Trust-region-reflective algorithm, using MATLAB's `lsqnonlin`, was used to solve the optimization problem to obtain the fits shown in Figure 4.6.

Visually, the fits shown in Figure 4.6 are reasonable for all tailpipe signals. These fits are quantified in Table 4.2 using the values of average modeling error, in ppm and as a fraction (r_{mean}) of average value of the true signals. Note that the average error for tailpipe NOx and tailpipe NH_3 is less than 1 ppm for both DG and EUL catalysts. However, it is still 37% of the average value of true tailpipe NOx for the DG catalyst, which is around 2 ppm. The average error for tailpipe N_2O is around 0.2 ppm for the DG catalyst and around 6.4 ppm for the EUL catalyst, which is about 23% of the average value of true tailpipe N_2O. Average error values in Table 4.2 demonstrate that very low modeling error could still be a significant fraction of the true signal value if the signal itself is small. But, it will be shown in Chapter 5 that a model-based diagnostic method could be designed to handle modeling

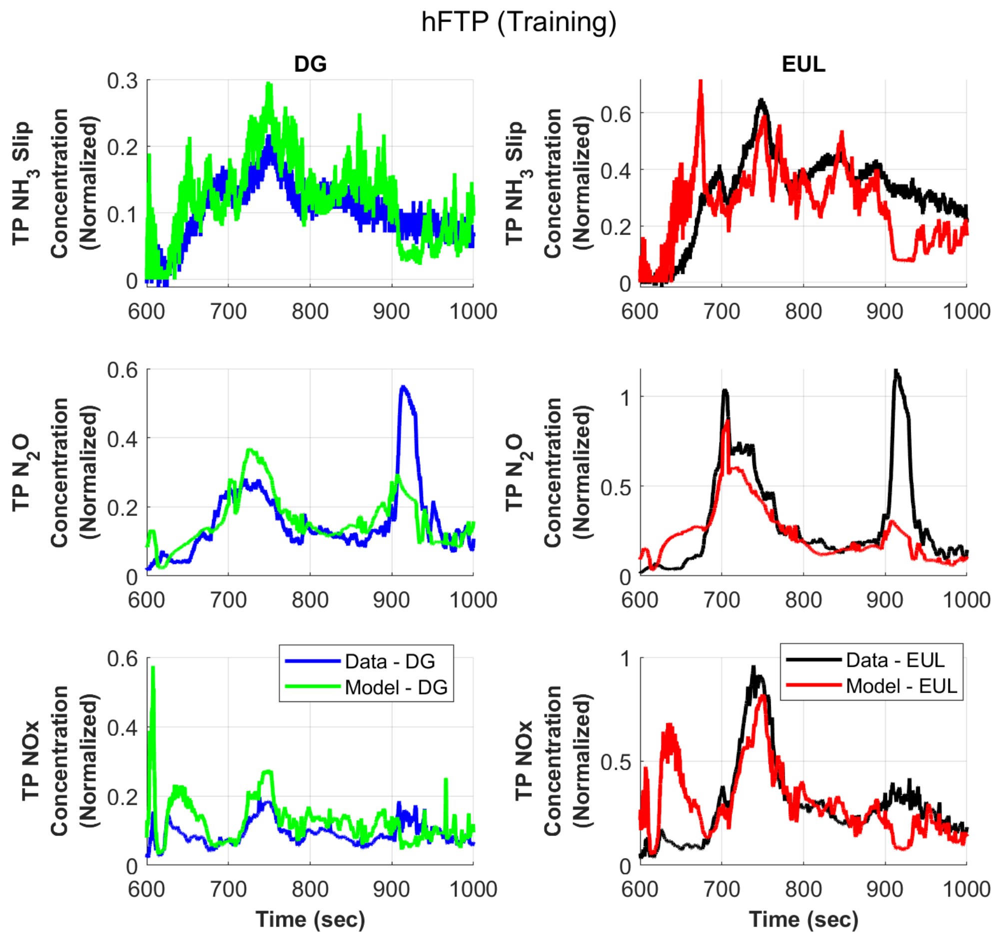

Figure 4.6. TP signal fits for degreened and EUL catalysts after calibrating the model on hFTP cycle.

error up to 10 ppm in tailpipe NOx. So, even if the modeling error is significant with respect to the true signal value, the model can be considered accurate enough for the OBD method in Chapter 5 to capture the aging signatures if the modeling error is less than 10 ppm.

One observation from Figure 4.6 is that the model is not able to capture the second spike in tailpipe N_2O between 900-950 seconds. The reason for this spike is not exactly clear at this point, but it could be due to conditions favoring NH_3 desorption, such as relatively low engine-out NOx, low flow rate and high exhaust temperature, leading to high SCR-out NH_3, which then gets primarily converted to tailpipe N_2O due to conditions where ASC's selectivity to N_2O is high. Our model's inability to capture this spike could primarily be attributed to the SCR model underestimating SCR-out NH_3 at that time. This will be analyzed more carefully in future to improve model calibration.

Table 4.2. Average modeling error, in ppm and as a fraction (r_{mean}) of average value of the true signal, to quantify the tailpipe signal fits for hFTP shown in Figure 4.6.

	Avg Error ($\bar{e}$,ppm)		Avg True Value ($\bar{y}_{i,\text{TP}}$, ppm)		$r_{\text{mean}} = \frac{\bar{e}}{\bar{y}_{i,\text{TP}}}$	
	DG	EUL	DG	EUL	DG	EUL
TP NH_3	0.28	0.79	1.75	5.36	0.16	0.15
TP N_2O	0.23	6.43	14.37	27.67	0.01	0.23
TP NOx	0.67	0.12	1.83	5.81	0.37	0.02

It should be noted that the pre-exponential coefficient, S_1, of the catalyst NH_3 storage capacity was the only free parameter when calibrating the model for the EUL catalyst. Therefore, the only difference between parameters for the degreened and the EUL catalysts is S_1. It is likely that other parameters, if left free, could also have taken different values for the EUL catalyst than the degreened one. But since the model could capture the trends due to aging by just changing S_1, it can be concluded that S_1 is adequate to capture the catalyst age. However, the effect of other parameters could be explored in future work.

4.3.6 Model Validation

cFTP, RMC, and truck data are used to validate the SCR+ASC model. This section will present the model validation results on these data-sets.

4.3.7 Model Validation on cFTP Cycle

The validation fits for both degreened and EUL catalysts are shown in Figure 4.7.

The average modeling error, in ppm and as a fraction (r_{mean}) of average value of the true signal, is shown in Table 4.3 to quantify the validation fits shown in Figure 4.7. Very small values of true TP NH_3 signals lead to large r_{mean} values and bad visual fit for the EUL

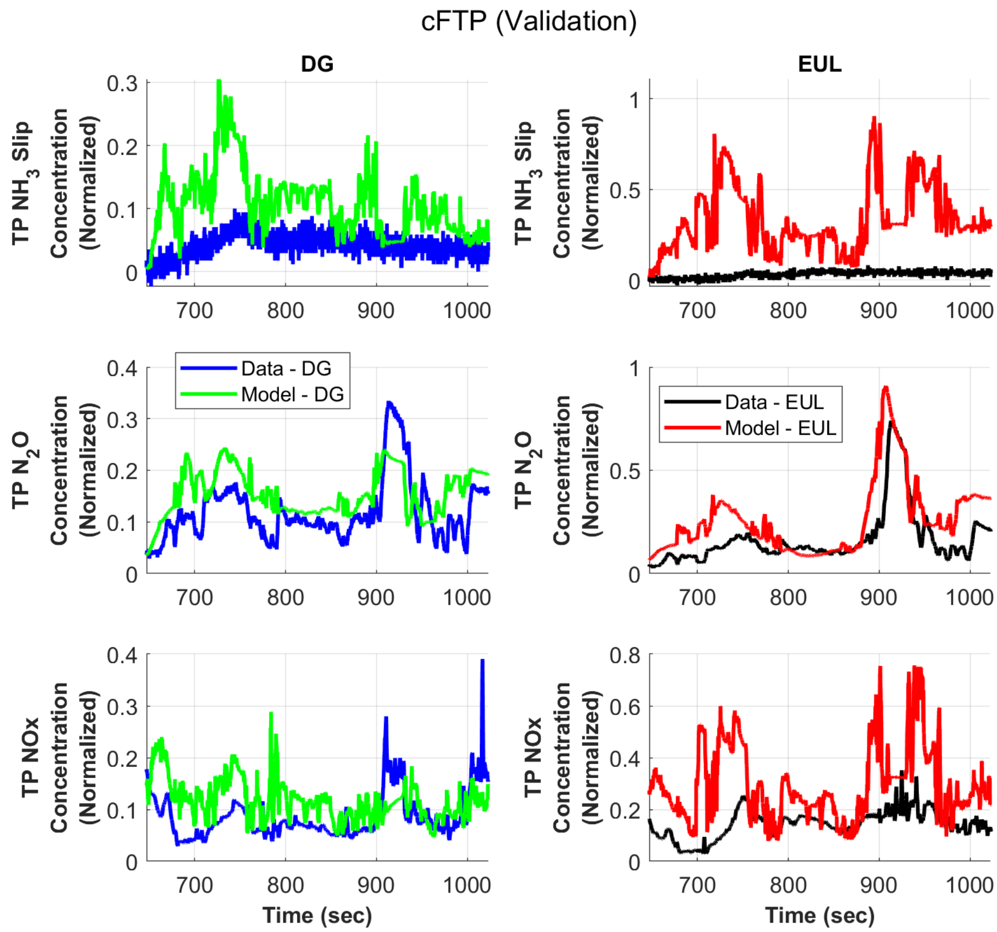

Figure 4.7. TP signal fits after ASC calibration for degreened and EUL catalysts for cFTP, which was used for validation.

catalyst, but the fit is reasonable as the average error values are less than 10 ppm. Visual fits for TP N_2O and NOx are decent, supported by low average error values. Large r_{mean} values can again be attributed to small signal values.

4.3.8 Model Validation on RMC Cycle

Ideally, the training data for the ASC look-up tables should cover a wider range of temperature and flow rate than the validation data because look-up tables can not extrapolate. However, the maximum temperature across the FTP cycles is 270^{o}C. But the temperature

Table 4.3. Average modeling error, in ppm and as a fraction (r_{mean}) of average value of the true signal, to quantify the tailpipe signal fits for cFTP shown in Figure 4.7.

	Avg Error ($\bar{e}$,ppm)		Avg True Value ($\bar{y}_{i,\text{TP}}$, ppm)		r_{mean}	
	DG	EUL	DG	EUL	DG	EUL
TP NH_3	4.2	8.1	0.6	0.5	6.39	17.31
TP N_2O	2.4	7	9.7	13.4	0.24	0.52
TP NOx	0.5	2.7	1.8	2.9	0.25	0.91

for the RMC cycle ranges from 260^{o}C to 350^{o}C. Therefore, the look-up tables in Figure 4.5 have to be extended for the RMC cycle by following the procedure in Section 4.3.4 using the ASC parameter values (p_1, p_2, p_3, p_4) obtained from calibrating the model on the hFTP cycle. The updated curves for NH_3 conversion efficiency and selectivities vs temperature and flow rate are shown in Figure 4.8.

It can be observed from Figure 4.9 that reasonable fits, quantified by low average error values in Table 4.4, were obtained for both degreened and EUL catalysts.

Table 4.4. Average modeling error, in ppm and as a fraction (r_{mean}) of average value of the true signal, to quantify the tailpipe signal fits for RMC shown in Figure 4.9.

	Avg Error ($\bar{e}$,ppm)		Avg True Value ($\bar{y}_{i,\text{TP}}$, ppm)		r_{mean}	
	DG	EUL	DG	EUL	DG	EUL
TP NH_3	0.34	0.98	2.14	2.18	0.16	0.45
TP N_2O	0.93	3.81	13.03	9.42	0.07	0.40
TP NOx	1.52	5.52	15.42	15.79	0.1	0.35

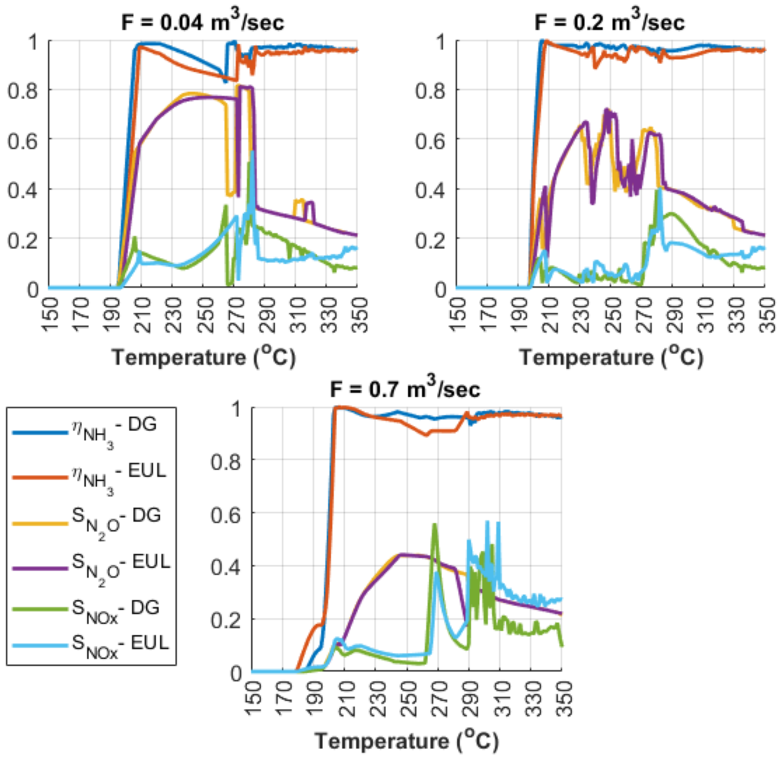

Figure 4.8. $\eta_{\mathrm{NH_3}}$, S_{NOx}, and $S_{\mathrm{N_2O}}$ vs temperature and flow rate, extended to RMC cycle.

4.3.9 Model Validation on Truck Data

Since the duty cycles for the trucks are different from the cycles in test-cell data, the pre-exponential coefficient of the NOx reduction reaction (A_{SCR}) had to be adjusted to make the model work for truck data. Also, since the catalyst degradation levels on the trucks are unknown, the model is considered to be "performing reasonably" if any of the following conditions is satisfied:

1. The measured TP NOx is close to the TP NOx value estimated by the DG catalyst model, or

2. The measured TP NOx is close to the TP NOx value estimated by the EUL catalyst model, or

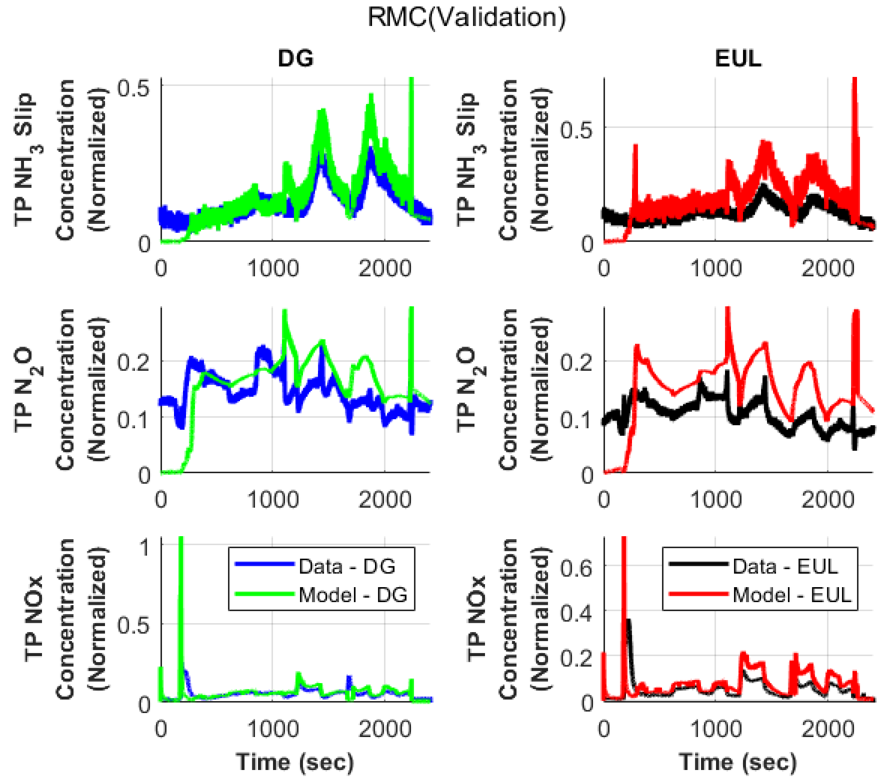

Figure 4.9. Tailpipe signal fits for degreened and EUL catalysts for RMC, which was used for model validation.

3. the measured TP NOx is more than the TP NOx value estimated by the DG catalyst model but less than the EUL catalyst model.

These conditions will be elaborated and quantified in the next section. An example of each of these conditions from the truck data is shown in Figure 4.10. It can be concluded from the values in Table 4.5 that the model behaves reasonably, based on the three points mentioned above, for a significant number of points for all four trucks.

Using a simple cross-sensitivity model to improve the fits: Since the commercial tailpipe NOx sensor on the trucks is cross-sensitive to NH_3, the results in Table 4.5 could be improved by incorporating a simple model for cross-sensitivity. The tailpipe NOx and

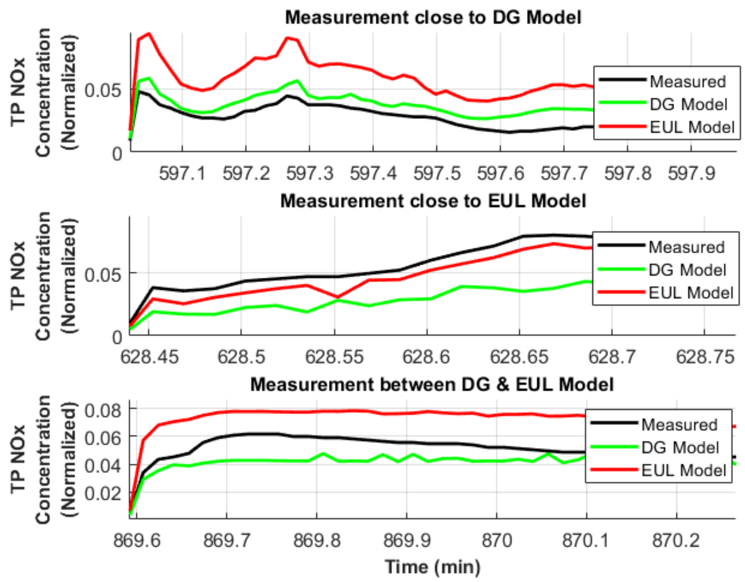

Figure 4.10. Examples from truck data where the model behaves reasonably.

Table 4.5. Model performance on truck data quantified by the number and percentage of points where model behaves reasonably.

	Truck 1	Truck 2	Truck 3	Truck 4
No. of points where T>200^{o}C	32036	57852	67500	55678
No. of points where model is reasonable	18515	47919	41591	24253
%. of points where model is reasonable	57.8%	82.8%	61.6%	43.5%

NH_3 values can be combined as follows to incorporate cross-sensitivity in both DG and EUL models:

$$y_{\mathrm{NOx,cross}} = y_{\mathrm{NOx,TP,model}} + \chi \left(y_{\mathrm{NH_3,TP,model}} \right)$$

Though the cross-sensitivity factor χ can vary with temperature, it is a common approach to use a constant value for simplicity [42]–[44]. It has been reported in [43] that the cross-sensitivity factor can range from 0 to 2. Therefore, in this paper, χ was varied from 0 to 2 for each truck to find the value that results in the best fit. From the curves shown in Figure 4.11, it can be concluded that the fits improved significantly for each truck by using this simple cross-sensitivity model with an appropriate χ. After incorporating cross-sensitivity, the percentage of points where the model is reasonable increased to 86.6%, 85.6%, 69.8%, and 80% for Trucks 1 to 4, respectively.

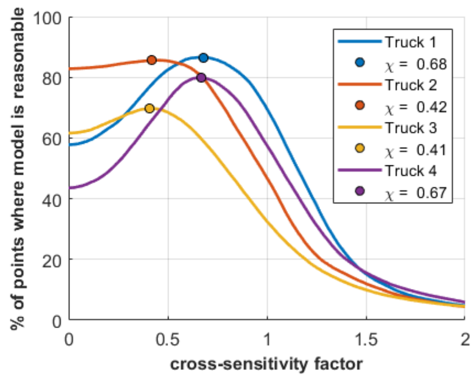

Figure 4.11. Percentage of points where the DG and EUL models behave reasonably for the truck data vs the cross-sensitivity factor χ.

The next chapter will discuss the model-based OBD method with well-defined enable conditions applied to both test-cell and truck data.

5. MODEL-BASED OBD STRATEGIES

Two OBD methods based on the DG and EUL catalyst models are presented in this chapter. The key idea for both methods is to infer catalyst degradation level by comparing the measured tailpipe NOx to its value estimated by both DG and EUL models. Note that a key assumption in this chapter is that the model-based OBD methods should be applied to the same engine-aftertreatment combination as the one used for model calibration. The first five sections will describe the enable conditions, precise diagnostic criteria, and results on both test-cell and truck data for the first method. The last section will present the second OBD method, which is based on the stochastic version of the SCR-ASC model.

5.1 Model-based Enable Conditions

Unlike a controller, OBD doesn't need to run at all times. It is important to pick the right conditions to activate the OBD. These conditions are called enable conditions. The enable conditions should minimize false positives and false negatives while maintaining a good In-use-performance-monitoring-ratio (IUMPR).

The fundamental objective of formulating enable conditions is to detect and pick operating conditions where a degraded catalyst would perform significantly differently from a degreened one. In other words, the enable conditions need to pick operating conditions which are likely to produce aging signatures.

Since the OBD needs to detect catalyst degradation on commercial trucks using just tailpipe NOx measurements, we tried to find operating conditions in test-cell data where more than 10% difference in deNOx efficiency of the DG and the EUL catalysts was observed.

However, observations from test-cell data, such as the one shown in Figure 5.1, showed that very similar operating conditions could lead to very different separability between DG and EUL catalysts based on %deNOx. Despite very similar values of DEF dosing, engine-out NOx, temperature, and flow rate, the difference between %deNOx of DG and EUL catalyst is more than 10% for the operating conditions plotted in blue and very small for the ones plotted in red. This shows that the separability between DG and aged catalysts depends not just on the present operating conditions but on the dynamics that happened in the past, which could be captured by a model. This establishes the importance of formulating model-based enable conditions.

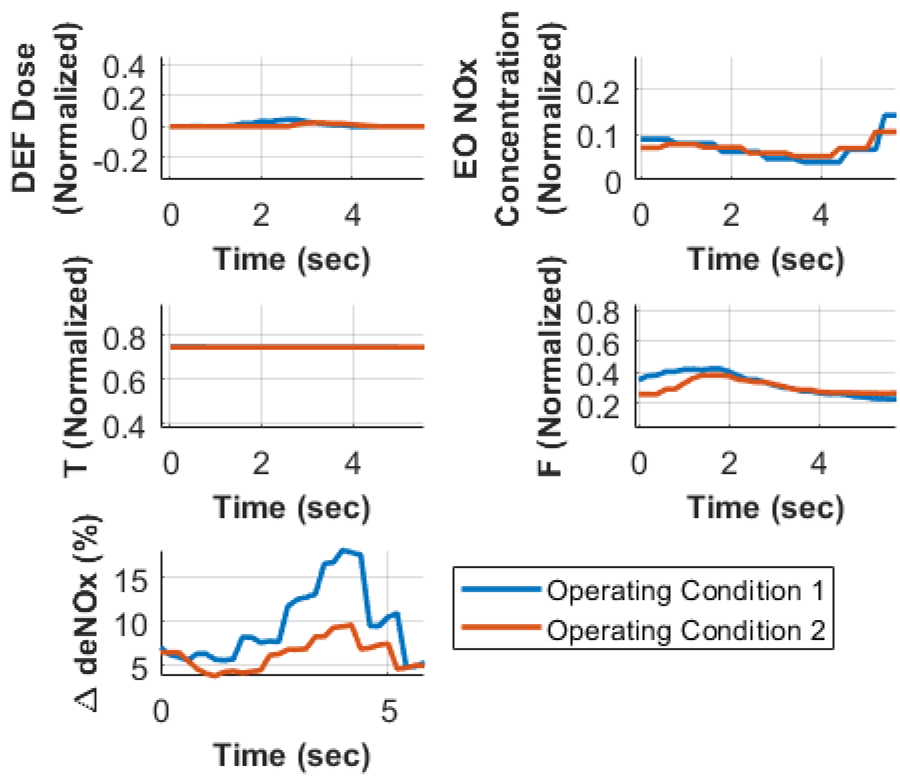

Figure 5.1. A section of test-cell data showing that very similar operating conditions could lead to different separability between DG and EUL catalysts based on %deNOx.

In this thesis, the following steps are proposed to pick operating conditions where aging signatures are expected to occur according to the SCR-ASC model:

1. **Filter 1: Run both DG and EUL catalyst models** so that model-out TP NOx values could be compared to measured TP NOx. Since the SCR-ASC model can't run at temperatures less than 200°C, only the points where the SCR bed temperature is greater than 200°C are selected in this step.

2. **Filter 2:** From the points selected in step 1, **select points where the model behaves reasonably**, i.e., at least one of the following conditions is satisfied:

$$
\begin{aligned}
&|y_{\text{NOx,TP,meas}} - y_{\text{NOx,TP,DG model}}| < 20 \text{ ppm OR} \\
&\frac{|y_{\text{NOx,TP,meas}} - y_{\text{NOx,TP,DG model}}|}{y_{\text{NOx,TP,meas}}} < 0.2 \text{ OR} \\
&|y_{\text{NOx,TP,meas}} - y_{\text{NOx,TP,EUL model}}| < 20 \text{ ppm OR} \\
&\frac{|y_{\text{NOx,TP,meas}} - y_{\text{NOx,TP,EUL model}}|}{y_{\text{NOx,TP,meas}}} < 0.2 \text{ OR} \\
&y_{\text{NOx,TP,DG model}} < y_{\text{NOx,TP,meas}} < y_{\text{NOx,TP,EUL model}}
\end{aligned}
\tag{5.1}
$$

The threshold in modeling error is chosen to be 20 ppm or 20%, because the commercial NOx sensor has an uncertainty of 10 ppm or 10%, and the maximum average modeling error in tailpipe NOx across the three drive cycles was slightly less than 10 ppm. So, the measurement and modeling uncertainty were combined to choose 20 ppm or 20% as the threshold for this enable condition.

3. **Filter 3:** From the points selected after the first two steps, **select points where differences between DG and EUL catalysts can be expected based on the SCR-ASC model**. This can be quantified either based on %deNOx or TP NOx. For %deNOx-based filter 3, the points where $(\eta_{\text{deNOx,DG model}} - \eta_{\text{deNOx,EUL model}}) > 10\%$ are selected. The threshold for %deNOx-based separation was chosen as 10% based on observations from test-cell data such that it is not too low to be affected by measurement or modeling errors and not too high to exclude a lot of points from the data.

   The other option for this enable condition is to quantify the separation in DG and EUL catalysts based on TP NOx, where the points that satisfy all of the following conditions are selected:

$$
\begin{aligned}
&y_{\text{NOx,TP,EUL model}} - y_{\text{NOx,TP,DG model}} > 20 \text{ ppm AND} \\
&\frac{y_{\text{NOx,TP,EUL model}} - y_{\text{NOx,TP,DG model}}}{y_{\text{NOx,TP,DG model}}} > 0.2 \text{ AND} \\
&\frac{y_{\text{NOx,TP,EUL model}} - y_{\text{NOx,TP,DG model}}}{y_{\text{NOx,TP,EUL model}}} > 0.2
\end{aligned}
\tag{5.2}
$$

Since the modeling error in tailpipe NOx for both DG and EUL catalyst models is up to 10 ppm, a difference of up to 20 ppm in $y_{\text{NOx,TP,DG model}}$ and $y_{\text{NOx,TP,EUL model}}$ could be because of modeling error. So, to ensure that the difference is due to an aging signature, 20 ppm or 20% was chosen as the threshold to quantify the separation based on tailpipe NOx.

4. **Filter 4:** From the points selected after the first three steps, **select points where the tailpipe NH_3 is too low for cross-sensitivity to significantly affect tailpipe NOx sensor readings.** In the existing literature, 2 is reported as the maximum cross-sensitivity factor [43]. So, this enable condition should select points where the tailpipe NOx sensor reading with maximum cross-sensitivity, $y_{\text{NOx}} + 2y_{\text{NH}_3}$, is not too different from the true reading, y_{NOx}, to affect the result of diagnostics. Therefore, this enable condition selects the points that satisfy the following conditions:

$$\begin{bmatrix} 2y_{\text{NH}_3\text{,TP,DG model}} < 5 \text{ ppm} \\ \text{OR} \\ 2y_{\text{NH}_3\text{,TP,DG model}} < 0.05y_{\text{NOx,TP,DG model}} \end{bmatrix}$$
$$\text{AND}$$
$$\begin{bmatrix} 2y_{\text{NH}_3\text{,TP,EUL model}} < 5 \text{ ppm} \\ \text{OR} \\ 2y_{\text{NH}_3\text{,TP,EUL model}} < 0.05y_{\text{NOx,TP,EUL model}} \end{bmatrix}$$

Since the goal of this enable condition is to select points where y_{NH_3} is too small for cross-sensitivity to affect the result of diagnostics, the threshold was chosen as 25% of the thresholds in Filter 2 and Filter 3.

5.2 Diagnostic criteria

For a perfect model and with perfect TP NOx measurements, the TP NOx measurements from a DG catalyst can be expected to overlap with the TP NOx estimated from the DG model. As the catalyst degrades, the TP NOx measurements will be higher than the value estimated by the DG model, and their difference will be higher for higher degradation. For an EUL catalyst, the measurement will overlap with the value estimated by the EUL model. However, there will be false positives and false negatives because of uncertainties in the model and imperfect measurements. This means that the TP NOx measurements can be closer to the DG model at some sample points and to the EUL model at others. However, if the enable conditions are designed effectively to minimize false positives and false negatives then the TP NOx measurements will align with the correct model according to the aging level. Based on this, the following diagnostic metric is defined to be applied to the points selected after the four filters in Section 5.1.

The key idea in this metric is to classify each point, selected after applying the enable conditions, as either DG, EUL, or none. Let N_{DG} and N_{EUL} be the number of points classified as DG and EUL, respectively. Then the degradation level is quantified by the ratio of N_{EUL} to N_{DG}. Higher $N_{\text{EUL}}/N_{\text{DG}}$ would imply higher degradation.

The diagnostic metric classifies a point as DG if the measured TP NOx is closer to the value estimated by the DG model than the one by the EUL model, i.e.

$$|e_{\text{NOx,TP,DG model}}| < |e_{\text{NOx,TP,EUL model}}|,$$

where

$$e_{\text{NOx,TP,DG model}} = y_{\text{NOx,TP,meas}} - y_{\text{NOx,TP,DG model}}$$
$$e_{\text{NOx,TP,EUL model}} = y_{\text{NOx,TP,meas}} - y_{\text{NOx,TP,EUL model}}$$

Similarly, a point is classified as EUL if the measured TP NOx is closer to the value estimated by the EUL model than the one by the DG model, i.e.

$$|e_{\text{NOx,TP,DG model}}| > |e_{\text{NOx,TP,EUL model}}|$$

Note that every point is guaranteed to be classified as either DG or EUL by this metric.

Also note that this diagnostic metric is designed to compare the degradation level across various catalysts. Therefore, rather than giving an absolute aging level, it will give aging level relative to a baseline catalyst with known aging level.

5.3 Results with test-cell data

We will now apply the enable conditions in Section 5.1 to monitor both DG and EUL catalysts during the three drive cycles in test-cell data:

1. **Filter 1**: We run both DG and EUL models for all three cycles, and only select points where SCR-bed temperature is greater than 200^{o}C.

2. **Filter 2**: We then select the points where the model behaves reasonably. It can be observed from Table 5.1 that this filter removes less than 5% of the points selected after the first filter. This implies that the model behaves reasonably in all three cycles for almost every point where the temperature is greater than 200^{o}C, which is expected because of good agreement between test-cell data and models.

3. **Filter 3**: From the points selected after applying the first two filters, this filter selects the points where aging signature can be expected based on DG and EUL catalyst models. This can be quantified either based on %deNOx efficiency or TP NOx from DG and EUL models. It can be observed from Table 5.1 that this filter removes most of the points. Based on %deNOx, very few but non-zero number of points are selected from all three cycles. However, no points are selected from cFTP and hFTP cycles if the filter is applied based on TP NOx.

4. **Filter 4**: This filter selects points where the TP NH_3, from both EUL and DG catalysts, is too low for cross-sensitivity to affect the OBD results. Over the three drive cycles, this filter removed 78% of the points selected after %deNOx-based filter 3 and no points were selected from the RMC cycle. When applied to the points selected after TP NOx-based filter 3, only 1.2% of the points got selected after this filter. In this case, all the selected points are from RMC because the TP NOx-based filter 3 removed all points from cFTP and hFTP.

Table 5.1. Number of points selected in test-cell data after applying the enable conditions

<table>
<tr><td colspan="2"></td><td colspan="2">cFTP</td><td colspan="2">hFTP</td><td colspan="2">RMC</td></tr>
<tr><td colspan="2"></td><td>DG</td><td>EUL</td><td>DG</td><td>EUL</td><td>DG</td><td>EUL</td></tr>
<tr><td colspan="2">Total no. of points</td><td>6014</td><td>6013</td><td>6012</td><td>6012</td><td>12005</td><td>12005</td></tr>
<tr><td colspan="2">Filter 1: No. of points where T>200^oC</td><td>2864</td><td>2885</td><td>3173</td><td>3177</td><td>12005</td><td>12005</td></tr>
<tr><td colspan="2">Filter 2: No. of points where model is reasonable</td><td>2863</td><td>2885</td><td>3170</td><td>3174</td><td>11458</td><td>11362</td></tr>
<tr><td rowspan="2">Filter 3: No. of points where aging signature is expected based on DG and EUL models</td><td>Based on %deNOx</td><td>37</td><td>55</td><td>138</td><td>38</td><td>18</td><td>46</td></tr>
<tr><td>Based on TP NOx</td><td>0</td><td>0</td><td>0</td><td>0</td><td>1177</td><td>879</td></tr>
<tr><td rowspan="2">Filter 4: No. of points where TP NH_3 is too low for cross-sensitivity</td><td>after %deNOx-based filter 3</td><td>8</td><td>0</td><td>55</td><td>9</td><td>0</td><td>0</td></tr>
<tr><td>after TP NOx-based filter 3</td><td>0</td><td>0</td><td>0</td><td>0</td><td>1</td><td>24</td></tr>
</table>

After filtering the data using enable conditions, the diagnostic metric was applied to the selected points. It can be observed from Table 5.2 that the diagnostic metric correctly classified all points from the DG catalyst as DG for all three cycles, resulting in $N_{\text{EUL}}/N_{\text{DG}} = 0$. For the EUL catalyst, this metric correctly classified 22 points as EUL out of 24 points selected from the RMC cycle by TP NOx-based enable conditions, resulting in $N_{\text{EUL}}/N_{\text{DG}} = 22/2 = 11$. However, this metric incorrectly classified all 9 points selected from hFTP by %deNOx-based enable conditions as DG for the EUL catalyst. These results were combined over the three drive cycles and are shown in Table 5.3. It can be observed from Table 5.3 that %deNOx-based enable conditions selected 72 points whereas only 25 points were selected by TP NOx-based enable conditions. None of the enable conditions resulted in false positives, i.e., DG catalyst identified as EUL. For %deNOx-based enable conditions, 9 out of 72 points resulted in false negatives, i.e., EUL catalyst reported as DG, and only 2 out of 25 points for

TP NOx-based enable conditions resulted in false negatives. These results show that the TP NOx-based enable conditions are more selective and hence more robust to false negatives.

Table 5.2. Results of applying diagnostic metric to the test-cell data selected after applying the enable conditions (Filters 1 to 4).

		cFTP		hFTP		RMC	
		DG	EUL	DG	EUL	DG	EUL
%deNOx-based enable conditions	No. of points selected after applying Filters 1 to 4	8	0	55	9	0	0
	$N_{\mathrm{EUL}}/N_{\mathrm{DG}}$	0/8	0/0	0/55	0/9	0/0	0/0
TP NOx-based enable conditions	No. of points selected after applying Filters 1 to 4	0	0	0	0	1	24
	$N_{\mathrm{EUL}}/N_{\mathrm{DG}}$	0/0	0/0	0/0	0/0	0/1	22/2

Testing OBD method's robustness to cross-sensitivity and measurement noise: Since the OBD has to work with commercial NOx sensors on trucks, it is important to test its robustness to cross-sensitivity and measurement noise. The cross-sensitivity factor can change as a function of other signals such as temperature, but the worst-case scenario was simulated in test-cell data by using the maximum possible value of 2 for the cross-sensitivity factor. Since commercial tailpipe NOx sensors have measurement error up to 10 ppm, the measurement noise was simulated using a Gaussian distribution with zero mean and 10/3 ppm of standard deviation (since 99% of values sampled from a Gaussian distribution lie within ±3 times the standard deviation). Therefore, cross-sensitivity and measurement noise were simulated in test-cell data using the following equation:

$$y_{\mathrm{NOx,simulated}} = y_{\mathrm{NOx,TP,meas}} + 2y_{\mathrm{NH_3,TP,meas}} + \mathcal{N}(0, (10/3)^2)$$

Then instead of $y_{\mathrm{NOx,TP,meas}}$, $y_{\mathrm{NOx,simulated}}$ was compared to model-out TP NOx when applying the enable conditions and the diagnostic metric. The results of this exercise are shown in Table 5.3. It can be observed from Table 5.3 that almost identical results were obtained for a cross-sensitive NOx signal without measurement noise, suggesting that the enable conditions and the diagnostic metric are robust to cross-sensitivity. Addition of noise to the cross-sensitivity signal resulted in some false positives, but the majority of points were still correctly classified as degreened or EUL. Therefore, the diagnostic metric can be considered to be robust to both cross-sensitivity and noise.

Table 5.3. OBD results combined over the three drive-cycles for clean, cross-sensitive, and noisy tailpipe NOx sensor readings.

		Perfect TP NOx measurement ($y_{\mathrm{NOx,TP,meas}}$)	With cross-sensitivity ($y_{\mathrm{NOx,TP,meas}}$ $+2y_{\mathrm{NH_3,TP,meas}}$)	With cross-sensitivity and noise ($y_{\mathrm{NOx,TP,meas}}$ $+2y_{\mathrm{NH_3,TP,meas}}$ $+\mathcal{N}(0,(10/3)^2)$)
%deNOx-based enable conditions	Points selected	72	72	72
	Correctly identified as DG	63	63	58
	False positive (DG identified as EUL)	0	0	5
	Correctly identified as EUL	0	0	7
	False negative (EUL identified as DG)	9	9	2
Tailpipe NOx-based enable conditions	Points selected	25	25	25
	Correctly identified as DG	1	1	1
	False positive (DG identified as EUL)	0	0	0
	Correctly identified as EUL	22	23	20
	False negative (EUL identified as DG)	2	1	4

5.4 Results with truck data

The number of points selected from each truck after applying the enable conditions are shown in Table 5.4. Note that filter 2, which selects the points where the model behaves reasonably, is more selective for truck data than the test-cell data. In test-cell data, this filter removed less than 5% of the points selected after filter 1, which was expected because the model was calibrated on test-cell data. But in truck data, only 43% to 83% points were selected after filter 2. This was still a significant number of points as more than 18000 points were selected from all trucks. Filter 3, which selects the points where aging signature can be expected based on DG and EUL catalyst models, removed a significant number of points as it did for test-cell data. Based on %deNOx, filter 3 selected less than 0.6% of the points remaining after filter 2 from all four trucks. It was less restrictive based on tailpipe NOx as up to 32% of the points were selected. For the points selected after %deNOx-based filter 3, the cross-sensitivity based filter 4 selected 75% of the points. And it selected 67% of the points selected after TP NOx-based filter 3.

Table 5.4. Number of points selected in truck data after applying the enable conditions

<table>
<tr><td colspan="2"></td><td>Truck 1</td><td>Truck 2</td><td>Truck 3</td><td>Truck 4</td></tr>
<tr><td colspan="2">Total no. of points</td><td>33834</td><td>66133</td><td>79987</td><td>69848</td></tr>
<tr><td colspan="2">Filter 1: No. of points where T>200^oC</td><td>32036</td><td>57852</td><td>67500</td><td>55678</td></tr>
<tr><td colspan="2">Filter 2: No. of points where model is reasonable</td><td>18515</td><td>47919</td><td>41591</td><td>24253</td></tr>
<tr><td rowspan="2">Filter 3: No. of points where aging signature is expected based on DG and EUL models</td><td>Based on %deNOx</td><td>46</td><td>89</td><td>253</td><td>137</td></tr>
<tr><td>Based on TP NOx</td><td>619</td><td>272</td><td>13286</td><td>2284</td></tr>
<tr><td rowspan="2">Filter 4: No. of points where TP NH_3 is too low for cross-sensitivity</td><td>after %deNOx-based filter 3</td><td>28</td><td>86</td><td>159</td><td>121</td></tr>
<tr><td>after TP NOx-based filter 3</td><td>477</td><td>254</td><td>8823</td><td>1503</td></tr>
</table>

The results of applying the diagnostic metrics to points selected from both %deNOx-based and tailpipe NOx-based enable conditions are shown in Table 5.5. $N_{\mathrm{EUL}}/N_{\mathrm{DG}}$ vs the number of miles on each truck is shown in Figure 5.2. Higher $N_{\mathrm{EUL}}/N_{\mathrm{DG}}$ implies higher degradation, therefore the plots in Figure 5.2 show the aging trends reported by the diagnostic metrics vs the number of miles on each truck.

Since the actual degradation levels on these trucks is not known, the results can't be validated yet. However, it is encouraging that the diagnostic metric gave almost identical trends for both types of enable conditions. The only difference between the two trends is that the truck with 484k miles is reported to be more aged than the one with 271k miles for %deNOx-based enable conditions and vice versa for TP NOx-based enable conditions. This is because factors such as DPF regeneration, and different driving styles could result in

Table 5.5. Results of applying diagnostic metrics to the truck data selected after applying the enable conditions (Filters 1 to 4) based on %deNOx and tailpipe NOx.

		Truck 1	Truck 2	Truck 3	Truck 4
%deNOx-based enable conditions	No. of points selected after applying Filters 1 to 4	28	86	159	121
	$N_{\mathrm{EUL}}/N_{\mathrm{DG}}$	1/27	43/43	63/96	71/50
TP NOx-based enable conditions	No. of points selected after applying Filters 1 to 4	477	254	8823	1503
	$N_{\mathrm{EUL}}/N_{\mathrm{DG}}$	180/297	127/127	2126/6697	886/617

higher degradation on a truck with lesser miles on it. Another consistent result from both enable conditions is that the truck with 711 kmiles is reported to have significantly higher degradation compared to the other three trucks. Even though these results could not be validated yet, mostly similar and sensible trends using different enable conditions increase the confidence in the relative aging levels, and is an encouraging result.

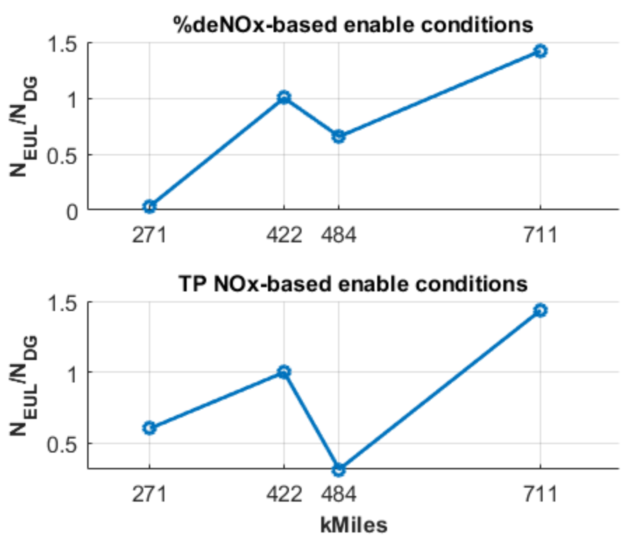

Figure 5.2. Aging trends reported by diagnostic metrics vs the number of miles on each truck. Higher $N_{\mathrm{EUL}}/N_{\mathrm{DG}}$ implies higher degradation

5.5 Impact of uncertainty in initial NH_3 storage on OBD results

For the results presented so far, the model was run assuming zero initial NH_3 storage. However, the initial NH_3 storage would be non-zero during most of the operation of a truck. Therefore, it is important to analyze the robustness of the OBD method to uncertainty in initial NH_3 storage. To do this, both degreened and EUL models were run for 100 different values of initial NH_3 storage fraction from 0 to 1, in increments of 0.01, for each truck. The OBD method was then applied to the truck data to calculate the $N_{\mathrm{EUL}}/N_{\mathrm{DG}}$ ratio for each initial NH_3 storage fraction for each truck, which is plotted in Figure 5.3. It can be observed from Figure 5.3 that $N_{\mathrm{EUL}}/N_{\mathrm{DG}}$ ratio, and hence the aging trend reported by the diagnostic metric across the four trucks, changes significantly with the initial NH_3 storage value, which implies that the OBD is not robust to uncertainty in initial NH_3 storage.

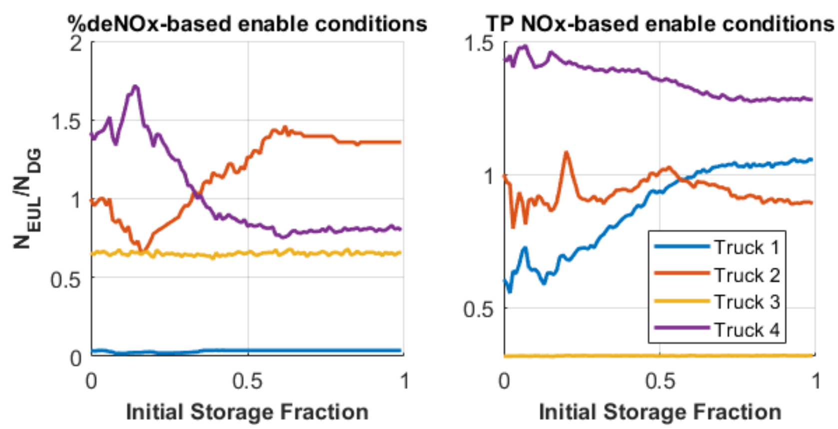

Figure 5.3. $N_{\mathrm{EUL}}/N_{\mathrm{DG}}$ vs initial NH_3 storage fraction before incorporating the enable condition designed to handle the uncertainty in initial NH_3 storage.

5.5.1 Designing an enable condition to make the OBD robust to uncertainty in initial NH_3 storage

Since the OBD method uses model-out tailpipe NOx and NH_3 values, the time-series of tailpipe NOx and tailpipe NH_3 of the model run with different initial NH_3 storage values were analyzed to determine the cause of the OBD method's high sensitivity to initial NH_3 storage value. Since the model was run for 100 different values of initial NH_3 storage, it resulted in 100 different values of tailpipe NOx and NH_3 at each time-stamp. To visualize the impact of the initial NH_3 storage on these signals, the difference between the maximum and minimum value at each time-stamp was plotted for both tailpipe NOx and NH_3. This was done for the entire truck data, but a segment of the data is shown in Figure 5.4 to demonstrate the key result of this analysis. It can be observed from Figure 5.4 that the difference between maximum and minimum value, of both tailpipe NOx and NH_3 across all initial NH_3 storage values, converges to almost zero in less than 10 minutes. This implies that all initial NH_3 storage values converge to almost identical values of model-out tailpipe NOx and NH_3 values in around 10 minutes.

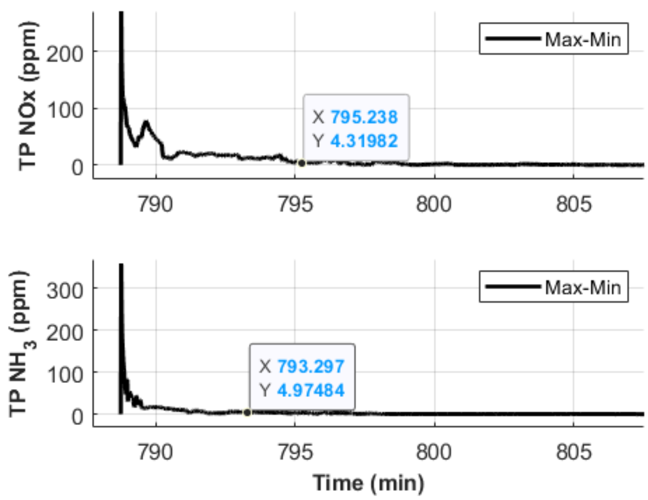

Figure 5.4. Time-series plot of difference between maximum and minimum value of model-out tailpipe NOx and NH_3 across all initial NH_3 storage values.

Therefore, to make the OBD method robust to uncertainty in initial NH_3 storage ($x_{3,0}$), another enable condition is added to only select points where the maximum variation in model-out tailpipe NOx and NH_3 due to uncertainty in initial NH_3 storage is less than 5 ppm for both degreened and EUL models. This enable condition is defined as Filter 5, and selects the points that satisfy the following conditions:

$$\left[\begin{array}{c}\max\limits_{x_{3,0}\in(0,1)}(y_{\text{NOx,TP,DG model}}) - \min\limits_{x_{3,0}\in(0,1)}(y_{\text{NOx,TP,DG model}}) < 5\text{ppm} \\ \text{AND} \\ \max\limits_{x_{3,0}\in(0,1)}(y_{\text{NH}_3\text{,TP,DG model}}) - \min\limits_{x_{3,0}\in(0,1)}(y_{\text{NH}_3\text{,TP,DG model}}) < 5\text{ppm}\end{array}\right]$$

AND

$$\left[\begin{array}{c}\max\limits_{x_{3,0}\in(0,1)}(y_{\text{NOx,TP,EUL model}}) - \min\limits_{x_{3,0}\in(0,1)}(y_{\text{NOx,TP,EUL model}}) < 5\text{ppm} \\ \text{AND} \\ \max\limits_{x_{3,0}\in(0,1)}(y_{\text{NH}_3\text{,TP,EUL model}}) - \min\limits_{x_{3,0}\in(0,1)}(y_{\text{NH}_3\text{,TP,EUL model}}) < 5\text{ppm}\end{array}\right]$$

5.5.2 Number of points selected for diagnostics after applying Filter 5

The results of applying this enable condition to test-cell data are shown in Table 5.6. It can be observed that Filter 5 removed all the points that were selected from cFTP and hFTP cycles after applying the first four %deNOx-based enable conditions. Filter 5 did not remove any points that were selected from the RMC cycle by tailpipe NOx-based enable conditions. The five enable conditions are designed to make the OBD robust to modeling errors, cross-sensitivity, and uncertainty in initial NH_3 storage but the results from Table 5.6 show that these enable conditions lead to a very small IUMPR for the test-cell data. This demonstrates the difficulty in designing enable conditions that are robust and yet lead to a high IUMPR.

The results of applying Filter 5 to truck data are summarized in Table 5.7. Compared to test-cell data, a reasonable number of points were selected from all four trucks after applying the five enable conditions. This is because the on-road driving cycles on trucks are much longer than the FTP and RMC cycles, which results in more opportunities for the OBD to get enabled.

Table 5.6. Results of applying the initial NH_3 storage-based enable condition, Filter 5, to test-cell data.

		cFTP		hFTP		RMC	
		DG	EUL	DG	EUL	DG	EUL
%deNOx-based enable conditions	No. of points selected after applying Filters 1 to 4	8	0	55	9	0	0
	No. of points selected after applying Filter 5	0	0	0	0	0	0
	$N_{\mathrm{EUL}}/N_{\mathrm{DG}}$	0/0	0/0	0/0	0/0	0/0	0/0
TP NOx-based enable conditions	No. of points selected after applying Filters 1 to 4	0	0	0	0	1	24
	No. of points selected after applying Filter 5	0	0	0	0	1	24
	$N_{\mathrm{EUL}}/N_{\mathrm{DG}}$	0/0	0/0	0/0	0/0	0/1	22/2

5.5.3 OBD method's robustness to uncertainty in initial NH_3 storage after incorporating Filter 5

The $N_{\mathrm{EUL}}/N_{\mathrm{DG}}$ ratio vs initial NH_3 storage fraction for each truck after incorporating this enable condition is shown in Figure 5.5. It can be observed from Figure 5.5 that the $N_{\mathrm{EUL}}/N_{\mathrm{DG}}$ ratio remains almost constant across different initial NH_3 storage, which implies that the aging trend reported by the OBD is now robust to uncertainty in initial NH_3 storage.

5.6 Stochastic model-based OBD

The model-based approach discussed so far does binary classification as it classifies each sample point as either degreened or EUL. In this section, a stochastic model-based OBD method is introduced, which can assign a non-binary value proportional to the probability of a sample point belonging to a degreened or an EUL catalyst. Note that the stochastic model-based OBD method presented in this work is a preliminary attempt to demonstrate the feasibility of this approach and lay the foundation for a more detailed implementation in future work.

Table 5.7. Results of applying initial NH_3 storage-based enable condition, Filter 5, to truck data.

		Truck 1	Truck 2	Truck 3	Truck 4
%deNOx-based enable conditions	No. of points selected after applying Filters 1 to 4	28	86	159	121
	No. of points selected after applying Filter 5	27	74	157	103
	$N_{\mathrm{EUL}}/N_{\mathrm{DG}}$	1/26	40/34	61/96	58/45
TP NOx-based enable conditions	No. of points selected after applying Filters 1 to 4	477	254	8823	1503
	No. of points selected after applying Filter 5	350	203	8744	1397
	$N_{\mathrm{EUL}}/N_{\mathrm{DG}}$	144/206	114/89	2111/6633	857/540

5.6.1 Stochastic model obtained using simplified Bayesian model calibration

For this approach, a stochastic version of the SCR-ASC model is derived using a simplified version of the Bayesian approach for model calibration. An introduction to the Bayesian approach for model calibration could be found in Lecture 20 of the Spring 2020 course on "Introduction to Uncertainty Quantification" by Dr. Ilias Bilionis at Purdue University [45].

The main goal of the Bayesian approach is to find a probability density function, instead of a single value, for the model parameters. Let $\theta \in \mathbb{R}^{12}$ be the unknown parameters of the SCR-ASC model, y be the tailpipe measurements, and $f(\theta)$ be the SCR-ASC model represented as a function that takes parameter values as the input and gives model-out tailpipe values for a particular drive cycle in test-cell data as the output. The key idea is to define:

1. **A prior probability density** for θ, $p_{\mathrm{prior}}(\theta)$, based on any prior knowledge about the parameters that is available before looking at the measurements.

2. **A likelihood model** $p_{\mathrm{likeli}}(y \mid f(\theta))$, which should be defined such that it satisfies the properties of a probability density function and is a non-increasing monotonic

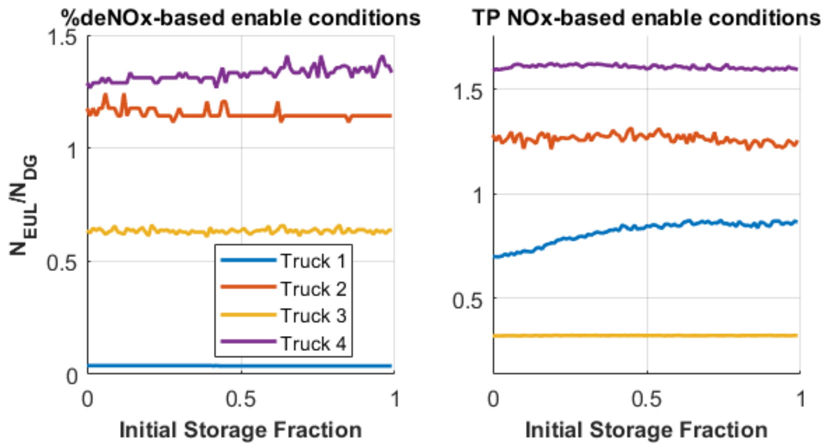

Figure 5.5. $N_{\mathrm{EUL}}/N_{\mathrm{DG}}$ vs initial NH_3 storage fraction after incorporating the enable condition designed to handle the uncertainty in initial NH_3 storage (Filter 5).

function of the modeling error, which can be defined as $\|y - f(\theta)\|^2$. In other words, $p_{\mathrm{likeli}}(y \mid f(\theta))$ should increase as the modeling error is decreased. A common choice for the likelihood is a Gaussian distribution with mean at $f(\theta)$ and a tunable standard deviation σ.

$$p_{\mathrm{likeli}}(y \mid f(\theta)) = \mathcal{N}(y \mid f(\theta), \sigma^2), \tag{5.3}$$

where $\mathcal{N}(x \mid \mu, \sigma^2)$ denotes the value of the probability density of a Gaussian distribution, with mean μ and standard deviation σ, at x.

Using the Bayes rule, the posterior probability density, $p_{\mathrm{post}}(\theta \mid y)$, on parameter θ, given the measurements y, is:

$$p_{\mathrm{post}}(\theta \mid y) \propto p_{\mathrm{likeli}}(y \mid f(\theta)) p_{\mathrm{prior}}(\theta) \tag{5.4}$$

Equation 5.4 implies that the posterior probability density will be higher for the parameters that result in good model fit and are close to the values based on prior knowledge. In other words, the posterior probability density will be low at parameters that:

- result in poor model fit and are far from the value based on prior knowledge,

- result in good model fit but are very far from the value based on prior knowledge, and

- are close to the value based on prior knowledge but result in very poor model fit.

In this work, there is no prior information available about the parameters, and hence p_{prior} can be considered uniform, which implies that

$$p_{\text{post}}(\theta \mid y) \propto p_{\text{likeli}}(y \mid f(\theta)) = \mathcal{N}(y \mid f(\theta), \sigma^2) \propto \mathrm{e}^{-\frac{\|y-f(\theta)\|^2}{2\sigma^2}}.$$

For this work,

$$p_{\text{post}}(\theta \mid y) = p_{\text{post}}(\theta \mid y_{\text{TPNOx,meas,RMC}}) = 3\mathrm{e}^{-\frac{\left\|e_{\text{NOx,RMC}}\right\|^2}{2\times10^6}}, \tag{5.5}$$

where $e_{\text{NOx,RMC}}$ is the difference between measured ($y_{\text{TPNOx,meas,RMC}}$) and model-out tailpipe NOx for the RMC cycle. The tailpipe NOx signal was chosen because OBD has to work using tailpipe NOx measurements, and RMC cycle was chosen because it covers a wider range of tailpipe NOx than cFTP and hFTP. The proportionality constant of 3, and $\sigma = 1000$ were chosen so that the maximum value of p_{post} is close to 1, which would make it easier to design thresholds for the OBD method. Note that p_{post} will be higher for parameters that give better fit on the tailpipe NOx signal in RMC cycle.

After defining the posterior probability density, the next step in the Bayesian approach is to sample the parameter values from this distribution. This process is not trivial and advanced methods such as Markov Chain Monte Carlo sampling are used because usually it is not possible to obtain an analytical formulation of the posterior probability density. For the simplified approach in this work, the parameters for both degreened and EUL models are sampled as follows:

1. Sample 500 parameter values from a Gaussian distribution with mean at the parameter values obtained after the traditional model calibration in Section 4.3.5, and standard deviation at one tenth of the mean value.

2. Run the model and calculate p_{post}, using Equation 5.5, for each parameter value sampled in step 1.

3. Pick 20 parameters with the highest p_{post} values.

These 20 parameters, with the corresponding p_{post} values parametrize the stochastic SCR-ASC model, which will be used to formulate the stochastic model-based OBD approach discussed in the next section.

5.6.2 OBD method based on the stochastic model

The key idea for this method is still to compare the measured tailpipe NOx to the model-out tailpipe NOx from both degreened and EUL models. In the previous method, a single value of measured tailpipe NOx was compared to a single model-out value from both degreened and EUL models at each time-stamp to classify a sample point as either degreened or EUL. Instead of binary classification at each time-stamp, this method will use the probability distribution of the measurement noise and the posterior distribution on 20 parameters, sampled for the stochastic model, to calculate a non-binary value that is proportional to the probability of the measured tailpipe NOx value belonging to a degreened or an EUL catalyst.

The following steps describe the method in detail:

1. Similar to the previous OBD method, the first enable condition for this method is to select points where the temperature is greater than 200^oC because the look-up tables in the SCR-ASC model can't work at temperatures lower than 200^oC. This enable condition is identical to Filter 1, which was defined in Section 5 for the previous method.

2. At any time-stamp, there is one tailpipe NOx value from the measurement ($y_{\text{TPNOx,meas}}$), and 20 tailpipe NOx values from the 20 parameters sampled for each of the degreened and the EUL models. Let $y_{\text{TPNOx},\theta_{\text{model},i}}$ be the model-out tailpipe NOx values using the i^{th} parameter value sampled for that model. Whenever required, the subscript "model" in $y_{\text{TPNOx},\theta_{\text{model},i}}$ will be replaced by "DG" or "EUL" to refer specifically to the degreened or the EUL model, respectively. Let $p_{\text{meas}}(y_{\text{TPNOx},\theta_{\text{model},i}})$ be the probability density of measurement noise at $y_{\text{TPNOx},\theta_{\text{model},i}}$. Since commercial tailpipe NOx sensors

have measurement error up to 10 ppm, p_{meas} is assumed to be Gaussian with zero mean and 10/3 ppm of standard deviation (since 99% of values sampled from a Gaussian distribution lie within ±3 times the standard deviation). Therefore, $p_{\text{meas}}(y_{\text{TPNOx},\theta_{\text{model},i}})$ is given by:

$$\begin{aligned} p_{\text{meas}}(y_{\text{TPNOx},\theta_{\text{model},i}}) &= \mathcal{N}(y_{\text{TPNOx},\theta_{\text{model},i}} - y_{\text{TPNOx,meas}} \mid 0, (10/3)^2) \\ &= \frac{1}{3.33\sqrt{2\pi}} \mathrm{e}^{-\frac{(y_{\text{TPNOx},\theta_{\text{model},i}} - y_{\text{TPNOx,meas}})^2}{2(3.33)^2}}, \end{aligned} \tag{5.6}$$

To make it easier to define thresholds for the OBD method, p_{meas} in Equation 5.6 will be scaled so that the maximum value of p_{meas} is close to one. After scaling, p_{meas} is given by

$$p_{\text{meas}}(y_{\text{TPNOx},\theta_{\text{model},i}}) = \mathrm{e}^{-\frac{(y_{\text{model},\theta_i} - y_{\text{TPNOx,meas}})^2}{2(3.33)^2}}. \tag{5.7}$$

3. Let $\theta_{\text{DG},i}$ and $\theta_{\text{EUL},i}$ be the i^{th} parameters sampled for the degreened and the EUL models, respectively. Using Equation 5.5, calculate

$$\begin{aligned} p_{\text{post}}(\theta_{\text{DG},i} \mid y_{\text{TPNOx,meas,RMC,DG}}) &= 3\mathrm{e}^{-\frac{\left\| y_{\text{TPNOx},\theta_{\text{DG},i}} - y_{\text{TPNOx,meas,RMC,DG}} \right\|^2}{2\times 10^6}}, \\ p_{\text{post}}(\theta_{\text{EUL},i} \mid y_{\text{TPNOx,meas,RMC,EUL}}) &= 3\mathrm{e}^{-\frac{\left\| y_{\text{TPNOx},\theta_{\text{EUL},i}} - y_{\text{TPNOx,meas,RMC,EUL}} \right\|^2}{2\times 10^6}} \end{aligned} \tag{5.8}$$

   for every $i \in \{1, 2, \ldots, 20\}$.

4. Calculate the following joint probability densities at $y_{\text{TPNOx},\theta_{\text{DG},i}}$ and $y_{\text{TPNOx},\theta_{\text{EUL},i}}$ for every $i \in \{1, 2, \ldots, 20\}$:

$$\begin{aligned} p_{\text{joint,DG}}(y_{\text{TPNOx},\theta_{\text{DG},i}}) &= p_{\text{meas}}(y_{\text{TPNOx},\theta_{\text{DG},i}}) p_{\text{post}}(\theta_{\text{DG},i} \mid y_{\text{TPNOx,meas,RMC,DG}}) \\ p_{\text{joint,EUL}}(y_{\text{TPNOx},\theta_{\text{EUL},i}}) &= p_{\text{meas}}(y_{\text{TPNOx},\theta_{\text{EUL},i}}) p_{\text{post}}(\theta_{\text{EUL},i} \mid y_{\text{TPNOx,meas,RMC,EUL}}) \end{aligned} \tag{5.9}$$

5. Integrate $p_{\text{joint,DG}}(y_{\text{TPNOx},\theta_{\text{DG},i}})$ and $p_{\text{joint,EUL}}(y_{\text{TPNOx},\theta_{\text{EUL},i}})$ as follows to calculate the probability of $y_{\text{TPNOx,meas}}$ belonging to a degreened (P_{DG}) or an EUL (P_{EUL}) catalyst.

$$
\begin{aligned}
P_{\text{DG}} &= \int_{i=1}^{20} p_{\text{joint,DG}}(y_{\text{TPNOx},\theta_{\text{DG},i}}) \\
P_{\text{EUL}} &= \int_{i=1}^{20} p_{\text{joint,EUL}}(y_{\text{TPNOx},\theta_{\text{EUL},i}})
\end{aligned}
\tag{5.10}
$$

This process is visually illustrated in Figure 5.6. P_{DG} is the area shaded in green in Figure 5.6a, and P_{EUL} is the area shaded in red in Figure 5.6.

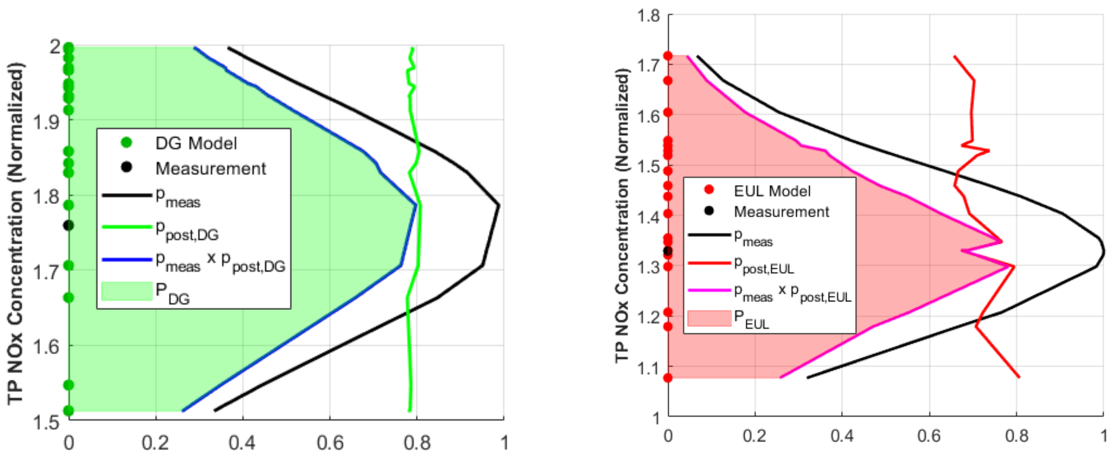

(a) The green area is P_{DG}

(b) The red area is P_{EUL}

Figure 5.6. Visual demonstration of the process of calculating (a) P_{DG} and (b) P_{EUL} at a time-stamp.

6. Then for each sample point, define P_{diff} as

$$
P_{\text{diff}} = P_{\text{DG}} - P_{\text{EUL}}. \tag{5.11}
$$

So, P_{diff} should be a large positive number for a degreened catalyst and a large negative number for an EUL catalyst. A small value of P_{diff} implies an indeterminate aging level resulting from either a small aging signature or poor model performance from both degreened and EUL models. Therefore, $|P_{\text{diff}}| > P_{\text{thres}}$ is added as an enable condition to remove points where the models are unreliable or the aging signatures are too small.

Therefore, this enable condition is equivalent to Filters 2 and 3 in the previous method. Based on observations from the test-cell data, 1.5 is chosen as the threshold P_{thres}. An example of each of the three cases i.e. $P_{\text{diff}} > P_{\text{thres}}$, $P_{\text{diff}} < -P_{\text{thres}}$, and $|P_{\text{diff}}| < P_{\text{thres}}$ is shown in Figure 5.7. For the sample point shown in Figure 5.7a, the measured tailpipe NOx is closer to the twenty model-out tailpipe NOx values from the degreened model than the ones from the EUL model. This implies that the probability of the tailpipe NOx measurement belonging to a degreened catalyst (P_{DG}) is higher than EUL (P_{EUL}), which results in a large positive P_{diff}. Similarly, the probability of the sample point in Figure 5.7b belonging to an EUL catalyst is higher than degreened, which results in a large negative P_{diff}. The sample point in Figure 5.7c is an example of an indeterminate point as it is almost equally likely to belong to either a degreened or an EUL catalyst, which is quantified by a small P_{diff}.

7. The metric reported by this OBD method is the value of P_{diff} averaged over all the points where enable conditions are satisfied. The average value is denoted by $\bar{P}_{\text{diff}}$. Higher $\bar{P}_{\text{diff}}$ implies lower degradation.

Results from applying this OBD method to the test-cell data are summarized in Table 5.8. Note that this OBD results in a much better IUMPR as it gets enabled at 10,291 points across the entire test-cell data, as opposed to only 2,388 points getting selected after applying the first three filters or enable conditions (including both %deNOx-based and TP NOx-based enable conditions) in the previous method.

Table 5.8. Results of applying the stochastic model-based OBD method to the test-cell.

	cFTP		hFTP		RMC	
	DG	EUL	DG	EUL	DG	EUL
No. of points selected after applying enable conditions equivalent to Filters 1 to 3	7	255	47	241	5409	4332
$\bar{P}_{\text{diff}}$	-1.8	-2	0.6	-2	1.7	-2.9

Another observation from Table 5.8 is that $\bar{P}_{\text{diff}}$ is negative for the degreened catalyst in cFTP cycle, which implies a significant number of false positives. It was observed that all false positives were from the start of the cycle where the impact of uncertainty in initial NH_3

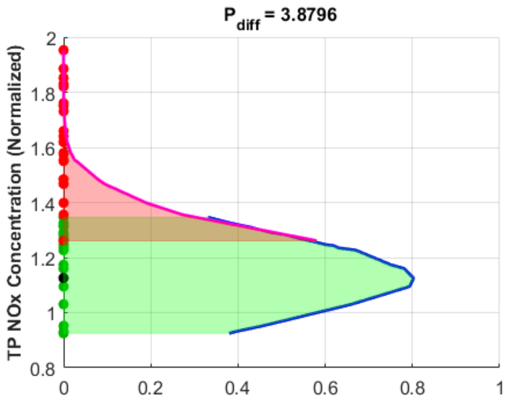

(a) $P_{\mathrm{DG}} > P_{\mathrm{EUL}} \implies P_{\mathrm{diff}} > 1.5$

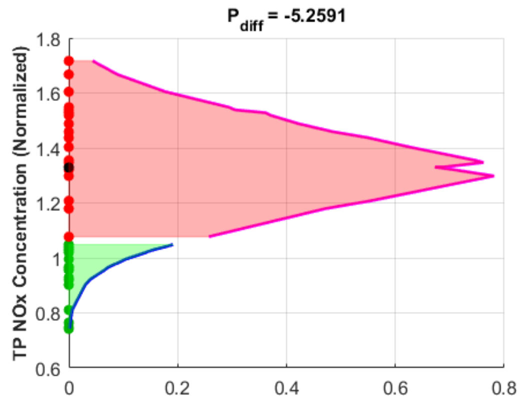

(b) $P_{\mathrm{DG}} < P_{\mathrm{EUL}} \implies P_{\mathrm{diff}} < -1.5$

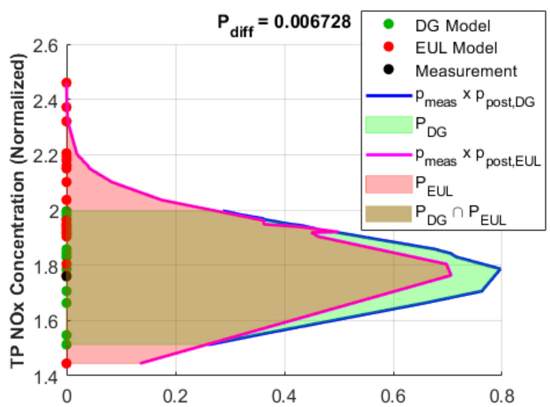

(c) $P_{\mathrm{DG}} \approx P_{\mathrm{EUL}} \implies P_{\mathrm{diff}} \approx 0$

Figure 5.7. An example of each of the three cases: (a) $P_{\mathrm{diff}} > P_{\mathrm{thres}}$, (b) $P_{\mathrm{diff}} < -P_{\mathrm{thres}}$, and (c) $|P_{\mathrm{diff}}| < P_{\mathrm{thres}}$. The OBD will be enabled at the sample points (a) and (b), but not (c).

storage is significant. Therefore, this was fixed by including the initial NH_3 storage-based enable condition, defined by Filter 5 in Section 5.5.1. The results after applying Filter 5 are summarized in Table 5.9.

Table 5.9. Results on test-cell data after incorporating the initial NH_3 storage-based enable condition, Filter 5, in the stochastic model-based OBD method.

	cFTP		hFTP		RMC	
	DG	EUL	DG	EUL	DG	EUL
No. of points selected after applying Filter 5	0	224	2	103	3605	3906
$\bar{P}_{\text{diff}}$	0	-2	1.8	-1.9	2.5	-2.9

5.6.3 Enable condition to make the stochastic OBD method robust to NOx sensor's cross-sensitivity to NH_3

To test the stochastic OBD method's robustness to tailpipe NOx sensor's cross-sensitivity to NH_3, the worst-case cross-sensitivity was simulated in test-cell data by using the maximum possible value of 2 for the cross-sensitivity factor, as shown in Equation 5.12.

$$y_{\text{NOx,cross}} = y_{\text{NOx,TP,meas}} + 2y_{\text{NH}_3\text{,TP,meas}} \tag{5.12}$$

Tailpipe NOx sensor's cross-sensitivity to NH_3 can make a degreened catalyst look like EUL, resulting in false positives. This is demonstrated, in Figure 5.8, by a section of tailpipe NOx vs time data for the degreened catalyst taken from the RMC cycle. The black line is the cross-sensitive NOx signal, $y_{\text{NOx,cross}}$. The green and the red bands show the range of tailpipe NOx values estimated by the stochastic models for the degreened and the EUL catalysts, respectively. It can be observed from Figure 5.8a that the cross-sensitive NOx signal is aligning much better with the values predicted by the EUL model, which results in $P_{\text{EUL}} > P_{\text{DG}}$ leading to $P_{\text{diff}} < -1.5$ as shown in Figure 5.8b. Therefore, the stochastic OBD method would report the degreened catalyst as EUL for the section of data shown in Figure 5.8.

The results of applying the stochastic OBD method on the entire test-cell data with the cross-sensitive tailpipe NOx values ($y_{\text{NOx,cross}}$) are shown in Table 5.10. It can be observed that the $\bar{P}_{\text{diff}}$ is negative for the degreened catalyst for all three cycles, which shows that

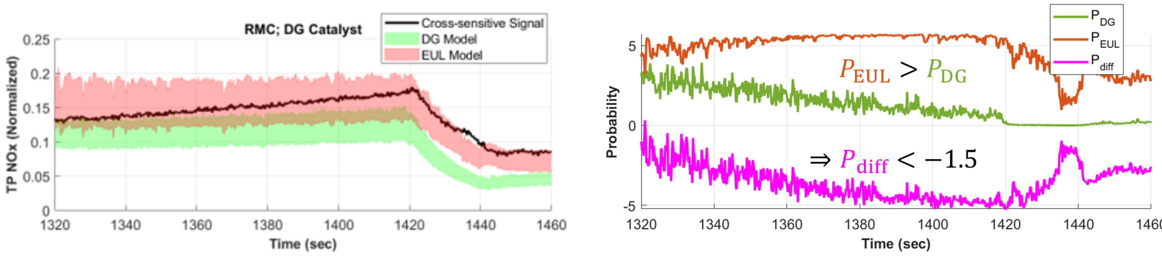

(a) Section of TP NOx vs time data from the RMC cycle for the DG catalyst.

(b) Probability calculations showing $P_{\mathrm{EUL}} > P_{\mathrm{DG}} \implies P_{\mathrm{diff}} < -1.5$

Figure 5.8. Segment of tailpipe NOx vs time data from the RMC cycle demonstrating that cross-sensitivity can make a degreened catalyst look like EUL: (a) the black line, representing the cross-sensitive tailpipe NOx measurement from a DG catalyst, aligns better with the EUL model than the DG model, quantified by the probabilities plotted in (b), which shows that $P_{\mathrm{EUL}} > P_{\mathrm{DG}} \implies P_{\mathrm{diff}} < -1.5$. This demonstrates that cross-sensitivity can make the stochastic OBD method report a degreened catalyst as EUL, leading to false positives.

cross-sensitivity makes the method report the degreened catalyst as EUL for all three cycles in the test-cell data.

Table 5.10. Results of applying the stochastic model-based OBD to test-cell data with cross-sensitive tailpipe NOx measurement (simulated using Equation 5.12).

	cFTP		hFTP		RMC	
	DG	EUL	DG	EUL	DG	EUL
No. of points selected after applying Filters 1, 2, 3, and 5	28	408	27	4	3460	4823
$\bar{P}_{\mathrm{diff}}$	-1.6	-2.5	-1.9	-1.6	-1.1	-3

The key idea to make the method robust to cross-sensitivity is as follows. For a catalyst that looks like EUL, calculate the probability that the measurement could actually be a cross-sensitive signal from a degreened catalyst. This is defined as $P_{\mathrm{DG,cross}}$ and calculated using the following equation.

$$P_{\mathrm{DG,cross}} = \int_{i=1}^{20} p_{\mathrm{meas}}(y_{\mathrm{TPNOx},\theta_{\mathrm{DG},i}} + y_{\mathrm{TPNH_3},\theta_{\mathrm{DG},i}})p_{\mathrm{post}}(\theta_{\mathrm{DG},i} \mid y_{\mathrm{TPNOx,meas}}) \tag{5.13}$$

Then the OBD must be disabled if $P_{\text{DG,cross}} \approx P_{\text{EUL}}$. In other words, the OBD should be disabled for NOx measurements which are equally likely to be either accurate NOx values for an EUL catalyst or cross-sensitive NOx values for a degreened catalyst. This situation is demonstrated in Figure 5.9. The same segment of data as in Figure 5.8a is shown in Figure 5.9a. As discussed earlier, cross-sensitivity makes the degreened catalyst look like EUL for this segment resulting in $P_{\text{EUL}} > P_{\text{DG}}$. However, it can be observed from Figure 5.9b that $P_{\text{DG,cross}} \approx P_{\text{EUL}}$, which implies that it is equally likely that the measurement is a cross-sensitive NOx value for a degreened catalyst.

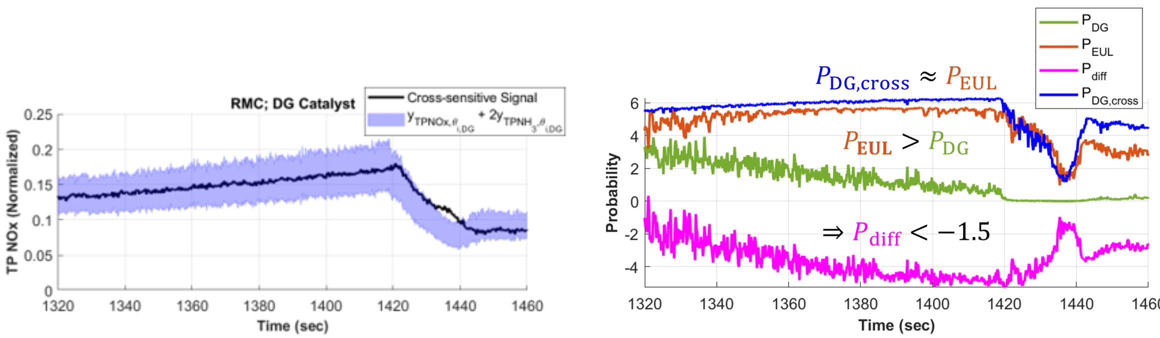

(a) Section of TP NOx vs time data from the RMC cycle for the DG catalyst.

(b) Probability calculations showing $P_{\text{EUL}} > P_{\text{DG}} \implies P_{\text{diff}} < -1.5$, and $P_{\text{DG,cross}} \approx P_{\text{EUL}}$

Figure 5.9. Segment of tailpipe NOx vs time data from the RMC cycle showing an example of NOx measurements, which are equally likely to be accurate measurements from an EUL catalyst or cross-sensitive NOx values for a degreened catalyst: (a) for the same segment of data as shown in Figure 5.8a, the black line, representing the cross-sensitive tailpipe NOx measurement from a DG catalyst, aligns with the cross-sensitive TP NOx values predicted by the DG catalyst model. This is quantified by the probabilities plotted in (b), which shows that $P_{\text{EUL}} > P_{\text{DG}} \implies P_{\text{diff}} < -1.5$ and $P_{\text{DG,cross}} \approx P_{\text{EUL}}$. OBD should be disabled for such situations to improve robustness to cross-sensitivity.

The precise enable conditions are defined as follows. Disable the OBD if:

$$\begin{aligned} &P_{\text{EUL}} - P_{\text{DG}} > 1.5 \text{ AND} \\ &|P_{\text{EUL}} - P_{\text{DG,cross}}| < 1.5 \end{aligned} \tag{5.14}$$

Since the enable condition to handle the cross-sensitivity was defined as Filter 4 in Section 5.1, this enable condition is also defined as Filter 4 for consistency across the two methods. OBD results for worst-case cross-sensitivity after incorporating this enable condition are listed in Table 5.11. It can be observed that this enable condition disabled the OBD for the degreened catalyst for both cFTP and hFTP. The OBD was still enabled at a significant number of points in the RMC cycle, and the degreened catalyst was correctly reported to be degreened even in the presence of worst-case cross-sensitivity as implied by the positive value of $\bar{P}_{\text{diff}}$.

Table 5.11. Results of applying the stochastic model-based OBD to test-cell data with cross-sensitive tailpipe NOx measurement (simulated using Equation 5.12), after applying Filter 4.

	cFTP		hFTP		RMC	
	DG	EUL	DG	EUL	DG	EUL
No. of points selected after applying Filters 1, 2, 3, 4 and 5	0	19	0	1	1228	2656
$\bar{P}_{\text{diff}}$	N/A	-3.6	N/A	-1.7	2.4	-3.1

6. CONCLUSION AND FUTURE WORK

6.1 Summary of key contributions and conclusions

1. **Observations and insights from test-cell and on-road data** about challenges of designing robust and accurate OBD for SCR-ASC are presented:

    - In the test-cell data, the most prominent aging signatures were observed in tailpipe N_2O, which is a signal often ignored in SCR OBD literature. The aging signatures in tailpipe NOx, the only tailpipe measurement in commercial trucks, are very small. Small aging signatures could make an OBD method susceptible to false positives due to NOx sensor's cross-sensitivity to NH_3. Moreover, some of the most prominent aging signatures in tailpipe NOx were observed during operating conditions, such as low temperatures ($< 200^o$C), where commercial NOx sensors would be off. This demonstrated the challenges posed by limitations of commercial NOx sensors towards robust OBD design.
    - An OBD method based on tailpipe NOx sensor could look at aging signatures in terms of either tailpipe NOx concentration or %deNOx efficiency. Based on the results from OBD methods presented in this thesis, it was observed that %deNOx would be a better metric for the cFTP and hFTP cycles, and tailpipe NOx concentration would be a better metric for the RMC cycle.
    - It was observed that the range of engine-out and tailpipe NOx covered during on-road vehicle operation is much larger than during FTP and RMC cycles in test-cell. Therefore a model or a model-based OBD method validated on FTP and RMC cycles may not necessarily work under on-road operating conditions and vice versa.

2. **A novel diagnostics-oriented SCR-ASC model:** The SCR-ASC model presented in this work is a simple diagnostics-oriented model that models the SCR using traditional three-state ODE model and ASC using static look-up tables that determine ASC's NH_3 conversion efficiency and its selectivity to NOx and N_2O as a function of temperature and flow rate. Since these look-up tables were calibrated for tempera-

tures ranging from 200^{o}C to 350^{o}C, this model can't be used for temperatures outside this range as the look-up tables can't extrapolate. Results show that the SCR-ASC model can capture the aging signatures in tailpipe NOx, NH_3, and N_2O reasonably well for cFTP, hFTP, and RMC cycles in the test-cell data. After slight re-calibration and combining with a simple model for commercial NOx sensor's cross-sensitivity to NH_3, the model works reasonably well for on-road data from commercial trucks. The two model-based OBD methods designed using this model showed reasonable results across test-cell and on-road data. This demonstrates that unlike a control-oriented model, a diagnostics-oriented model does not need to be accurate under all operating conditions. A diagnostics-oriented model only needs to accurately capture the general trends that occur as a result of aging during operating conditions where clear aging signatures can be observed.

3. **Model-based enable conditions:** To achieve accurate and robust diagnostics, it is very important for OBD methods to be equipped with carefully designed enable conditions to achieve a good IUMPR while minimizing false positives and false negatives. An important contribution of this work is the clearly defined model-based enable conditions for two OBD methods. It was demonstrated that the enable conditions increase the robustness of the OBD methods to model inaccuracy, uncertainty in initial NH_3 storage, and NOx sensor's cross-sensitivity to NH_3. However, increasing the robustness resulted in more restrictive enable conditions. Therefore, the results of applying these enable conditions demonstrated the fundamental difficulty of robust SCR monitoring due to the trade-off between the number of points where the enable conditions are satisfied and the robustness of the diagnostics results to uncertainties.

4. **Two model-based OBD methods:** Two model-based OBD methods are presented in this work. The first method does a binary classification at each sample point by labeling each sample point as either degreened or EUL. Results on test-cell data showed that this method is capable of correctly identifying the aging levels of degreened and EUL catalysts with zero false positives and very few false negatives. The method was also shown to be robust to NOx sensor's cross-sensitivity to NH_3 when the tailpipe NOx

and NH_3 signals in test-cell data were combined to simulate worst-case cross-sensitivity. Simulating both cross-sensitivity and measurement noise in test-cell data resulted in some false positives but the majority of points were still correctly classified as degreened or EUL. Results on truck data show encouraging trends between relative degradation level and the number of miles on the four trucks. A drawback with this method was that very few sample points were selected from the test-cell data after applying the enable conditions, which demonstrates the challenge with designing model-based enable conditions that are robust to false positives and false negatives but still lead to good IUMPR.

Unlike the first method, the second OBD method assigns a non-binary value to each sample point, which is proportional to the probability of that point belonging to a degreened or an EUL catalyst. This method uses a stochastic version of the proposed SCR-ASC model, which is derived using a simplified version of the Bayesian approach for model calibration. This method results in a much better IUMPR than the first one and can still correctly classify the degreened and EUL catalysts for all three cycles in the test-cell data.

6.2 Key Challenges

1. **Implementing the OBD on actual trucks:** Both OBD methods presented in this work involve running the differential equation and look-up table-based SCR-ASC model. The deterministic model-based method requires running two models, the degreened and the EUL catalyst models, and the stochastic model-based OBD method requires to run forty models (twenty times for the degreened catalyst model and twenty for the EUL catalyst model). It may not be computationally feasible to run these models in real-time on the on-board micro-controller in trucks. Since the OBD doesn't need to report the catalyst age in real time, the models could be run at a remote server and communicate with the on-board micro-controller over the air. Exact implementation of this would be a significant step towards running the proposed OBD methods on commercial trucks.

2. **Stringent emission regulations:** As the NOx emission regulations become more stringent, it would become harder to detect differences between degreened and EUL catalysts as the difference between tailpipe NOx emissions from degreened and EUL catalysts could start becoming smaller than the measurement and modeling errors. One option to resolve this would be to use more accurate NOx sensors. However, due to the lack of improvement in accuracy of commercial NOx sensors over the years, this would imply that the diagnostics-oriented SCR-ASC model would need to become more accurate for effective and robust OBD as the emission regulations become more stringent.

3. **Coupling of model accuracy and model-based enable conditions:** The accuracy of the diagnostics-oriented SCR-ASC model in this work was an important factor when designing the model-based enable conditions for the proposed OBD methods. This process demonstrated that the model accuracy and enable conditions are coupled with each other, and improvements in model accuracy in future would lead to changes in enable conditions and vice versa. Therefore, making improvements in the model and designing the enable conditions should not be considered as independent tasks and should be done in parallel as two tightly linked aspects of the same task.

6.3 Future Work

1. **Comprehensive model validation using more data and/or high-fidelity model:** In this work, the proposed SCR-ASC models for degreened and EUL catalysts were calibrated using the hFTP cycle and validated using the cFTP and RMC cycles in test-cell data. Since the degradation levels of the catalysts on the four trucks were unknown, the model performance on the truck data was considered "reasonable" if the tailpipe NOx measurements from the trucks lie between the model-out tailpipe NOx values from the degreened and the EUL catalyst models. Even if the degradation level of the catalyst on a truck was known, a model calibrated using the hFTP cycle might not work for the very different operating conditions encountered during on-road operation. Another challenge with validating the model using on-road data is unavailability

of tailpipe NH_3 measurements and cross-sensitive tailpipe NOx measurements in commercial trucks. Therefore, for a more comprehensive model validation, the following options are suggested:

- To validate the degreened and EUL catalyst models for operating conditions encountered during on-road vehicle operation, test-cell data for customized drive cycle(s), with operating conditions similar to truck data, for degreened and EUL catalysts should be used.
- Degreened and EUL are the extreme aging levels. To validate the SCR-ASC model for intermediate aging levels, test-cell data for a catalyst at an intermediate aging level run under cFTP, hFTP, RMC, and custom drive cycle(s) with "on-road" operating conditions should be used.
- Even though using real data for model validation is ideal, collecting data that meets all the requirements for a comprehensive model validation, such as the ones listed above, may not be practical. A good alternate in that case is to validate the simple diagnostics-oriented model against a high-fidelity partial differential equation (PDE) model for SCR-ASC. Unlike experimental data, signals such as SCR-out NOx and NH_3 would be available from the high-fidelity simulation. This will allow for individual calibration and validation of the low-fidelity SCR and ASC models. Also, simulating multiple aging levels using the high-fidelity model is much easier than getting access to catalysts at intermediate aging levels.
- Therefore, a comprehensive validation, for several degradation levels and under a wide range of operating conditions, of low-fidelity diagnostics-oriented SCR and ASC models against a high-fidelity PDE model for SCR-ASC followed by experimental validation could be a viable future direction.

2. **Validation of the diagnostic trends reported on the truck data:** Diagnostics results on truck data show encouraging trends between relative degradation level and the number of miles on the four trucks. However, these results could not be validated at this stage because the aging levels of the catalysts on these trucks are unknown.

Therefore, on-road data from truck(s) with known aging level(s) should be used to validate these results. This could be data from a new truck with a degreened catalyst and/or data collected right before replacing an EUL catalyst on an old truck.

3. **Further development of stochastic model-based OBD:** Good IUMPR and correct identification of degreened and EUL catalysts for the three cycles in the test-cell data are encouraging results for the stochastic model-based OBD method. However, a preliminary version of this method was presented in this thesis based on a simplified implementation of the Bayesian approach for model calibration. In future, a more rigorous version of the Bayesian approach should be used to refine the method. For example, in the preliminary implementation presented here, an analytical form of the posterior probability distribution was defined for model parameters by choosing specific values of the proportionality constant and standard deviation. This simplified the process of calculating posterior probability density at various parameter values. In the more rigorous implementation, advanced methods such as Markov Chain Monte Carlo sampling must be used to sample parameters from a posterior probability density function, whose analytical formulation is unknown. A more detailed implementation of the Bayesian approach coupled with the detailed framework of the stochastic model-based OBD method equipped with a complete set of enable conditions presented here would result in a promising model-based OBD method.

REFERENCES

[1] W. A. Majewski, *What are diesel emissions*, https://www.dieselnet.com/tech/emi_intro.php, 2012 (accessed April 28, 2017).

[2] J. Coan, *Vehicle emissions standards are a regulatory success story*, https://dieselnet.com/standards/us/ld.php, 2017 (accessed April 28, 2017).

[3] *Epa announces largest voluntary recall of medium- and heavy-duty trucks*, https://archive.epa.gov/epa/newsreleases/epa-announces-largest-voluntary-recall-medium-and-heavy-duty-trucks.html, 2018 (accessed November 28, 2021).

[4] K. K. Jain, "Modeling of nh 3 storage in vanadia-based scr catalyst for urea-dosing control in a dieselelectric hybrid car," M.S. thesis, Purdue University, 2017.

[5] J. R. Hiremath, "Development of urea-scr dosing control strategies for a diesel electric hybrid car," M.S. thesis, Purdue University, 2015.

[6] S. 1. Title 13, *Malfunction and diagnostic system requirements - 2004 and subsequent model-year passenger cars, light-duty trucks, and medium-duty vehicles and engines.* https://govt.westlaw.com/calregs/Document/IE92473B8992248378C3C5ABA362FE285?viewType=FullText&originationContext=documenttoc&transitionType=CategoryPageItem&contextData=(sc.Default), (accessed Nov 30, 2021).

[7] S. 1. Title 13, *On-board diagnostic system requirements - 2010 and subsequent model-year heavy-duty engines.* https://govt.westlaw.com/calregs/Document/IEE0FE47680F8470A80C1595EFDD80ABE?viewType=FullText&originationContext=documenttoc&transitionType=CategoryPageItem&contextData=(sc.Default), (accessed Nov 30, 2021).

[8] *United states: On-board diagnostics: California obd*, https://dieselnet.com/standards/us/obd_ca.php, (accessed Nov 30, 2021).

[9] *United states: On-board diagnostics: Federal obd*, https://dieselnet.com/standards/us/obd_fed.php, (accessed Nov 30, 2021).

[10] *United states: On-board diagnostics*, https://dieselnet.com/standards/us/obd.php, (accessed Nov 30, 2021).

[11] A. R. Emissions Compliance and C. Science Division, *Workshop for 2018 hd obd regulations update*, https://ww2.arb.ca.gov/sites/default/files/classic/msprog/obdprog/hdobd_2017wspresentation.pdf, 2018 (accessed Nov 30, 2021).

[12] M. Romijn and U. Kumar, *California hd obd programsummary of 2018 amendments*, https://dieselnet.com/news/2018/12obd.php, 2018 (accessed Nov 30, 2021).

[13] *Carb approves heavy-duty obd amendments, adopts real nox and co2 tracking*, https://dieselnet.com/news/2018/11carb.php, 2018 (accessed Nov 30, 2021).

[14] P. Chen and J. Wang, "Estimation and adaptive nonlinear model predictive control of selective catalytic reduction systems in automotive applications," *Journal of Process Control*, vol. 40, pp. 78–92, 2016.

[15] Y. Ma and J. Wang, "Observer-based estimation of aging condition for selective catalytic reduction systems in vehicle applications," *Journal of Dynamic Systems, Measurement, and Control*, vol. 139, no. 2, p. 021 002, 2017.

[16] K. Jiang, F. Yan, and H. Zhang, "Hydrothermal aging factor estimation for two-cell diesel-engine scr systems via a dual time-scale unscented kalman filter," *IEEE Transactions on Industrial Electronics*, vol. 67, no. 1, pp. 442–450, 2019.

[17] A. Matsumoto, K. Furui, M. Ogiso, and T. Kidokoro, "Model-based obd logic utilizing adsorption and desorption model of nh 3 in scr catalyst," SAE Technical Paper, Tech. Rep., 2016.

[18] A. D. Herman, M.-C. Wu, and D. D. Cabush, *Diagnostic methods for selective catalytic reduction (scr) exhaust treatment system*, US Patent App. 12/327,945, Apr. 2010.

[19] J. M. Perrin and S. P. Levijoki, *Diagnostic systems and methods for selective catalytic reduction (scr) systems based on nox sensor feedback*, US Patent 9,657,630, May 2017.

[20] M.-J. Kim, J.-I. Chun, and S.-H. Kwon, *Fault diagnosis method of scr system and an apparatus thereof*, US Patent 9,664,089, May 2017.

[21] H. S. Surenahalli, "Dynamic model based state estimation in a heavy duty diesel aftertreatment system for onboard diagnostics and controls," Ph.D. dissertation, Michigan Technological University, 2013.

[22] J. Y. Kim, Y. Cheng, J. E. Patterson, P. M. Laing, and C. K. Lambert, “Modeling study of urea scr catalyst aging characteristics,” SAE Technical Paper, Tech. Rep., 2007.

[23] T. J. Toops, K. Nguyen, A. L. Foster, *et al.*, “Deactivation of accelerated engine-aged and field-aged fe–zeolite scr catalysts,” *Catalysis Today*, vol. 151, no. 3-4, pp. 257–265, 2010.

[24] H.-W. Jen, J. W. Girard, G. Cavataio, and M. J. Jagner, “Detection, origin and effect of ultra-low platinum contamination on diesel-scr catalysts,” *SAE International Journal of Fuels and Lubricants*, vol. 1, no. 1, pp. 1553–1559, 2009.

[25] J. Gieshoff, A. Schäfer-Sindlinger, P. Spurk, J. Van Den Tillaart, and G. Garr, “Improved scr systems for heavy duty applications,” SAE Technical Paper, Tech. Rep., 2000.

[26] R. Daya, S. Y. Joshi, J. Luo, R. K. Dadi, N. W. Currier, and A. Yezerets, “On kinetic modeling of change in active sites upon hydrothermal aging of cu-ssz-13,” *Applied Catalysis B: Environmental*, vol. 263, p. 118 368, 2020.

[27] R. Daya, C. Desai, and B. Vernham, “Development and validation of a two-site kinetic model for nh 3-scr over cu-ssz-13. part 1. detailed global kinetics development based on mechanistic considerations,” *Emission Control Science and Technology*, vol. 4, no. 3, pp. 143–171, 2018.

[28] Y. Cheng, L. Xu, J. Hangas, M. Jagner, and C. Lambert, “Laboratory postmortem analysis of 120k mi engine aged urea scr catalyst,” *SAE Transactions*, pp. 187–194, 2007.

[29] M. Devarakonda, G. Parker, J. H. Johnson, V. Strots, and S. Santhanam, “Adequacy of reduced order models for model-based control in a urea-scr aftertreatment system,” SAE Technical Paper, Tech. Rep., 2008.

[30] M.-F. Hsieh, “Control of diesel engine urea selective catalytic reduction systems,” Ph.D. dissertation, The Ohio State University, 2010.

[31] J. Hu, J. Zeng, and L. Wei, “Failure diagnosis and tolerant control method for hydrothermally aged scr system by utilizing ekf observer and mrac controller,” *Energy*, vol. 156, pp. 103–121, 2018.

[32] J. Hu, J. Zeng, L. Wei, and F. Yan, "Improving the diagnosis accuracy of hydrothermal aging degree of v2o5/wo3–tio2 catalyst in scr control system using an gs–pso–svm algorithm," *Sustainability*, vol. 9, no. 4, p. 611, 2017.

[33] S. Stadlbauer, H. Waschl, and L. del Re, "Adaptive scr model for mpc control including aging effects," SAE Technical Paper, Tech. Rep., 2015.

[34] C. M. Schär, C. H. Onder, H. Geering, and M. Elsener, "Control-oriented model of an scr catalytic converter system," SAE Technical Paper, Tech. Rep., 2004.

[35] D. Upadhyay and M. Van Nieuwstadt, "Modeling of a urea scr catalyst with automotive applications," in *ASME International Mechanical Engineering Congress and Exposition*, vol. 36290, 2002, pp. 707–713.

[36] A. Pezzini, M. Canova, S. Onori, G. Rizzoni, and A. Soliman, "A methodology for fault diagnosis of diesel nox aftertreatment systems," *IFAC Proceedings Volumes*, vol. 42, no. 8, pp. 911–916, 2009.

[37] X. Yuan, H. Liu, and Y. Gao, "Diesel engine scr control: Current development and future challenges," *Emission Control Science and Technology*, vol. 1, no. 2, pp. 121–133, 2015.

[38] I. Nova and E. Tronconi, *Urea-SCR technology for deNOx after treatment of diesel exhausts*. Springer, 2014.

[39] J. Zhao, Z. Chen, Y. Hu, and H. Chen, "Urea-scr process control for diesel engine using feedforward-feedback nonlinear method," *IFAC-PapersOnLine*, vol. 48, no. 8, pp. 367–372, 2015.

[40] A. R. Ofoli, "Experimental demonstration of ammonia storage and slip modeling with control for an scr aftertreatment system," *IEEE Transactions on Industry Applications*, vol. 50, no. 4, pp. 2342–2348, 2014.

[41] S. Shrestha, M. P. Harold, K. Kamasamudram, A. Kumar, L. Olsson, and K. Leistner, "Selective oxidation of ammonia to nitrogen on bi-functional cu–ssz-13 and pt/al2o3 monolith catalyst," *Catalysis Today*, vol. 267, pp. 130–144, 2016.

[42] A. Bonfils, Y. Creff, O. Lepreux, and N. Petit, "Closed-loop control of a scr system using a nox sensor cross-sensitive to nh3," *Journal of Process Control*, no. 2, pp. 368–378, 2014.

[43] M.-F. Hsieh and J. Wang, "Development and experimental studies of a control-oriented scr model for a two-catalyst urea-scr system," *Control Engineering Practice*, vol. 19, no. 4, pp. 409–422, 2011.

[44] C. M. Schar, C. H. Onder, and H. P. Geering, "Control of an scr catalytic converter system for a mobile heavy-duty application," *IEEE Transactions on Control Systems Technology*, vol. 14, no. 4, pp. 641–653, 2006.

[45] *Lecture 20 - inverse problems/model calibration: Bayesian approach*, https://github.com/PredictiveScienceLab/uq-course/blob/SP2020/lectures/lecture_20.ipynb, (accessed December 8, 2022).

VITA

Kaushal Kamal Jain is from Jaipur city in India. His is interested in modeling, estimation, and controls of automotive and robotic systems. He has seven years of research experience working on modeling, estimation, controls and diagnostics of the automotive urea-SCR system. He received the degree of Bachelor of Technology in Mechanical Engineering from Indian Institute of Technology Guwahati in May 2015. He joined the Master of Science in Mechanical Engineering (M.S.M.E.) program at Purdue University in Fall 2015. He worked on parameter identification and observer design to estimate NH_3 storage in an SCR catalyst for his Masters thesis under the supervision of Dr. Peter H. Meckl. After receiving the degree of Master of Science in Mechanical Engineering from Purdue University in July 2017, he decided to continue working with Dr. Meckl towards a PhD in Mechanical Engineering from Purdue University. During the initial years of his PhD, he extended his M.S. thesis work on nonlinear parameter identification and analysis of control-oriented models for urea-SCR system. Later, Dr. Meckl and Kaushal collaborated with Dr. Pingen Chen's research group at Tennessee Technological University to secure sponsorship and data from Cummins Inc. to work on designing on-board diagnostics for SCR-ASC system in diesel engine aftertreatment. This project became the main focus of his PhD research. He plans to defend his PhD thesis in December 2022.

PUBLICATION(S)

Journal Articles

K. K. Jain, P. H. Meckl, P. Chen and K. Yang, "Diagnostics-oriented model for SCR-ASC," *International Journal of Prognostics and Health Management*, vol. 14, no. 3, 2023.

K. K. Jain, J. R. Hiremath, and P. H. Meckl, "A new parameter identification for control-oriented urea-SCR models," in preparation

K. K. Jain and P. H. Meckl, "Review and analysis of control-oriented urea-SCR models," in preparation

Conference Proceedings

K. K. Jain, J. R. Hiremath, and P. H. Meckl, "Term-by-term observer design method to estimate NH 3 storage in SCR catalyst," in *2020 American Control Conference (ACC)*, pp. 4899-4904. IEEE, 2020.

R. Ganne, **K. K. Jain**, P. H. Meckl, H. Angre, and J. R. Hiremath, "Computationally efficient urea-dosing controllers for urea-SCR," in *Dynamic Systems and Control Conference*, Vol. 84270. American Society of Mechanical Engineers, 2020.